Synthesis of Bi-functional Oxygen Donor Neutral Ligands and their Coordination Chemistry with Lanthanide(III) and Uranyl(VI) ions.

By

BAL GOVIND VATS

CHEM01201204008

Bhabha Atomic Research Centre

A thesis submitted to the
Board of Studies in Chemical Sciences

In partial fulfillment of requirements

for the Degree of

DOCTOR OF PHILOSOPHY

of

HOMI BHABHA NATIONAL INSTITUTE

August, 2017

Homi Bhabha National Institute

Recommendations of the Viva Voce Committee

As members of the Viva Voce Committee, we certify that we have read the dissertation prepared by BAL GOVIND VATS entitled “ Synthesis of Bi-functional Oxygen Donor Neutral Ligands and their Coordination Chemistry with Lanthanides(III) and Uranyl(VI) ions” and recommend that it may be accepted as fulfilling the thesis requirement for the award of Degree of Doctor of Philosophy.

Chairman - Dr. V. K. Jain **Date:**

Guide / Convener – Dr. S. Kannan **Date:**

Examiner – Prof. Prasenjit Ghosh **Date:**

Member 1- Dr. S. K. Ghosh **Date:**

Member 2- Dr. P. K. Mohapatra **Date:**

Member 3- Dr. (smt.) S. Banerjee **Date:**

Final approval and acceptance of this thesis is contingent upon the candidate’s submission of the final copies of the thesis to HBNI.

I/We hereby certify that I/we have read this thesis prepared under my/our direction and recommend that it may be accepted as fulfilling the thesis requirement.

Date:

Place:

Guide

(S. Kannan)

STATEMENT BY AUTHOR

This dissertation has been submitted in partial fulfillment of requirements for an advanced degree at Homi Bhabha National Institute (HBNI) and is deposited in the Library to be made available to borrowers under rules of the HBNI.

Brief quotations from this dissertation are allowable without special permission, provided that accurate acknowledgement of source is made. Requests for permission for extended quotation from or reproduction of this manuscript in whole or in part may be granted by the Competent Authority of HBNI when in his or her judgment the proposed use of the material is in the interests of scholarship. In all other instances, however, permission must be obtained from the author.

(BAL GOVIND VATS)

DECLARATION

I, hereby declare that the investigation presented in the thesis has been carried out by me. The work is original and has not been submitted earlier as a whole or in part for a degree / diploma at this or any other Institution / University.

(BAL GOVIND VATS)

List of Publications arising from the thesis

Journal

1. Extraction and structural studies of an unexplored monoamide, N,N′-dioctyl, α-hydroxy acetamide with lanthanide(III) and actinide(III) ions

S.Kannan, **Bal Govind Vats**, I.C. Pius, D. M. Noronha, P. S. Dhami, P. W. Naik and Mukesh Kumar, *Dalton Trans.*, **2014** , *43*, 5252-5255

2. Synthetic, structural, extraction and theoretical studies of uranyl nitrate dithio-diglycolamide compounds

B.G. Vats, S. Kannan, I.C. Pius, D.M. Noronha, D.K. Maity, M.G.B. Drew, *Polyhedron*, **2014**, 75, 81–87

3. Steric effects in complexes of diphenyl(2-pyridyl)phosphine oxide with the uranyl ion. Synthetic, structural and theoretical studies

Bal Govind Vats, S. Kannan, K. Parvathi, D.K. Maity, M.G.B. Drew, *Polyhedron*, **2015**, *89*, 116–124

4. Ligand Field Asymmetry Controlled Luminescent Europium(III) and Samarium(III) Tris(β-diketonate) Complexes of Diphenyl-(2-pyridyl-N-oxide)- Phosphine Oxide

Bal Govind Vats, Shanmugaperumal Kannan, Mukesh Kumar and Micheal G. B. Drew, *Chem. Select*, **2017**, *2*, 3683-3689

5. Synthesis, structural and extraction studies of new bifunctional ligand with uranium

Bal Govind Vats, J.S. Gamare, S. Kannan, I.C. Pius, D.M.Noronha and M. Kumar *Inorg. Chim. Acta,* **2017,** 467, 1-6

6. Novel approach for extraction of plutonium and americium from aqueous complexing media

Bal Govind Vats, I.C. Pius, D.M. Noronha and S. Kannan, J. Radioanal. Nucl. Chem., **2018**, 1-8

Conferences

1. Europium and samarium β-diketonate complexes with diphenyl-2-pyridyl phosphine oxide: Synthesis and photoluminescence

Bal Govind Vats, S.Kannan and M.G.B.Drew, 5th Interdisciplinary Symposium on Materials Chemistry (ISMC-2014) held at BARC, Mumbai during Dec. 9-13, 2014, Paper No. H-101, p.283.

2. Extraction of Am(III) and Pu (III) by a monoamide N,N-dioctyl-a-hydroxyacetamide from different acid media

Bal Govind Vats, I.C.Pius, D. M. Noronha and I. C. Pius, NUCAR-2015 held at BARC, Mumbai, Paper No. B-21, p.130

3. A new bi-functional Ligand for UO_2^{2+} and Pu^{4+} Extraction

Bal Govind Vats, I.C.Pius, D.M. Noronha, Mukesh kumar and S.Kannan, NUCAR-2017 held at KIIT, Bhubaneswar, Odisha during Feb. 6-10, 2017, Paper No,C-14, p.192

Others

1. Synthesis, structural and theoretical studies of dithiodiglycolamidcompounds of palladium(II)

Balgovind Vats, S. Kannan, Mahesh Sundararajan, Mukesh Kumar and M. G. B. Drew, *Dalton Trans.,* **2015**, *44*, 11867-11876.

(BAL GOVIND VATS)

Dedicated to........

My Mother

ACKNOWLEDGEMENTS

Firstly, I would like to express my sincere gratitude to my advisor Dr. S. Kannan for the continuous support of my Ph.D. study and related research for his patience, motivation and immense knowledge. A person with an amicable and positive disposition, Dr. Kannan has always made himself available to clarify my doubts despite his busy schedules and I consider it as a great opportunity to do my doctoral programme under his guidance and to learn from his research expertise.

His guidance helped me in all the time of research and writing of this thesis. I could not have imagined having a better advisor and mentor for my Ph.D. study.

I would like to extend my gratitude to my doctoral commitee members Dr. V. K. Jain, Dr. S. K. Ghosh, Dr. P. K. Mohapatra and Dr (smt.) S. Banerjee for their support and encouragement throghout my Ph.D. work.

I wish to acknowledge Dr. M.G.B. Drew and Dr. Mukesh Kumar for their help in carrying out the Single Crystal XRD for my compounds. I would like to acknowledge Dr. I.C. Pius and Dr. D. M. Noronha for helping me in solvent extraction experiments. I would like to thank national NMR facility, TIFR and Dr. V. K. Jain to allow me to record the NMR spectra.

I would like to acknowledge Dr. D. K. Maity (Associate Dean, HBNI) for performing theoretical calculation to support the experimental findings of this thesis

I would like to thank my Heavenly Teacher Shri M. P. Shukla for His Grace, benevolence and for giving me the strength to overcome many trying moments to pursue my dreams.

Thanks are due to my friends Pallavi Singhal and Adish Tyagi who always supported me in thin and thick of the time. I am also most grateful to my mother and family for their belief in me and their constant prayers. Finally, and most importantly, I would like to thank my wife Kusum. Her support, encouragement, quiet patience and unwavering love were undeniably the bedrock upon which the past six years of my life have been built. Her tolerance of my occasional bad moods is a testament in itself of her unyielding devotion and love.

Table of Contents

Chapter 4: Synthesis, coordination, structural and photoluminescence studies of (diphenyl-(2-pyridyl) phosphine oxide and diphenyl-(2-pyridyl-N-oxide) phosphine oxide) with lanthanides and uranyl nitrate 77

Synopsis

For selective extraction of lanthanide and actinides cations from nuclear waste, bi-functional ligands like malonamides, CMPO (carbamoylphosphine oxide), succinamides, bis-phosphine oxides and picolinamides represent an important class of extractants. The incinerable organic amide based extractants have shown excellent and promising results in the process chemistry of lanthanides and actinides from nitric acid media as compared to the conventional tributyl phosphate (TBP) ligand. The chemistry of the uranyl ion with bi-functional ligands has shown great interest, not only from a separation point of view, but also due to the interesting properties exhibited in the solid state. The co-extraction of An (III) and Ln (III) from HLLW (High Level Liquid Waste) solution followed by group separation of actinides from lanthanide is proposed (SANEX process). Several reagents were synthesized in last two decades for this purpose and their extraction properties with trivalent actinides and lanthanides from HLLW solution have been studied. Among them, the carbamoyl methyl phosphine oxides, (TRUEX process) trialkyl phosphine oxides (TRPO process), di-isodecyl phosphoric acid (DIDPA process), malonamides (DIAMEX process) and tetra alkyl diglycolamide (TODGA or TEHDGA) have shown excellent extraction properties for actinide and lanthanide ions from HNO_3 medium. However, in most of the cases they show very high D values even in lower acidities ($< 0.5M$) and therefore need very low acidities for stripping (which is not advisable in plant operation) or complexing agents. Many novel bi-functional ligands containing the combinations of carbamoyl group (C=O), phosphine oxide group (P=O) and N-oxide (N-O) groups have been explored in recent years by Paine et. al. for actinides and lanthanides separations from nuclear waste. Still, there is a scope to modify these types of ligand systems to explore the coordination chemistry of novel bi-functional system with lanthanides and actinides. So in this thesis work, we have explored some novel unexlpored bi-functional ligand systems for the coordination and extraction studies of lanthanide and actinide ions.

The thesis consists of five chapters and the details are given below.

Chapter 1 : Introduction

This chapter deals with a brief introduction to different types of ligands relevant to the extraction of lanthanide and actinide ions from the spent fuel and the factors affecting the coordination number and geometry around the metal ions. It also deals with different types of bi-functional ligands used in the different stages of the nuclear fuel cycle and the structural studies with uranyl and lanthanide ions. Finally, the scope of the present work is discussed.

Chapter 2: Synthesis, coordination and structural studies of dithiodiglycolamide based ligands with the uranyl(VI) ion.

2.1 Synthesis of ligands and complexes with the uranyl(VI) ion: The general reactions for the synthesis of ligands and their complex with uranyl(VI) are represented in Scheme **1**.

2.2 Results and discussion: All the ligands and their compounds with uranyl(VI) nitrate were characterized for CHN analysis followed by IR and NMR techniques. The structures for the complexes $[UO_2(NO_3)_2(CH_2SCH_2CON\{C_4H_9\}_2)_2]$ and $[UO_2(NO_3)_2C_7H_6(SCH_2CON\{C_4H_9\}_2)_2]$ were deduced by single crystal XRD. The molecular structure of one of the compound is shown in Fig. 1, which confirms the spectral observations.

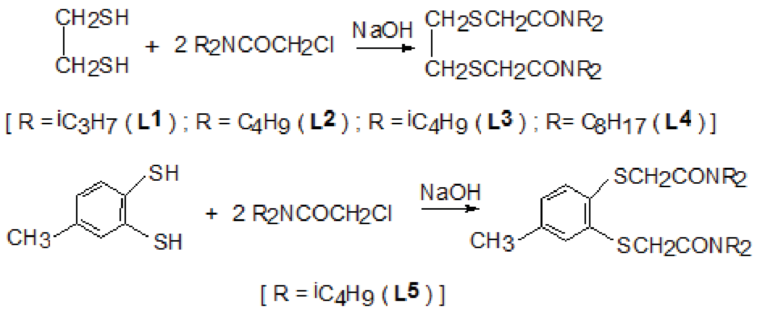

$$UO_2(NO_3)_2.6H_2O \;+\; L \longrightarrow UO_2(NO_3)_2.L$$

Where L = L^1 (**1**), L^2 (**2**), L^3 (**3**), L^5 (**4**)

Scheme : 1

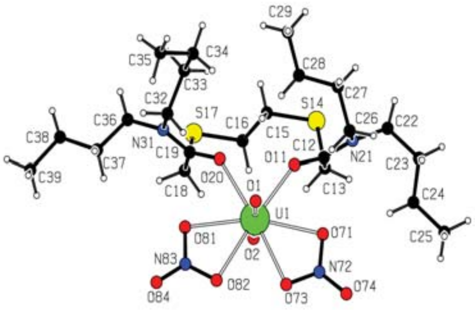

Fig. 1. Molecular Structure of [$UO_2(NO_3)_2(CH_2SCH_2CON\{C_4H_9\}_2)_2$]

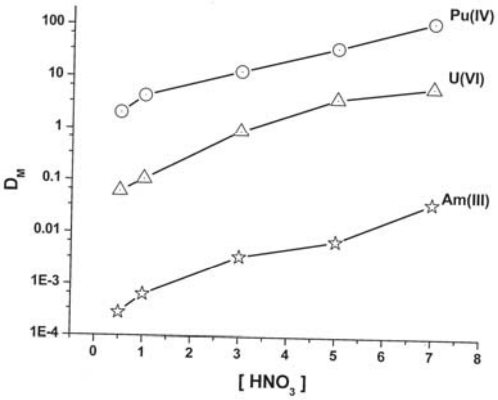

Fig. 2. Distribution ratio vs. [HNO_3] for UO_2(VI), Pu (IV) and Am (III) ions with 0.2 M **L^4** in dodecane .

The extraction studies were carried out by using the ligand **L^4** in dodecane with UO_2(VI), Pu(IV) and Am(III) ions at tracer level (using ^{233}U, ^{239}Pu and ^{241}Am tracers) from nitric acid medium to assess the feasibility of using this ligand (0.2 M) for extraction purposes. The observed distribution ratios follow the order of : $D_{Pu(IV)} >> D_{UO2(IV)} >> D_{Am(III)}$ (Fig. 2) and are similar to those observed for the other bi-functional ligands reported in the literature.

2.3 Conclusions: The coordination chemistry of dithio-diglycolamide ligands with uranyl (VI) nitrate shows a chelating mode of bonding for these ligands. The dioctyl based ligand shows an appreciable extraction for uranyl (VI) and plutonium (IV) ions from the nitric acid medium into *n*-dodecane. The extracted ions could be stripped back quantitatively using 0.5 M HNO_3 or a mixture of 0.5 M HNO_3 + 0.5 M $H_2C_2O_4$, respectively.

Chapter 3: Synthesis, coordination, structural and extraction studies of α-hydroxy acetamide based ligands with lanthanide(III) and uranyl(VI) ions.

3.1 Synthesis of ligands and their uranyl and lanthanide complexes: The synthesis of ligand and their complexes with lanthanide (III) and urany l(VI) ions are shown in Scheme -2.

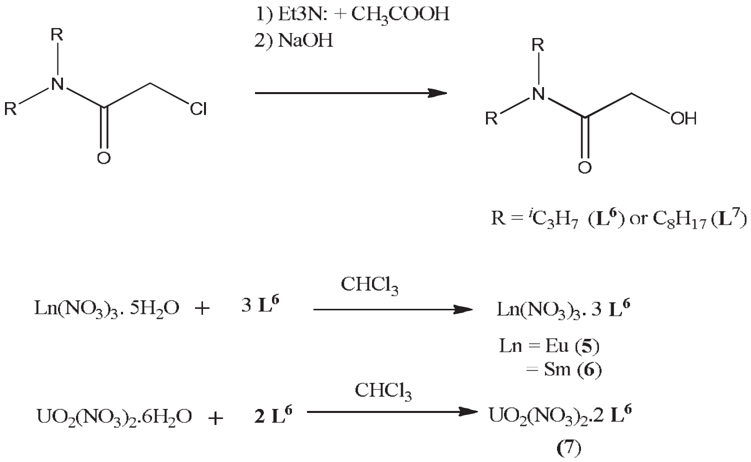

Scheme -2

3.2 Results and discussion: The ligands and their compounds of uranyl (VI) and lanthanide (III) ions were characterized by CHN analysis and IR and NMR spectroscopic techniques. Single crystal structures of the europium (III) and uranyl (VI) complexes are shown in figures 3 and 4, respectively. The extraction studies of Am (III), Pu (IV), UO$_2$ (VI), Eu (III), Sr (II), and Cs (I) ions from different concentrations

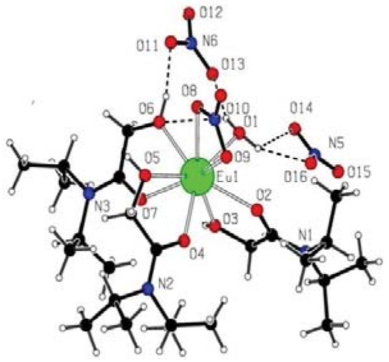

Fig. 3. Molecular structure of [Eu(NO$_3$)$_3$

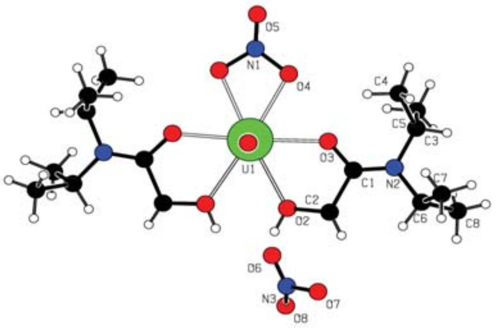

Fig. 4. Molecular structure of [UO$_2$(NO$_3$)$_2$

$((^{i}Pr)_2NCOCH_2OH)_3.H_2O]$ $((^{i}Pr)_2NCOCH_2OH)_2]$

of HNO_3 show that the order of extraction is: $D_{Pu} >> D_{Am} > D_{Eu} >> D_{UO2}$ above 3M HNO_3 (D_{Sr} and D_{Cs} are negligible at all acidities studied) (figure 5) . Extraction studies using 0.2 M of $\mathbf{L}^7$ in dodecane with 100 times diluted simulated HLLW solution from 4M HNO_3 showed that more than 99% of α, 64% of β and 47 % of γ activities could be extracted in a single contact. Extraction studies of Pu(IV) and Am (III) with $\mathbf{L}^7$ from different acidic media containing complexing as well as non-complexing anions have also been explored for the separation these ions from different types of liquid wastes.

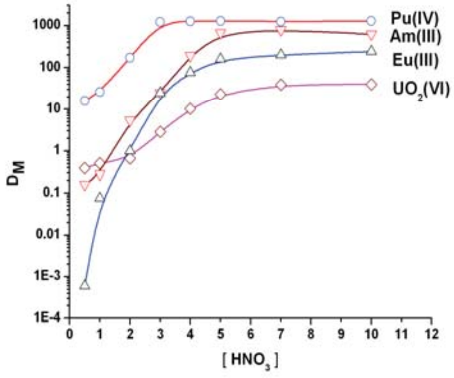

Fig.5. Distribution ratios for Pu (IV), Am (III), Eu (III) and UO_2 (VI) versus [HNO_3] in 0.2 M $\mathbf{L}^7$ in dodecane

3.3 : Conclusions: A new bi-funtional ligand is developed for extraction of trivalent lanthanide and actinide ions above 3 M HNO_3 and quantitative back extraction by 0.5 M HNO_3 showed the potential nature of this novel monoamide extractant. The structures of the Eu (III) and Sm (III) nitrates show that the ligands acts as a neutral bidentate chelating ligand and bonds through the hydroxyl and carbamoyl oxygen atoms to metal center. This ligand shows very good extraction properties towards tetravalent as well as trivalent actinides from highly complexing media like phosphoric acid.

Chapter 4: Synthesis, coordination, and photoluminescence studies of (diphenyl-(2-pyridyl) phosphine oxide and diphenyl-(2-pyridyl-*N*-oxide) phosphine oxide) with lanthanides and uranyl nitrate

4.1 Synthesis of ligands and complexes : The synthesis of ligands and their complexes with lanthanide(III) and uranyl(VI) ions are shown in Scheme -3 .

4.2 Results and discussion : The ligands and the complexes were characterized by CHN analysis, IR and NMR spectroscopy and XRD techniques. The molecular structures for both the uranyl (VI) compounds are given in figures 5 and 6 . The IR spectra of **8** and **9** clearly show that the water molecules from the starting compound are completely replaced by the ligand and structures of both compounds show that the ligand acts as a monodentate ligand and bonds through the phosphoryl oxygen atom to the uranyl(VI) centre. The geometries around uranyl(VI) ion are hexagonal and pentagonal bi-pyramidal respectively for complexes **8** and **9**. The lanthanide β-diketonate complexes of ligand $\mathbf{L^8}$ and $\mathbf{L^9}$ were prepared and characterized by IR and NMR spectroscopy and single crystal XRD. The structures of complexes $[Sm(C_4H_3SCOCHCOCF_3)_3\{(C_6H_5)_2PO(C_5H_4N)\}_2]$ and $[Sm(C_4H_3SCOCHCOCF_3)_3\{(C_6H_5)_2PO(C_5H_4N)\}_2]$ are shown in Fig. 7 and Fig. 8 respectively. The structures of the samarium(III) complexes shows that $\mathbf{L^8}$ behaves as a monodentate ligand and bonds through the P=O group whereas $\mathbf{L^9}$ behaves as a bidentate ligand and bonds through both P=O as well as N-O groups to metal centre. Photophysical properties of all the complexes were measured in the solid as well as in the solution states.

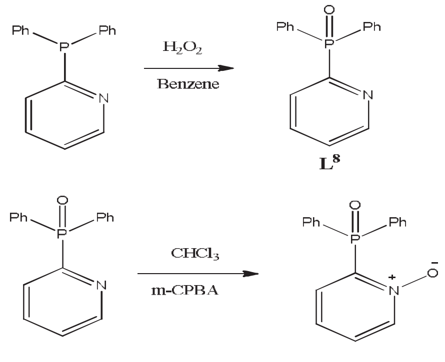

L^8

L^9

$$[UO_2(NO_3)_2\,.6H_2O] \quad + \quad \mathbf{2.\ L^8} \longrightarrow \quad [UO_2(NO_3)_2\,.2\,(\mathbf{L^8})] \; \mathbf{(8)}$$

$$[UO_2(DBM)_2\,.H_2O] \quad + \quad \mathbf{L^8} \longrightarrow \quad [UO_2(DBM)_2\,.(\mathbf{L^8})] \; \mathbf{(9)}$$

$$Ln(\overset{\frown}{O\,O})_3.2H_2O + 2\,\mathbf{L^8} \longrightarrow Ln(\overset{\frown}{O\,O})_3.2\,\mathbf{L^8}$$

When Ln=Eu, $\overset{\frown}{O\,O}$ = TTA (**10**)
$\overset{\frown}{O\,O}$ =DBM (**11**)
Ln=Sm, $\overset{\frown}{O\,O}$ = TTA (**12**)
$\overset{\frown}{O\,O}$ = DBM (**13**)

$$Ln(\overset{\frown}{O\,O})_3.2H_2O + \mathbf{L^9} \longrightarrow Ln(\overset{\frown}{O\,O})_3.\mathbf{L^9}$$

When Ln=Eu, $\overset{\frown}{O\,O}$ = TTA (**14**)
$\overset{\frown}{O\,O}$ =DBM (**15**)
Ln=Sm, $\overset{\frown}{O\,O}$ = TTA (**16**)
$\overset{\frown}{O\,O}$ = DBM (**17**)

$\overset{\frown}{O\,O}$ = Theonoyltrifluroacetonate (TTA)
and dibenzoylmethanate(DBM)

Scheme-3

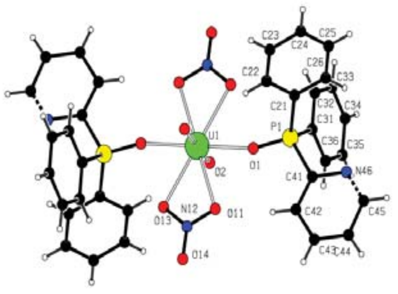

Fig. 5. Molecular structure of $[UO_2(NO_3)_2(\{C_6H_5\}_2POC_5H_5N)_2]$

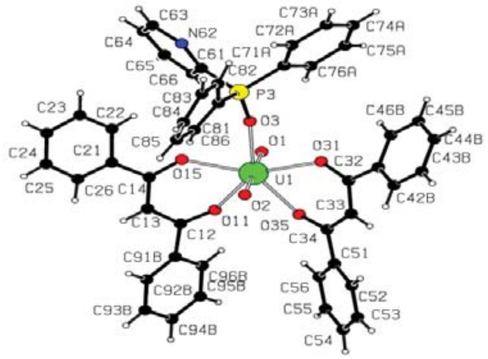

Fig. 6. Molecular structure of $[UO_2(C_6H_5COCHCOC_6H_5)_2(C_6H_5)_2POC_5H_5N\ ]$

Due to the increase in ligand field asymmetry around the metal centre (by changing ligand from **L^8** to **L^9**) the asymmetry ratios in the europium(III) tris(β-diketonate)-PONO complexes as measured by emission spectroscopy were increased from 19.1 % to 28.6% in the TTA complexes. This leads to an increase in the intrinsic quantum yield for the PONO complexes as compared to that of the PON complexes according to the recently reported Escalate Coodination Anisotropy (ECA) principle.

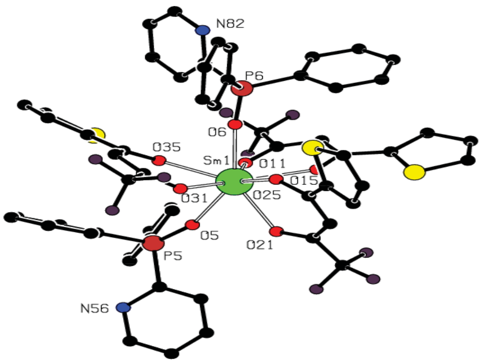

Fig. 7. Molecular structure of $[Sm(C_4H_3SCOCHCOCF3)_3\{(C_6H_5)_2PO(C_5H_4N)\}_2]$

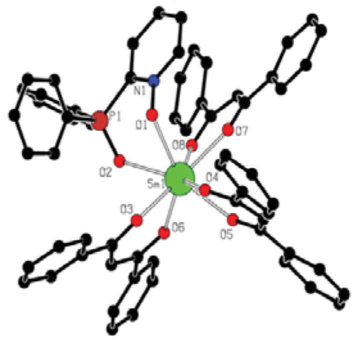

Fig. 8. Molecular structure of $[Sm(C_6H_5COCHCOC_6H_5)_3\{(C_6H_5)_2PO(C_5H_4NO)\}]$

4.3 Conclusions. The structural studies on the complexes of diphenyl(2-pyridyl)phosphine oxide with uranyl(VI) nitrate and uranyl(VI) bis(dibenzoylmethanate) show a monodentate mode of bonding for the ligand. The crystal structures of the lanthanide tris(β-diketonate) complexes, show a monodentate mode of bonding for $\mathbf{L}^{\mathbf{8}}$ and bidentate mode of bonding for $\mathbf{L}^{\mathbf{9}}$. All the complexes show good photophysical properties in the solid state as well as in solution states. It is observed that the increase in ligand field asymmery around the metal centre increases the asymmetry ratio of the Eu(III) emission bands, the quantum yield also increases.

Chapter 5: Synthesis, coordination, structural and extraction studies of (*N,N*-dialkyl carbamoyl methyl) (2-pyridyl-*N*-oxide) sulfide ligands with the uranyl(VI) ion.

5.1 Synthesis of ligands and complexes: The synthesis of ligands and their complexes with uranyl(VI) ion is given in Scheme 4.

5.2 Results and discussion: All the ligands and complexes were characterized by CHN analyses and FTIR and NMR spectroscopy. The IR spectra of complexes show that the water molecule from the starting compound $UO_2(NO_3)_2.6H_2O$ has been completely replaced by the ligands and the ligands are bonded to the uranyl(VI) ion through the C=O and N-O groups. The molecular structure of the

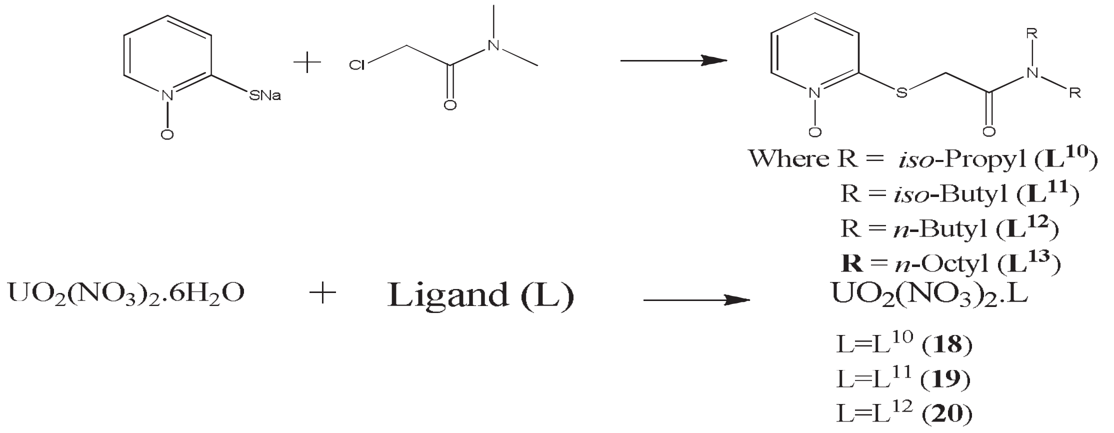

Scheme 4

compound $[UO_2(NO_3)_2\{C_5H_4NOSCH_2CON(^iBu)_2\}]$ shows (Fig. 9) the bidentate chelating mode of bonding for this ligand. Distribution ratios (D) for UO_2(VI) and Pu(IV) as a function of nitric acid concentration shows clearly that UO_2(VI) and Pu(IV) are extracted significantly from nitric acid concentrations of 1–7 M into dodecane (figure 10).

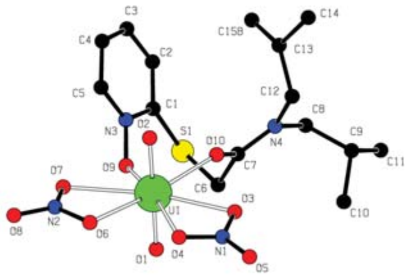

Fig. 9: Molecular structure of $[UO_2(NO_3)_2\{C_5H_4NOSCH_2CON(^iBu)_2\}]$

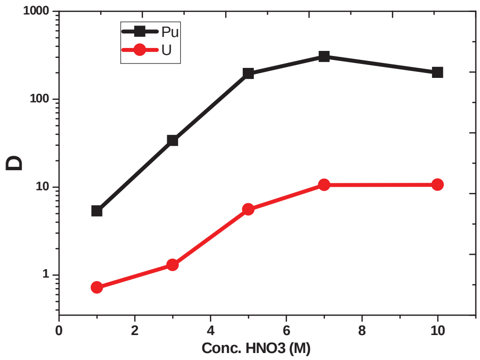

Fig.10 . Distribution ratios for Pu(IV) and UO_2(VI) versus $[HNO_3]$ in 0.2 M $\mathbf{L}^{13}$ in dodecane

5.3 Conclusion: The novel bi-functional ligands having N-O and C=O oxygen donor groups have been synthesized and characterized by IR and NMR spectroscopy. The complexes of uranyl (VI) nitrate with these ligands show that ligands are connected to the uranyl (VI) ion in a chelating mode. The extraction behaviour of the L^{13} ligand shows that uranyl (VI) and plutonium (IV) could be extracted from a nitric acid medium into dodecane significantly.

List of figures

List of schemes

List of Tables

Thesis Highlight

Name of the student: Bal Govind Vats **Enrolment No.:** CHEM01201204008
Name of CI/OCC: BARC
Thesis title:"Synthesis of Bi-functional Oxygen Donor Neutral Ligands and their Coordination Chemistry with Lanthanide(III) and Uranyl(VI) ions"
Discipline: CHEMICAL SCIENCES **Sub-Area of Discipline:** Coordination chemistry

In this thesis, the student has synthesized different types of bi-functional ligand systems namely, dithiodiglycolamide, N,N-dialkyl-α-hydroxy acetamide, diphenyl-2-pyridyl phosphine oxide(PON), diphenyl-2-pyridyl-N-oxide phosphine oxide (PONO) and *N, N*-dialkyl carbamoyl methyl-2-pyridyl-N-oxide sulphide. The coordination chemistry of these ligand systems was explored with uranyl(VI) and lanthanides(III) ions. Dithiodiglycolamide ligands behave as chelating ligands towards uranyl(VI) ion and form 11 membered metallocyclic ring. These ligands also extract actinides (tetravalent and hexavalent) from nitric acid medium. N,N-dialkyl-α-hydroxy acetamide show potential for group separation of lanthanides(III) and actinides(III) ions from high level waste. The coordination chemistry with lanthanides(III) ions and uranyl(VI) ion is also explored. In phosphine oxide system, the PON ligand shows monodentate behaviour towards uranyl nitrate and lanthanide β-diketonates, while pyridyl nitrogen remains uncoordinated. PONO ligand behaves as a bidentate donor through the phosphine oxide and N-oxide groups and shows its potential as a promising auxiliary ligand in lanthanide-β-diketonate systems, which are useful in optical display devices. The *N, N*-dialkyl carbamoyl methyl-2-pyridyl-N-oxide sulphide ligand is the first bi-functional ligand system containing both the N-oxide and carbamoyl functionality to be explored for actinide extraction. This ligand system shows appreciable extraction for tetravalent plutonium and hexavalent uranium ions.

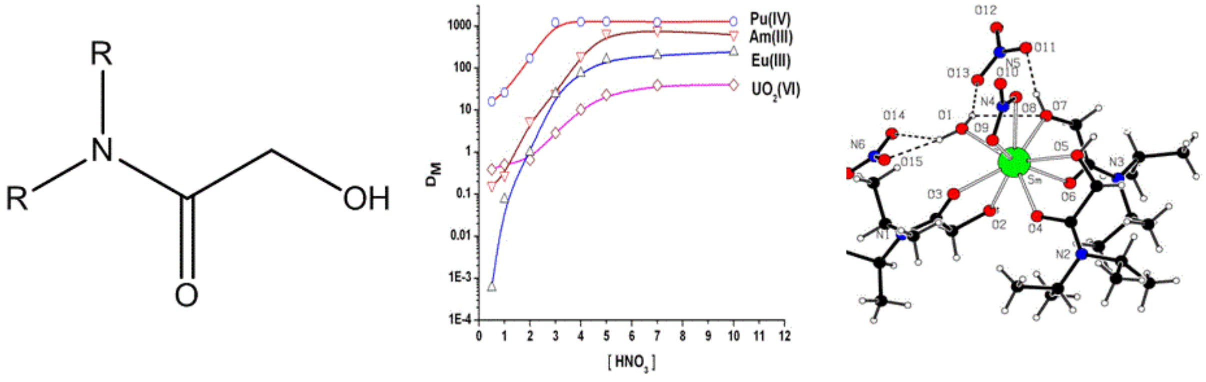

Figure 1: N,N-dialkyl-α-hydroxy acetamide ligand, Extraction of actinides and lanthanides and crystal structure of samarium(III) nitrate complex

Chapter -1

General Introduction

1.1: History of actinide chemistry

The first step in actinide chemistry research was the discovery of uranium by M. H. Klaproth in 1789 [1]. From 1789, the focus was on the discovery of new elements, which after the path breaking discovery of radioactivity in 1895 [2] shaped the discovery of highly fundamental particles like the proton and the neutron etc. With the discovery of artificial radioactivity in 1934 [3], several new phenomena were discovered. The most amazing as well as powerful phenomenon in the history of mankind i.e. nuclear fission was discovered eventually in 1938 [4] which led to the necessity of chemistry research in the actinides. The chase for separation and purification of plutonium from the fission and radioactive decay products led to the research on the organic extractants and their coordination chemistry with actinides. The pursuit for ^{235}U (a fissile isotope of the uranium) separation from the ^{238}U (a fertile isotope) led to the foundation for the more volatile organouranium compounds which further paved the way for organometallic chemistry of the actinides. The quest for highly selective extractant systems not only from the extraction point of view but also for the basic understanding of the electronic structure of the actinides in particular, have opened the path to explore the field of the actinide chemistry [5].

1.2 History of lanthanide chemistry

The lanthanides as compared to the actinides are well explored systems, first due to their non-radioactive nature (apart from Pm) and secondly due to their more applied nature in modern technology. The first discovery of lanthanides came to the light in 1787 when an unusual black mineral was found in Ytterby, Sweden. Later on, Gadolin found an impure form of yttria, which contains several lanthanide elements in smaller amounts. The first lanthanide, discovered in its pure form was cerium in 1803 by Berzelius and Klaproth. Later, Moseley proved that there are fourteen lanthanide elements between lanthanum and hafnium using X-ray spectroscopy. The rest of the elements were found later, separated from the same mineral. These elements were first named as ‘Rare Earths’ because of the rare abundance of the mineral which contains lanthanides. Lanthanides are technologically very important elements and their separation from the minerals in pure form is very difficult. Hence their chemistry was explored to get the pure elements and this is still a challenging area of research [6] .

1.3 Chemical properties of actinides and lanthanides

Actinides are long believed to behave like their f-block counterparts, the lanthanides, due to their chemical properties and size. Additionally, the poor shielding of the 4f and 5f orbitals from the nuclear charge results in a contraction of the ionic radius with increasing atomic number leading to the core like behaviour of the f-orbitals (known as the lanthanide and actinide contraction)[7]. As a consequence of this, the heavy actinides (Am-Lr) behave as lanthanides, predominantly existing in the +3 oxidation state. The greater radial extent of 5f and 6d orbitals as compared to 4f and 5d orbitals due to the relativistic effect, results in the more diverse chemical behaviour in the case of the lighter actinides.[8] In the electronic spectra, the actinide complexes are more influenced by the crystal field effect as compared to the lanthanides whereupon spin orbit and electron-electron interactions predominate [9]. Because of the energetically favourable electrons in the outer orbitals, actinides show variable oxidation states (Table 1.1) and the bonding is more covalent as compared to lanthanides[10]. In lanthanides, the 4f orbitals do not significantly take part in the bonding due to the core nature of the f orbitals which separates them from the transition metals as well as from the early actinides. The bonding is predominantly ionic in nature and electronic properties are generally not affected by the crystal field. The most stable oxidation state for lanthanides is +3 and dominates the coordination chemistry of the lanthanides[11]. Cerium also exists in the +4 oxidation state while europium and ytterbium can exist in the +2 oxidation state due to the f^0, f^7 and f^{14} configurations (Table 1.2).

Table 1.1: Oxidation states of actinides

Th	Pa	U	Np	Pu	Am	Cm	Bk	Cf	Es	Fm	Md	No	Lw
2	3	2	3	3	2	3	3	2	2	2	2	2	3
3	4	3	4	4	3	4	4	3	3	3	3	3	
4	5	4	5	5	4			4					
		5	6	6	5								
		6	7	7	6								
					7								

Table 1.2: Oxidation states of lanthanides

La	Ce	Pr	Nd	Pm	Sm	Eu	Gd	Tb	Dy	Ho	Er	Tm	Yb	Lu
					2	2						2	2	
3	3	3	3	3	3	3	3	3	3	3	3	3	3	3
	4	4	4					4	4					

Since the ligand field effect on 5f and 4f orbitals is very small, the complexes of actinides and lanthanides will not have a well defined coordination number and geometry for a given metal ion as compared to that of the analogous transition metal ions. The coordination number and geometry around a metal ion will be decided mainly by the charge and size of the metal ion and size of the ligands [12]. Actinide ions display relatively large ionic radii and therefore support higher coordination numbers of 8 to 10 and in rare cases 12 to 15 (Table 1.3), which is not seen in the transition metal ions. The coordination number of fourteen is reported in the adducts of $[Th(BH_4)_4]$ [13] and $[U(BH_4)_4]$[14] and only one complex with fifteen coordination number is reported in $[Th(H_3BNMe_2BH_3)_4]$[15] and the lowest coordination number of three is reported in $[Pu(N\{SiMe_3\}_2)_3]$[16] and $[U(N\{SiMe_3\}_2)_3]$[17].

Table 1.3: Coordination number and geometry of actinides complexes

C. N	Coordination geometries	Complex
3	Pyramidal	$[U(N\{SiMe_3\}_2)_3]$[17]
4	Tetrahedral	$U(O\text{-}2,6\text{-}{}^tBu_2C_6H_3)_4$ [18]
5	Distorted trigonal Pyramidal	$[U(NEt_2)_4]_2$[19] where Et = Ethyl
6	Octahedral	$[MO_2X_2L_2]$ (M = U, Np, Pu), $[MX_4L_2]$ [20] where X = Halide ion
7	Pentagonal bipyramidal	$[MO_2(\beta\text{-diketonate})_2.L]$ (M = U, Np, Pu) [21]
8	Cubic	MO_2 (M = Th, U, Np, Pu) [22]
8	Square antiprism	ThI_4[23]
8	Hexagonal bipyramidal	$[MO_2(NO_3)_2L_2]$,$[MO_2(OAc)_2.L_2]$ (M = U, Np, Pu) [24]
8	Bicapped trigonal prism	$PuBr_3$ [25]
9	Tricapped trigonal Prism	$[Pu(H_2O)_9][(CF_3SO_3)_3]$[26], $[Th(TTA)_4.TOPO]$[27] where TTA = Trifluorotheonoylacetonate and TOPO = Tri octyl phosphine oxide
9	Monocapped square antiprism	$[(DMF)Th(Tropolonate)_4]$[28] where DMF = Dimethylformamide
10	Bicapped square antiprism	$K_4[Th(C_2O_4)_4]$[29]
10	Dodecahedron	$[Th(NO_3)_4.(OPPh_3)_2]$[30]
11	All-capped trigonal prism	$[Th(NO_3)_4.5H_2O]$ [31]
12	Icosahedron	$[M(NO_3)_6]^{2-}$ (M = Th, Pu)[32]
14	Bicapped hexagonal antiprism	$[Th(BH_4)_4]$ [13], $[U(BH_4)_4.2THF]$[14] where THF = Tetrahydrofuran
15	-----	$[Th(H_3BNMe_2BH_3)_4]$[15]

L = H_2O, OPR_3 (R=alkyl), Amides

The low probability of the 4f electrons existing at the outer region of the ion permits very little (practically zero) effective overlap between the orbital of a lanthanide ion and any binding ligand. Thus lanthanide complexes typically have no covalent character and are not influenced by orbital geometries. So, the geometry around the metal centre is purely dictated by the size of the metal ion and the nature of the ligands. Complexes are held together by weaker electrostatic forces and thus the ligands alone dictate the symmetry and coordination of complexes. Steric factors therefore dominate, with coordinative saturation of the metal being balanced against inter-ligand repulsion. As there is no energetic reason to be locked into a single geometry, rapid intra-molecular and inter-molecular ligand exchange will take place in solution, which typically results in complexes which will rapidly fluctuate between all possible configurations in solution. The coordination numbers in most of the lanthanide complexes vary between 8 to 12 and very often 8 to 10 (Table 1.4). The highest coordination number of 12 is reported in many complexes of the type $[Ln(NO_3)_6]^{3-}$ and the lowest coordination number of 3 is reported in $[Ln\{N(SiMe_2)_2\}_3]$.

Table 1.4: Coordination number and geometry of lanthanide complexes

C. N	Coordination geometries	Complex
3	Pyramidal	$[Ln\{N(SiMe_3)_2\}_3]$[33]
4	Distorted Tetrahedral	$[(Me_3Si)_2N]_3Ln(\mu\text{-}Cl)Li(THF)_3$ [34]
5	Distorted trigonal Pyramidal	$(Piso)_2CeCl$ (1, Piso = [*t*BuC(NAr)$_2$]–, Ar = C_6H_2*i*Pr_2–2,6)[35]
6	Octahedral and trigonal prism	$Ln(tpip)_3$ (tpip = tetraphenylimidophosphinate)[36]
7	Monocapped trigonal prism	$[Ln(dbm)_3H_2O]$ (Ln = Sm, Er and Pr; dbm = dibenzoylmethane)[37]
8	Square antiprism, bicapped	$Ln(OO)_3.L$ (where OO = diketonate and

	trigonal prism	L=bidentate donor)[38]
9	Tricapped trigonal Prism	$[Ln(pcam)_3](CF_3SO_3)_3$ (pcam = pyridine-2,6-dicarboxamide) [39]
9	Monocapped square antiprism	$[LnL1(H_2O)](CF_3SO_3)_3\cdot 3H_2O]$ (L1= tetraamide DOTA)[40]
10	Bicapped square antiprism	$[Pr(NO_3)_3.L]$ (1), where L = N,N′-bis[1-(pyridin-2-yl)ethylidene]ethane-1,2-diamine [41]
11	All-capped trigonal prism	$[bpeH]^+[La(NO_3)_4(OH_2)(bpe)]^-$, where bpe = 1,2-bis(4-pyridyl)ethane [42]
12	Icosahedron	$[Sm(Tp^{Py})_2][BPh_4]$, where Tp^{py} = tris[3-(2-pyridyl)pyrazolyl]hydroborate)[43]

1.4 Coordination chemistry of actinides ions with ligands relevant to solvent extraction

Due to very small crystal field effect on the f-orbitals, the coordination number in f-block metal ions is governed by the size and charge of the metal ions. Coordination chemistry of lanthanides and actinide ions was of interest as it pertained to extraction of these ions from the aqueous medium. Classically, actinide-ligand complex formation in organic solvents is of direct importance to understanding and developing new biphasic aqueous-organic actinides separation chemistry, which is cornerstone of existing reprocessing schemes. Actinide organometallic chemistry is of importance from the point of view of answering the fundamental questions related to bonding, extent of covalency and electronic structure[44]. Establishing a more profound and detailed comprehension of basic bonding principles, trends, and electronic structure changes across the actinide series underpins the ability to manipulate and accurately model the behavior of all the relevant actinides in the nuclear fuel cycle and the geosphere. Moreover, many research papers have indicated the small molecule activation and very different reactivity modes for actinide organometallic complexes [45]. The most stable oxidation state of uranium is +6 and it exists in the form of uranyl (UO_2^{2+}) at ambient conditions. Uranyl nitrate exists as uranyl nitrate hexahydate $UO_2(NO_3)_2.6H_2O$ in the solid state and is the most important precursor for studying the coordination chemistry of uranyl with ligands which have potential for the solvent extraction from spent nuclear fuel. The four molecules are lattice water and only two water molecules are bonded to the uranium center in the primary coordination sphere. Four oxygens from two nitrate molecules are cordinated to the uranium froming a hexagonal bipyramidal structure as shown in figure 1.1 [46].

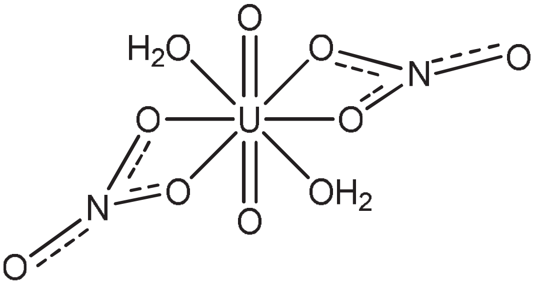

Figure 1.1: Structure for the uranyl nitrate dihydrate

The coordination chemistry of the uranyl ion is of utmost importance in the nuclear reprocessing industry. As actinides are hard Lewis acids, their coordination chemistry mostly deals with hard donor ligands like oxygen. Phosphine oxides and phosphonates are continuing to attract a great deal of increased attention because of their relevance in actinide separation in nuclear fuel reprocessing such as in the PUREX process (Plutonium Uranium Redox Extraction)[47]. Various types of neutral extractants having different donor groups have been studied and they were classified according to the number of donor centers present in the molecule, such as mono-functional, bi-functional, tri-functional etc. The coordination, extraction and structural properties of these extractants are completely different from each other and giving interesting geometries around the metal ions.

1.4.1 Neutral mono-functional extractants

Alkyl phosphate based tributyl phosphate (TBP) ligand, known as the workhorse for the nuclear reprocessing industry, is a monofunctional extractant which is widely used at the industrial scale in the PUREX process[48]. In PUREX process, the spent fuel in ~ 3M HNO_3 is extracted into an organic layer (dodecane) with TBP. The Pu(IV) and UO_2(VI) metal ions are extracted into oraganic phase and rest of the fission products remain in the aqueous stream Many other monofunctional analogues of phosphates like substituted amide[49], phosphine oxide [50], suphoxide[51] and *N*-oxide[52] derivatives have been investigated for the extraction of actinides form spent nuclear fuel. The extraction studies of actinides with monofunctional ligand systems clearly show that solvation adducts are formed by replacing water molecules from the inner coordination sphere. In all these cases, extraction mechanism could be expressed as:

$[MO_2(NO_3)_2.\ 2H_2O] + 2L \rightarrow [MO_2(NO_3)_2.\ 2L] + 2H_2O$ (M = U , Np or Pu)………(1.1)

$[M(NO_3)_4.nH_2O] + 2L \rightarrow [M(NO_3)_4.2L] + nH_2O$………(1.2)

(M = Th , U or Pu, n = 2 for Pu or U, n = 3 for Th and L = monofuntional ligands)

The structural studies of these complexes clearly shows the adduct formation as in $UO_2(NO_3)_2.2TIBP$ [53] (TIBP = Tri *iso*-butyl phosphate), $UO_2(NO_3)_2.2NBP$ (NBP=N-n-butyl-2-pyrrolidone) [54], etc. In all the monofunctional neutral oxygen donor ligand systems, hexagonal bipyramidal coordination geometries around uranium are observed as shown in figure 1.2.

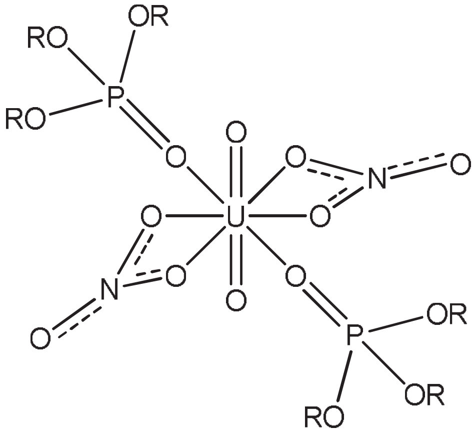

Figure 1.2: Coordination geometry around uranium in $UO_2(NO_3)_2.2TIBP$ (R= ^{i}butyl)

The strength of the metal ligand bonding can be predicted by determining the U-O (ligand) bond distances. As in the case of isobutyramide type ligands which have selectivity towards uranyl(VI) over tetravalent actinides (Th(IV), Pu(IV))[55]. The short U-O (ligand) distance (in the range of 2.35 Å - 2.42 Å) is a signature of strong binding interactions of the ligand to the uranyl(VI) centre [56]. It has been shown that the shorter this distance, the more will be the selectivity of uranyl(VI) over tetravalent actinides. The structures for the tetravalent nitrate complexes $[M(NO_3)_4(OPPh_3)_2]$ (M= Th , U)[57] show that the metal(VI) ion is surrounded by four nitrate and two phosphine oxide groups giving a coordination number of ten with dodecahedral geometry. Similar coordination geometries have been observed for other tetravalent nitrate-neutral ligand complexes.

1.4.2 Neutral bi and tri- functional extractants

Bi-functional extractants, such as carbamoyl methyl phosphonates (CMP), carbamoyl methyl phosphine oxides (CMPO), malonamides and bis(diaklyl phosphine oxide) methane and tri-functional ligands such as tetraalkyl diglycolamides have shown excellent extraction properties for the trivalent actinides in addition to that of tetra and hexavalent actinide ions [49b, 57a, 58]. The proposed complexes responsible for the extraction process were prepared by the reaction of the respective metal nitrates with these ligands in a stoichiometric ratio. The structures of complexes $[UO_2(NO_3)_2.CMPO]^{59}$ (Fig.1.3) $[UO_2(NO_3)_2CMP]$ [60], $[UO_2(NO_3)_2$. Malonamide$]^{58a}$ and $[UO_2(NO_3)_2$.(bis-phosphine oxide)] [61] show that the uranyl group is bonded to two nitrates and one neutral bi-functional ligand to give a hexagonal bi-pyramidal geometry.

The solid state structure for the tetravalent nitrate ion complex $[Th(NO_3)_4(CMP)_2]^{62}$ shows that the Th (IV) ion is surrounded by four nitrates and two CMP ligands in a icosahedron geometry. Both the nitrate and CMP groups act as bidentate chelating ligands to give a coordination number of twelve. The structure of the uranyl(VI) nitrate diglycolamide complex (Fig. 1.4) [58d, 63] shows that the uranyl group is bonded to two nitrate groups and one diglycolamide ligand. The diglycolamide ligand acts as tridentate chelating ligand and bonds through both the carbamoyl and ethereal oxygen atoms to the uranyl group.

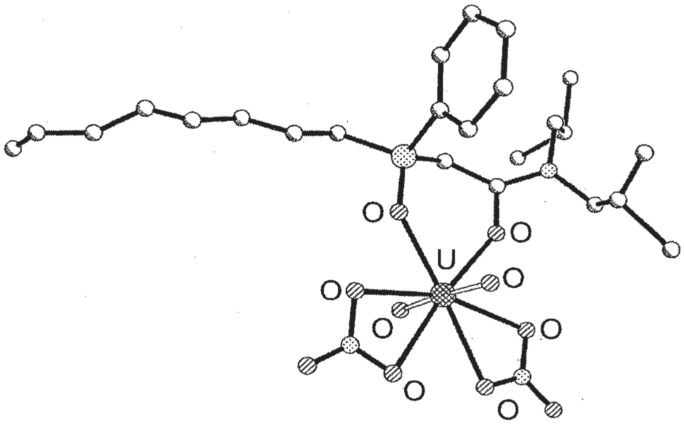

Figure 1.3: Structure of $[UO_2(NO_3)_2.CMPO]^{59}$

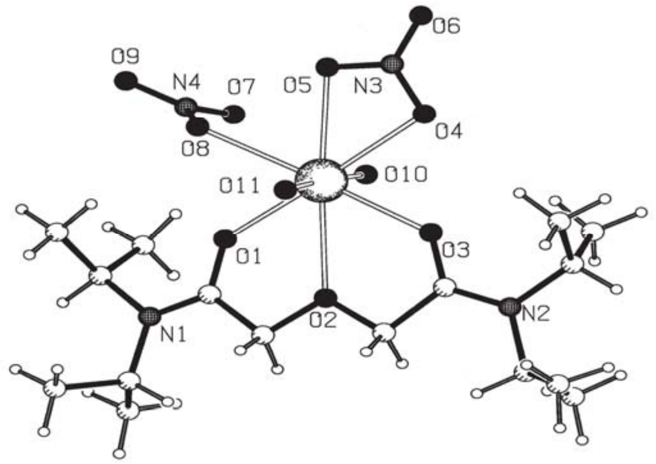

Figure 1.4: Structure of $[UO_2(NO_3)_2 L]$ (L = diglycolamide) [58d]

The structure of a symmetrical neptunyl (V) - diglycolamide compound is also reported and shows that the $[NpO_2]^+$ group is bonded to two of the diglycolamide ligands in a symmetrical fashion to give hexagonal bi-pyramidal geometry around the metal ion [64]. The positive charge on the complex is satisfied by the non-coordinating counter ion ClO_4^-. The tri-functional soft nitrogen containing ligands show better separation factors (S.F. value of Am(III) over Eu (III) upto 400) for the trivalent actinides over those of trivalent lanthanides[65].

1.4.3 Multiple neutral oxygen donor complexes: Crown ether complexes

The crown ethers are a very important class of extractants for the separation of actinide ions from their mixture. The nature of the complexes formed between the crown ether and metal ion is mainly decided by the experimental conditions employed during separation. The crown ethers form inclusion compounds (Fig. 1.5) with metal ions in the presence of non coordinating anions such as: ClO_4^- and $CF_3SO_3^-$[66]. The 18-crown-6 ligand selectively extracts NpO_2^+ or UO_2^{2+} from a perchloric acid medium and the structure of the isolated compound revealed that the NpO_2^+ or UO_2^{2+} ion is selectively encapsulated in the cavity of the crown ether. However, in the presence of coordinating anions such as: nitrate, sulphate etc, they form second sphere coordination complexes, in which the crown ether is hydrogen bonded to the water molecules, which are in the primary coordination sphere.[67]

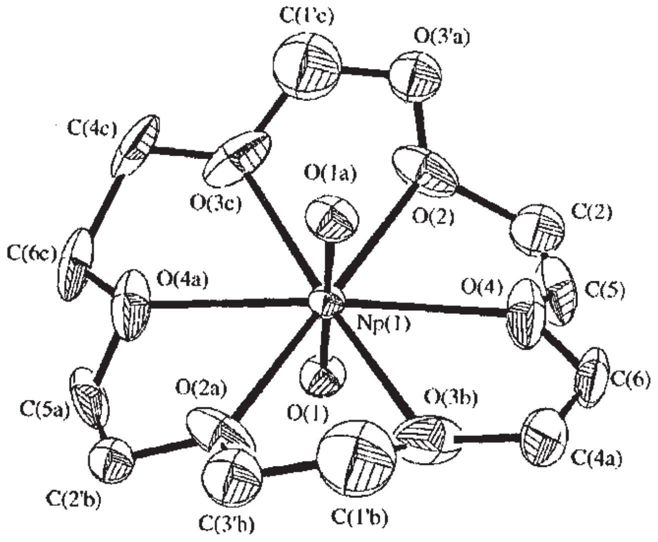

Figure 1.5: Structure of $[NpO_2(18C6)] (ClO_4^-)$[66]

1.4.4 Complexes of actinide ions with β-diketonates

A quite large number of acidic extractants were employed for the separation of actinide ions from acidic media and one of the well studied extractants are β-diketones[68]. These extractants possess acidic protons and can be easily dissociated to form complexes with the metal ions. These complexes are organic soluble and can be extracted in to an organic phase. Complexes responsible for the extraction in many of the cases were isolated in the solid state and characterized by using well known spectroscopic techniques, like IR spectroscopy and, ^1H and ^{19}F NMR spectroscopy. The structure of $[UO_2(TTA)_2.2H_2O]$ (TTA = theonoyl trifluroacetate)[69] (Fig. 1.6) shows that the uranyl(VI) group is bonded to two of the TTA units and one water molecule in the primary coordination sphere. The coordination number and geometry around the uranium (VI) ion is seven and pentagonal bi-pyramidal. A second water molecule is present in the second coordination sphere and hydrogen bonded to the first water molecule. The structures for the tetravalent metal β-diketonate complexes [M(OO)$_4$] (M = Th, U or Pu) (OO = β-diketonate anion) show that the metal ion is surrounded by four β-diketonate anions in a square anti-prismatic coordination geometry [70].

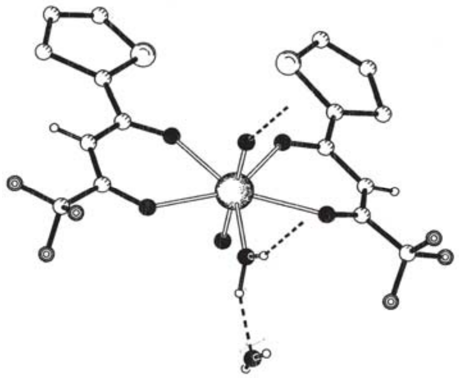

Figure 1.6: The Structure of [UO$_2$(TTA)$_2$.2H$_2$O] (dashed line means hydrogen bonding)

1.4.5 Synergistic extraction of actinide ions using mixtures of β-diketones and neutral extractants

The synergistic extraction of actinide ions from the acid media by using the mixture of β-diketones and neutral extractants is a well established procedure for the separation of tetravalent as well as hexavalent actinides [71]. The increase in extraction was due to the formation of more organic soluble metal complex with both the β-diketones and neutral extractants. A large number of complexes of actinide ions with the combination of β-diketonates and neutral extractants have been prepared in the solid state and characterized.

The structures of all complexes shows that the uranyl group is bonded to two of the β-diketonate anions and one neutral extractant (Fig 1.7) to give a pentagonal bi-pyramidal geometry around the metal ion. [21, 72]

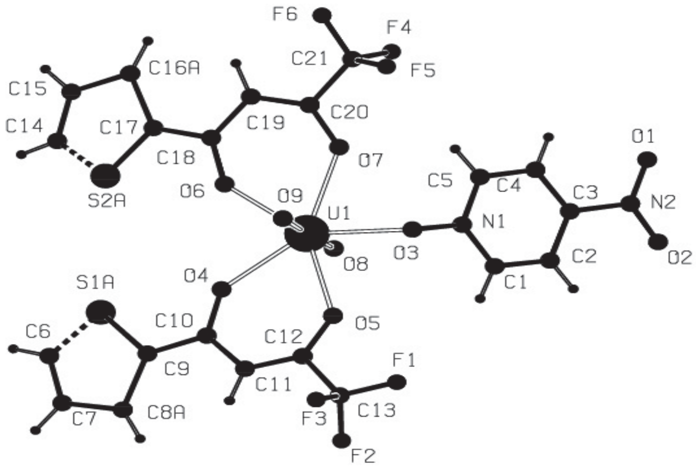

Figure 1.7: Structure of [$UO_2(TTA)_2$ p-NO_2-C_5H_5NO] (dashed line means disordering)

The structure of [Th(TTA)$_4$.TOPO][27] complex shows that the Th(IV) ion is surrounded by four TTA anions and one TOPO molecule in a tri-capped trigonal prismatic geometry. The β-diketonate acts as a bidentate chelating ligand and the TOPO acts as a monodentate ligand. Similar types of structures have been proposed for the other M (IV) ion –β-diketonate-neutral ligand complexes.

1.5 Coordination chemistry of lanthanide ions with ligands relevent to solvent extraction

Lanthanide nitrates are highly soluble in polar solvents such as water, alcohols, esters or nitriles. Lanthanide nitrates usually have the formula [$RE(NO_3)_3$ nH_2O] , where n = 6 for the lighter rare earth nitrates (lanthanum to neodymium) and n = 5 for the heavier rare earth nitrate (europium to lutetium) and this is caused by lanthanide contraction. In lanthanide nitrates, the nitrate groups usually behaves as a bidentate chelating ligand similar to reported in [$Ce(NO_3)_3(C_5H_7N_2CH_2CONBu_2)_2$].

1.5.1 Monodentate neutral ligand lanthanide nitrate compounds

Lanthanide nitrates form very weak complexes with monoamides, sulfoxides and phosphates [73]. In general, these ligands show very poor extractions for lanthanides from HNO_3 medium due to poor complexation of these ligands with lanthanide ions and lability of the ligand in the solution. However, the phosphine oxides show appreciable extraction for these ions from the nitric acid medium and a larger number of phosphine oxide compounds have been isolated in the solid state and structurally characterized. The phosphine oxides form either $[Ln(NO_3)_3(OPR_3)_3]$ or $[Ln(NO_3)_3(OPR_3)_4]$ (Fig. 1.8) types of complexes with coordination numbers that vary between 9 and 10.[74]

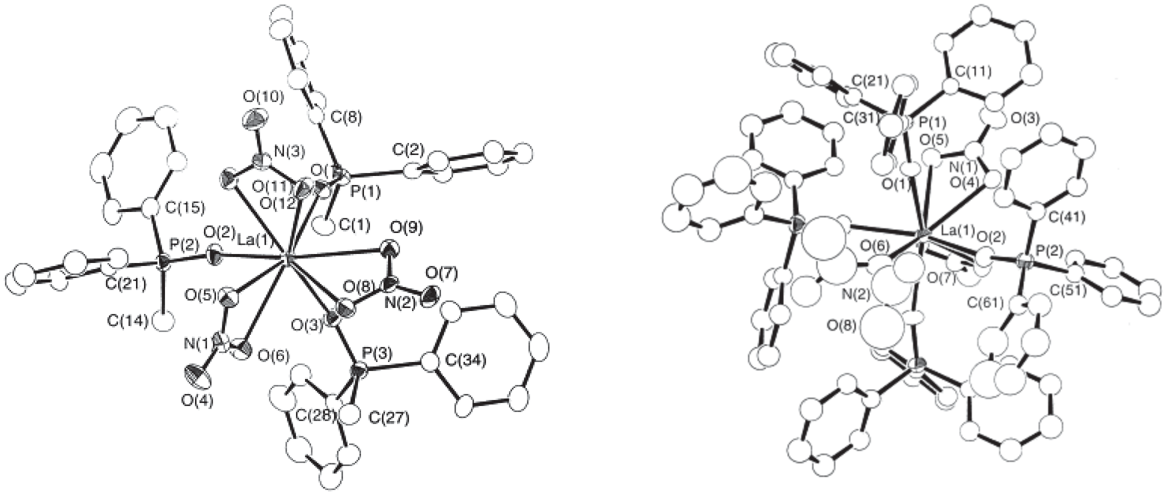

(a)

(b)

Figure 1.8: Structure of $[La(Ph_2MePO)_3(NO_3)_3]$ (a) and $[La(Ph_3PO)_4(NO_3)_3]$ (b)

1.5.2 Bidentate neutral ligand lanthanide nitrate compounds

Many bi-functional ligands such as carbamoyl methyl phosphonates, carbamoyl methyl phosphine oxides and carbamoyl methyl sulfoxide ligands show excellent extraction for lanthanide and actinide ions from a nitric acid medium [24, 75]. A number of compounds have been isolated in the solid state and have been structurally characterized for understanding the coordination chemistry of these ligands molecules which are important for the extraction point of view. All these ligands form 2:1 complexes with lanthanide nitrates with the formula $[Ln(NO_3)_3.2L]$ (where L = malonamides, carbamoyl methyl phosphonates, carbamoyl methyl phosphine oxides, carbamoyl methyl sulfoxide) in the solid state. In all cases, the ligands act as bidentate chelating ligands and bond through both the donor groups (Fig. 1.9). The coordination numbers and geometries are 10 and bi-capped square antiprism, respectively.

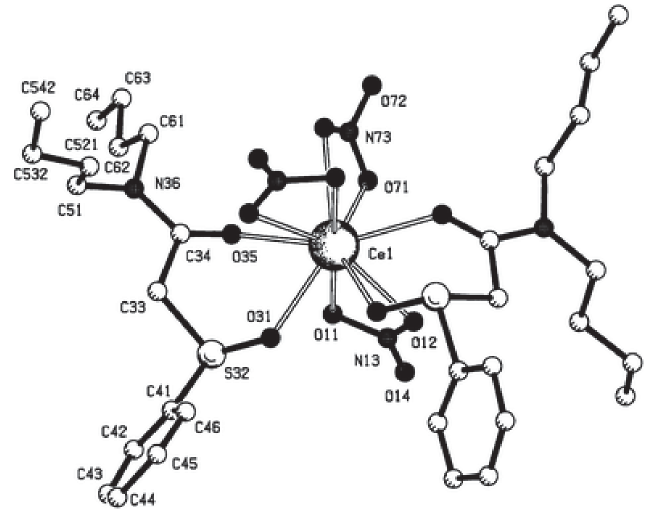

Figure 1.9: Structure of $[Ce\ (NO_3)_3(PhSOCH_2CON^iBu_2)_2]$

1.5.3 Tridentate neutral ligand lanthanide nitrate compounds

In recent years, tri-functional chelating ligands show excellent extractions for trivalent lanthanides and actinides from a nitric acid medium [63]. Among the trifunctional oxygen donor ligands, the most studied ligand systems are diglycolamide based ligands for trivalent actinide and lanthanide separations. For some of the cases, the lanthanide complexes have been isolated and structurally characterized. In all cases, the ligand acts as a tridentate chelating ligand and is bonded through both the carbamoyl and ethereal oxygen atoms to the metal centre. These ligands form 3:1 complexes of the formula $[LnL_3]^{3+}$ with lanthanide nitrates [58d, 76], in which the anions are outside the coordination sphere as shown in figure 1.9.

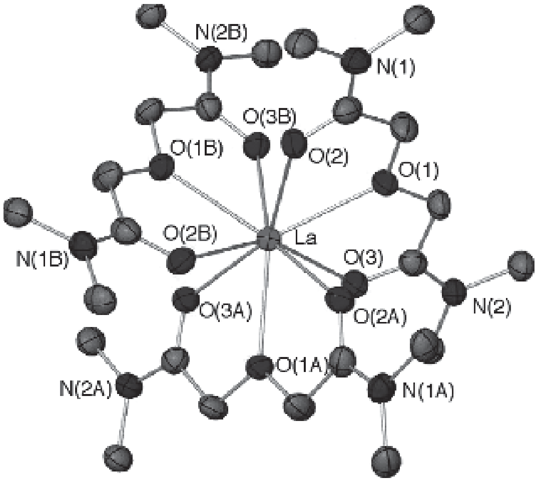

Figure 1.10: Structure of [LaL$_3$][La(NO$_3$)$_6$] where L=Diglycolamide

Tri-functional ligands containing a nitrogen donor centre also show good extraction for trivalent actinide ions over lanthanide ions and for some cases, the species responsible for the separation have been structurally characterized. In most of the cases, the ligand acts as a tridentate ligand and bonds through all nitrogen atoms to metal centre (Fig .1.11).[77]

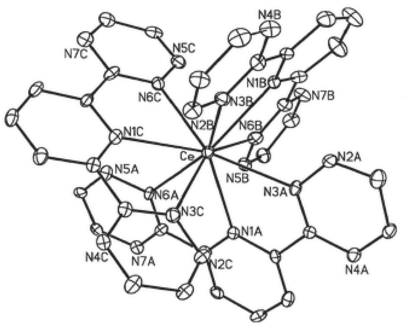

Figure 1.11: Structure of [Ce(Mebtp)$_3$]$^{3+}$ (Mebtp = 2,6-bis(5,6-dimethyl-1,2,4-triazin-3-yl)pyridine

1.5.4 Multiple neutral oxygen donor complexes: Crown ether complexes

Lanthanides do not form crown ether inclusion complexes readily in aqueous solution, due to the considerable hydration energy of the Ln^{3+} ion. These complexes are, however, readily synthesized by operating in non-aqueous solvents. Because many studies have been made with lanthanide nitrate complexes, coordination numbers are often high. Thus 12-coordination is found in $[La(NO_3)_3(18\text{-crown-}6)]$[78], 11-coordinate in $[La(NO_3)_3(15\text{-crown-}5)]$[79], and 10-coordinate in $[La(NO_3)_3(12\text{-crown-}4)]$[80]. Lanthanide chloride complexes often include water in the co-ordination sphere; thus the complex with the formula $[ErCl_3(12\text{-crown-}4).5H_2O]$ actually contains 9-coordinate $[Er(12\text{-crown-}4)(H_2O)_5]^{3+}$ cations [81] whilst $[NdCl_3(18\text{-crown-}6).4H_2O]$ is $[Nd(18\text{-crown-}6)Cl(H_2O)_2]Cl_2.2H_2O$. On reaction in MeCN/MeOH, 15-crown-5 reacts with neodymium chloride to form complexes with $[Nd(OH_2)_9]^{3+}$ and $[NdCl_2(OH_2)_6]^{+}$ ions hydrogen-bonded to the crown ether without any direct Nd–crown ether bonds[82]. By carrying out electrocrystallization, the water-free [Nd(15-crown-5)C_{l3}] species is obtained [83]. Lanthanides also make complexes with noncyclic linear polyethers such as glyme and other macrocycles like calixarenes [84].

1.5.5 Compounds of lanthanides with β-Diketonates

These are an important class of compounds with a general formula $[Ln(R^1COCHCO.R^2)_3]$. The acetylacetonates (acac), $Ln(acac)_3$ ($R^1 = R^2 = CH_3$) can readily be made from a lanthanide salt and acetylactone by adding sodium hydroxide:

$LnX_3 + 3\ Na(acac) \rightarrow Ln(acac)_3 + 3\ NaX$...........(1.3)

They crystallize as hydrates like $[Ln(acac)_3.(H_2O)_2]$ (Ln = La to Ho and Y) and $[Yb(acac)_3.(H_2O)]$. These compounds are difficult to dehydrate, even in vacuum as they decompose on heating, and on dehydration at room temperature tend to oligomerize to nonvolatile materials. They form Lewis base adducts like $[Ln(acac)_3.(Ph_3PO)]$ and $[Ln(acac)_3.(phen)]$ (7- and 8-coordinate, respectively). Using bulkier alkyl groups (for example R^1 and $R^2 = CMe_3$) affords more congested diketonate complexes like $[Ln(Me_3.CO.CH.CO.CMe_3)_3]$ that are more tractable, monomers in solution and sublime in vacuum at 100–200°C. In the solid state, they are dimers for Ln = La to Dy (CN 7) and monomers for Dy to Lu (CN 6) and have trigonal prismatic coordination. They tend to hydrate readily, forming adducts [e.g. capped trigonal prismatic $[Ln(DBM)_3(H_2O)]$][85].

Complexes of fluorinated diketones (R^1 $=CF_3$, R^2 $=CH_3$; R^1 $=R^2$ $=CF_3$; R^1 = C_4H_3S, R^2 = CF_3; R^1 = $CF_3CF_2CF_2$, R^2 = CMe_3) are also important. Again, the initial complexes obtained in synthesis are hydrates that can be dehydrated in vacuo. 2-Thenoyltrifluoroacetone complexes $[Ln(TTA)_3.2H_2O]$ are important in solvent extraction. Addition of phosphine oxides gives a synergistic improvement in extraction owing to the formation of phosphine oxide complexes.

1.6 Recent advances in separation of actinides from lanthanides from nuclear waste

The most remarkable advances in the industrial solvent extraction process are due to the requirement imposed by the nuclear industry. In fact, solvent extraction technology has been proved to be an efficient technique for this very hard task. The PUREX process is a well established process for the separation of uranium and plutonium from the spent nuclear fuel. The resultant high level waste contains very high activity and due to the presence of transuranics (having half lives thousands of years) means this waste has to be stored for an indefinite time period. Immense efforts have been made recently to develop advanced separation processes in order to maximize fuel resources and reduce the impact of nuclear waste while providing a proliferation-resistant fuel cycle (i.e., no pure plutonium is isolated)[86]. This is a part of the "Partitioning and Transmutation" strategy, where it is proposed that all of the actinides in spent nuclear fuel (SNF), including the minor actinides, can be separated and recycled as nuclear fuel. An alternate option is to "burn" the separated actinides, which will also result in conversion to short-lived fission product nuclides but without nuclear energy production for public consumption. This provides the added benefit of converting most of the long lived actinides in SNF to shorter-lived fission product nuclides compared to current spent fuel management options. As a result, the "Partitioning and Transmutation" strategy can significantly reduce the time it takes for SNF to decay to radioactivity levels of natural uranium and therefore the necessary design lifetime of any nuclear waste repository. [75a, 77a, 87]

One of the major separation challenges that need to be overcome for this strategy to be successful is the separation of minor actinides (americium and curium) from the lanthanide fission products. This is because the high neutron absorption cross sections of some of the lanthanide ions present in SNF both decrease the flux in a reactor and create more activation products, thereby making transmutation a less attractive option if the lanthanides cannot be separated from the actinides. Achieving this separation is extremely difficult because of the chemical similarities between americium, curium, and the lanthanides, which all most commonly exist in the +3 oxidation state in solution[88]. Consequently, organic molecules that can selectively extract actinides, in particular Am^{3+} and Cm^{3+}, over the Ln^{3+} ions are of great interest, as is evident by the number of different ligand systems and processes that have been developed by various groups in the field of partitioning [77a, 86b, 88-89]. Examples include the TALSPEAK (Trivalent Actinide Lanthanide Separation by Phosphorus reagent Extraction from Aqueous Komplexation) process [90], which uses diethylene-triamine-pentaacetic acid (DTPA) in a lactic acid solution to hold back Am^{3+} and Cm^{3+} in the aqueous phase while the lanthanide ions are extracted into the organic phase containing di(2-ethylhexyl)phosphoric acid, and the TRUEX (Trans Uranic Extraction) process[91], where the addition of *N*,*N*-diisobutyl carboylmethyl phosphine oxide to the organic phase in the core PUREX process allows Am^{3+} and Cm^{3+} to be extracted alongside UO_2^{2+} and Pu^{4+}, leaving the lanthanide ions and other fission products in the aqueous phase .

The SANEX (Selective Actinide EXtraction) solvent extraction process[92] is designed to separate the minor actinides from the lanthanide fission products in HLW (high level waste) and fission product separation (except the lanthanides) by DIAMEX (Diamide Extraction) using bifunctional amide ligands [93]. The promising molecules proposed very early for the selective extraction of An^{3+} (where, An = Actinides) over Ln^{3+} (Ln = Lanthanides) in a SANEX process were the tridentate 2,6-bis(5,6-dialkyl-1,2,4- triazin-3-yl)pyridines (BTPs) [94]. However, many of these extractant molecules have not been found suitable for the actinide lanthanide partitioning in plant scale extraction procedure due to the poor solubility, slow extraction kinetics and ineffective back extraction.The next triazinyl based ligand system for An/Ln separations, which was superior to BTPs, was 6,6'-bis-(5,5,8,8-tetramethyl-5,6,7,8-tetramethyl-5,6,7,8-tetrahydro-1,2,4-benzotriazin-3-yl)-2,2'-bipyridine ($CyMe_4$-BTBP). This extractant molecule has high separation factor (~150) for Am^{3+} over Eu^{3+}[89b, 92] and tested for real feed.solutions Here, it is to be noted that recoveries for minor actinides were impressive (>99.9%) but radiolytic stability of the ligand was poor. Moreover, kinetics was not improved as compared to BTPs[95]. To improve the kinetics of extraction, a conformationally rigid tetradentate ligand 2,9-bis(5,5,8,8-tetramethyl-5,6,7,8-tetrahydro-1,2,4-benzotriazin-3-yl)-1,10-phenanthroline ($CyMe_4$-BTPhen) was proposed [65]. This rigid ligand shows very high separation factors for Am^{3+} over Eu^{3+} (up to 400), with significantly faster kinetics of extraction compared to those found for $CyMe_4$-BTBP,. GANEX (Group Actinide Extraction) is a new concept for the recovery of actinides from Spent Nuclear Fuel. GANEX process consists of two cycles. The first cycle involves separation of uranium from spent fuel and in the second cycle remaining actinides are recovered from the fission products. GANEX process is devised for the separation of actinides where plutonium concentration during portioning process are high as compared to those found in current fuel reprocessing cycles.[96]. It will be difficult for a single extractant to achieve separation of group actinides with wide range of oxidation states in spent fuel Hence, different set of combination of extractants are proposed for the second cycle of GANEX process [97]. There is a good number of potential combination of different extractant like N,N,N′,N′-tetra-octyl diglycolamide (TODGA; used in DIAMEX) with DMDOHEMA, TODGA with TBP, and CyMe4-BTBP with TBP which are proposed for group extraction of actinides from spent fuel. The structure of the different ligand system is shown in Fig. 1.12.

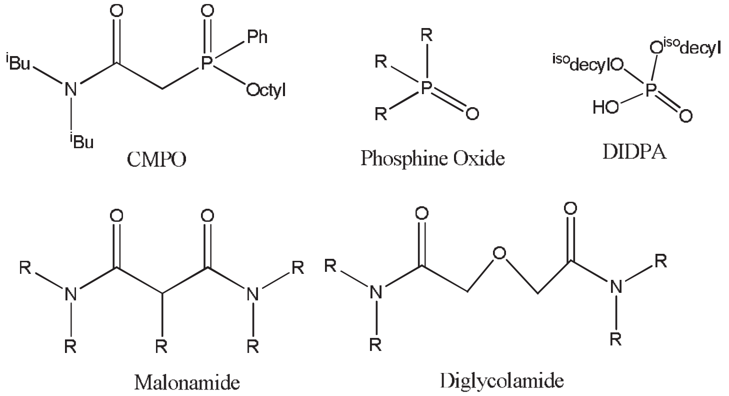

Figure 1.12: Structure of important ligand proposed for extraction of actinides

1.7 Scope of the present work

The above introduction on the coordination chemistry aspect of lanthanides and actinides gives a glimpses of the research efforts pertaining to the separation of these metal ions from spent nuclear fuel. Still, there are lot of active areas of research on the development of new ligand systems to understand the functionality of the ligand system under the solvent extraction conditions. The coordination chemistry aspect of the newly synthesized ligand systems is definitely going to play a major role in the selectivity as well as extractability of the metal ion from the aqueous phase. Many monofunctional, bifunctional and trifunctional molecules are reported so far for the separation process. Specially, bifunctional and trifunctional ligand systems are explored extensively for the separation of trivalent actinides and lanthanides. The uranyl (VI) coordination chemistry of monofunctional ligands is quite well explored. Bifunctional chelating ligand system with relevance to separations have mostly dealt with tri, tetra and hexavalent lanthanides and actinides.. Here, in this thesis we explored the chemistry of newly synthesized bifunctional neutral oxygen donor ligand systems for the separation and coordination chemistry of uranyl(VI), plutonium(IV) as well as lanthanide(III) ions. All the ligands and complexes prepared during the present investigation have been characterized by elemental analysis, IR and NMR (^{1}H and ^{31}P) spectroscopy. Selected complexes whose crystals could be grown were structurally characterized by single crystal XRD. For clarity the present thesis is subdivided as follows:

Chapter 2: Synthesis, coordination and structural studies of dithiodiglycolamide based ligands with the uranyl(VI) ion.

Chapter 3: Synthesis, coordination, structural and extraction studies of α-hydroxy acetamide based ligands with lanthanide(III), plutonium(IV) and uranyl(VI) ions.

Chapter 4: Synthesis, coordination, structural and photoluminescence studies of diphenyl-(2-pyridyl)phosphine oxide and diphenyl-(2-pyridyl-*N*-oxide) phosphine oxide) ligands with lanthanide(III) and uranyl(VI) ions.

Chapter 5: Synthesis, coordination and structural studies of (*N*,*N*-dialkyl carbamoyl methyl-2-pyridyl-*N*-oxide) sulfide ligands with the uranyl(VI) ion.

Chapter -2

Synthesis, coordination and structural studies of dithiodiglycolamide based ligands with the uranyl(VI) ion

2.1 Introduction

The coordination chemistry of uranium with neutral oxygen donor ligands is well established and matured field for the basic understanding of the process of extraction of uranium from the nuclear waste. The PUREX process, the workhorse of nuclear fuel recycling process, utilizes a neutral oxide donor namely, tributyl phosphate (TBP), as an extractant for plutonium and uranium from the spent fuel [98]. There are several disadvantages with TBP, such as third phase formation and incomplete incineration due to the phosphate groups. [99]. Thus, a number of alternatives to TBP, containing carbamoyl and other neutral oxygen donor ligands have been studied. Similar to the phosphine oxide functionality, many other hard oxygen donor molecules like amide (C=O) [49c], sulphoxide (S=O) [100] and N-oxide (N-O) [101] donor groups have been utilized for studying the coordination chemistry of the uranyl ion to better understand the extraction mechanisms at the molecular level. A number of bi-functional ligands having hard oxygen donors attracted considerable attention due to attractive f-element separation chemistry. Many ligands like bis(phosphine oxide) [102], diamides [58a, 103] and mixed donor liagnds like carbamoyl methyl phosphine oxide (CMPO) [104], carbamoyl methyl sulfoxide CMSO [24] have been attractive coordination targets for uranyl chemistry to understand the behaviour of these ligand systems in the solvent extraction of f-elements. Most of these ligand systems, which possess good extraction properties, show a bidentate chelating mode with uranyl nitrate as shown in Figure 2.1. Diamides like malonamides have shown very promising behaviour in terms of solvent extraction in the DIAMEX process [93]. It is reported that the nature of the spacer groups between the two functional groups play an important role in the solid state structure of the compounds formed. For example, in bi-functional amide ($R_2NCO(CH_2)_nCONR_2$, R = alkyl) compounds of uranyl nitrate, the number of CH_2 groups bridging the two amide groups decides the nature of complex.

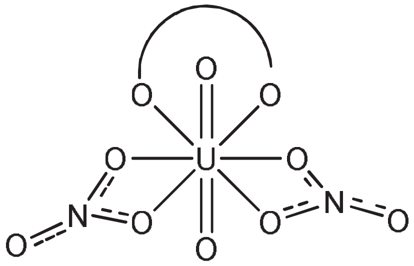

Where  – bifunctional oxygen donor neutral ligand

Figure 2.1: Uranyl nitrate coordination with a bifunctional oxygen donor neutral ligand

formed in the solid state [105] . When n = 1 or 2, the ligands always act as chelating ligand, where n = 3 or 4 they act as either chelating or bridging ligands and in cases where n = 5 or 6, they act exclusively as bridging ligands. The theoretical studies show that the modes of bonding for these ligands are energetically controlled. The compounds of uranyl nitrate with thio-diglycolamide[106] , bis(carbamoyl methyl) sulfoxide [107] and bis(carbamoyl methyl) sulfone (where n = 3) [108] also show bidentate chelating modes of binding for these ligands. However, the solid state structure of the uranyl nitrate 1, 2-phenylene bis(oxyacetamide) compound [109] shows a bidentate chelating mode of bonding for this ligand in the solid state, even though the carbamoyl groups are separated by a six atom bridge ($CH_2OC_6H_4OCH_2$). This is very much different from the one which is expected for all six atom CH_2 bridging ligand [105] (expected to be a bridging bidentate ligand). By changing the CH_2 groups to oxygen atoms completely changes the complexing properties of these bi-functional ligands in the solid state. The bi-functional dithio-glycolamide based ligands (Scheme 1) show selective extraction for palladium ions from HLLW and it has been proposed that they bond through both the thio-ether and amido groups to the metal centre[110] These ligands have two amide groups, and are expected to show extraction for actinide (VI) and (IV) ions from the nitric acid medium. However, no systematic work on the extraction and complex chemistry of these ligands with actinide ions are reported so far, we report herein the theoretical studies of dithio-glycolamide synthesis, structural studies with uranyl nitrate and extraction studies with U (VI), Pu (IV) and Am (III) ions.

2.2 Experimental

2.2.1 General Considerations: All reagents and solvents were of analytical grades and used as received. IR spectra were recorded as nujol mulls using a JASCO-610 FITR spectrometer. ^{1}H NMR spectra were recorded using a Bruker AMX-300 spectrometer. The chemical shifts (δ) are reported in ppm and coupling constants (J) are reported in hertz. Electrospray ionization mass spectrometric detection of positive ions in CH_2Cl_2 or CH_3COCH_3 were recorded using a MicrOTOF Q-II instrument. The samples were introduced in to the source with the syringe pump. Nitrogen was employed as both the drying and spraying gas with a source temperature of 180° C. The cone voltage was set to 45V, the voltage applied on the capillary was 1162 kV and the sample solution flow rate was 5 μL min^{-1}. Spectra were recorded from m/z of 100 to 1000.

2.2.2 Synthesis of $[(CH_2SCH_2CON\ (^iC_3H_7)_2)_2]$ (L^1): To a methanolic solution (10 mL) of ethylene-1, 2-dithiol (5.5 g, 0.059 mol), a methanolic solution (20 mL) of NaOH (4.7 g, 0.118 mol) was added slowly with stirring. The whole solution was stirred for 30 min. To this solution a solution of *N,N*-di-isopropyl carbamoyl methyl chloride (21 g, 0.118 mmol) in methanol (20 mL) was added slowly. The whole solution was stirred for 3 hours and then treated with 200 mL of 5% HCl solution. The organic layer formed was extracted with $CHCl_3$, dried over Na_2SO_4 and filtered. The solution on evaporation a yielded colorless crystalline solid in 75 % yield. ^{1}H NMR (25 °C, $CDCl_3$): δ = 1.20 (d, 12H, CH_3, ^{i}Pr , J = 6.6 Hz), 1.37 (d, 12H, CH_3, ^{i}Pr, J=6.6 Hz), 2.90 (s, 4H, $-CH_2S-$), 3.33 (s, 4H, $-SCH_2CO-$), 3.35

(m, 2H, CH, ^{i}Pr), 3.96 (m, 2H, CH, ^{i}Pr). IR (cm^{-1}): ν = 1624 (s) (C=O). Analysis (%): Calcd. for $C_{18}H_{36}N_2O_2S_2$: C, 57.4; H, 9.6; N, 7.4; S, 17.0; Found: C, 57.5; H, 9.5; N, 7.4; S, 17.2.

2.2.3 Synthesis of [(CH$_2$SCH$_2$CON (C$_4$H$_9$)$_2$)$_2$] (L^2): This was prepared similarly to $\mathbf{L^1}$ by using ethylene-1, 2-dithiol (5.5 g, 0.059 mol) and *N,N*-di *n*-butyl carbamoyl methyl chloride (24.2 g, 0.118 mol) in 82% yield. ^{1}H NMR (25 °C, $CDCl_3$): δ = 0.92 (m, 12H, CH_3, ^{n}Bu), 1.31 (m, 8H, $NCCCH_2$, ^{n}Bu), 1.53 (m, 8H, $NCCH_2$, ^{n}Bu), 2.92 (s, 4H, $-CH_2S-$), 3.27 (m, 8H, NCH_2 , ^{n}Bu) 3.32 (s, 4H, $-SCH_2CO-$). IR (cm^{-1}): ν =1637 (s) (C=O). Analysis (%): Calcd. for $C_{22}H_{44}N_2O_2S_2$: C, 61.6; H, 10.3; N, 6.5; S, 14.8; Found: C, 61.4; H, 10.4; N, 6.7; S, 14.9.

2.2.4 Synthesis of [(CH$_2$SCH$_2$CON (^{i}C$_4$H$_9$)$_2$)$_2$] (L^3): This was prepared similarly to $\mathbf{L^1}$ in 80% yield by using ethylene-1, 2-dithiol (5.5 g, 0.059 mol) and *N,N'*-di-isobutyl carbamoyl methyl chloride (24.2 g, 0.118 mol) in 80% yield. ^{1}H NMR (25 °C, $CDCl_3$): δ = 0.83 (d, 12H, CH_3 , ^{i}Bu, J = 7.2 Hz), 0.87 (d, 12H, CH_3, ^{i}Bu, J = 7.2 Hz), 1.88 (m, 2H, CH, ^{i}Bu), 1.98 (m, 2H, CH, ^{i}Bu), 2.88 (s, 4H, $-CH_2S-$), 3.08 (d, 4H, NCH_2, ^{i}Bu J = 7.5 Hz), 3.13 (d, 4H, NCH_2, ^{i}Bu, J = 7.5 Hz), 3.317 (s, 4H, $-SCH_2CO-$). IR (cm^{-1}): ν = 1644 (s) (C=O). Analysis (%): Calcd. for $C_{22}H_{44}N_2O_2S_2$: C, 61.6; H, 10.3; N, 6.5; S, 14.8; Found: C, 61.5; H, 10.5; N, 6.6; S, 14.8.

2.2.5 Synthesis of [(CH$_2$SCH$_2$CON (C$_8$H$_{17}$)$_2$)$_2$] (L^4): This was prepared similarly to $\mathbf{L^1}$ in 85% yield by using ethylene-1, 2-dithiol (3.4 g, 0.036 mol) and *N,N*-di n-octyl carbamoyl methyl chloride (23 g, 0.72 mol). ^{1}H NMR (25 °C, $CDCl_3$): δ = 0.86 (br, 12H, CH_3, C_8H_{17}), 1.26 (br, 40H, CH_2, C_8H_{17}), 1.52 (m, 8H, NC-CH_2, C_8H_{17}), 2.91 (s, 4H, $-CH_2S-$), 3.23 (m, 8H, NCH_2 , C_8H_{17}), 3.30 (s, 4H, $-SCH_2CO-$). IR (cm^{-1}): ν =1633 (s) (C=O). Analysis (%): Calcd. for $C_{38}H_{76}N_2O_2S_2$: C, 69.5; H, 11.7; N, 4.3; S, 9.8; Found: C, 69.4; H, 11.6; N, 4.2; S, 9.9.

2.2.6 Synthesis of [$C_7H_6(SCH_2CON\ (^iC_4H_9)_2)_2$] ($L^5$): This was prepared similarly to $\mathbf{L^1}$ in 81% yield by using tolyl-3, 4-dithiol (3.04 g, 0.0195 mol) and *N,N*-diisobutyl carbamoyl methyl chloride (8 g, 0.39 mol). ^{1}H NMR (25 °C, $CDCl_3$): $\delta = 0.85$ (m, 24H, CH_3, ^{i}Bu), 1.92 (m, 4H, CH, ^{i}Bu), 2.27 (s, 3H, $-CH_3$, tolyl), 3.13 (m, 8H, NCH_2, ^{i}Bu), , 3.73 (s, 2H, -SCH_2CO-), 3.76 (s, 2H, -SCH_2CO-), 6.97 (m, 1H, tolyl), 7.27 (br, 1H, tolyl), 7.39 (d, 1H, tolyl, J = 8.1 Hz) . IR (cm^{-1}): ν =1652 (s) (C=O). Analysis (%): Calcd. for $C_{27}H_{46}N_2O_2S_2$: C, 65.5; H, 9.4; N, 5.7; S, 13.0; Found: C, 65.4; H, 9.3; N, 5.8; S, 12.9.

2.2.7 Synthesis of [$UO_2(NO_3)_2(CH_2SCH_2CON\ (^iC_3H_7)_2)_2$] (1) : To a solution of $\mathbf{L^1}$ (250 mg, 0.67 mmol) in CH_2Cl_2 (20 mL), solid [$UO_2(NO_3)_2\cdot 6H_2O$] (335 mg, 0.66 mmol) was added and stirred for few minutes until all [$UO_2(NO_3)_2\cdot 6H_2O$] had dissolved to give a clear solution. This solution was filtered and layered with iso-octane. The solution on slow evaporation yielded a yellow crystalline solid, which was filtered, washed with hexane, and dried. Yield : 84 %. ^{1}H NMR (25 °C, CD_3COCD_3): $\delta = 1.55$ (d, 12H, CH_3, ^{i}Pr , J = 6.3 Hz), 1.66 (d, 12H, CH_3, ^{i}Pr , J = 6.3 Hz), 2.96 (s, 4H, -CH_2S-), 3.82 (s, 4H, -SCH_2CO-), 4.03 (m, 2H, -NCH, ^{i}Pr), 4.51 (m, 2H, -NCH**,** ^{i}Pr). IR (cm^{-1}): ν = 1578 (s, C=O). Analysis (%): Calcd. for $C_{22}H_{44}N_4O_{10}S_2U$: C, 28.1; H, 4.7; N, 7.3; S, 8.3; Found: C, 28.0; H, 4.8; N, 7.1; S, 8.5.

2.2.8 Synthesis of [$UO_2(NO_3)_2(CH_2SCH_2CON\ (C_4H_9)_2)_2$] (2): This was prepared similarly to **1** in 85% yield by using $\mathbf{L^2}$ (259 mg, 0.60 mmol) and [$UO_2(NO_3)_2\cdot 6H_2O$] (300 mg, 0.59 mmol). ^{1}H NMR (25 °C, $CDCl_3$): $\delta = 0.80$ (t, 6H, $CH_{3,}$ ^{n}Bu J = 7.4 Hz), 1.07 (t, 6H, $CH_{3,}$ ^{n}Bu J = 7.4 Hz), 1.27 (m, 4H, CH_2, ^{n}Bu), 1.55 (m, 4H, CH_2, ^{n}Bu), 1.81 (m, 4H, CH_2, ^{n}Bu), 1.92 (m, 4H, $CH_{2,}$ ^{n}Bu), 2.97 (s, 4H, -CH_2S-), 3.59 (s, 4H, -SCH_2CO-), 3.60 (t, 4H, NCH_2, ^{n}Bu J = 7.4 Hz), 3.754 (t, 4H, NCH_2, ^{n}Bu J = 7.4 Hz) . IR (cm^{-1}): ν =1600 (s) (C=O). Analysis (%): Calcd. for $C_{22}H_{44}N_4O_{10}S_2U$: C, 32.0; H, 5.4; N, 6.8; S, 7.8; Found: C, 32.1; H, 5.5; N, 6.9; S, 7.7.

2.2.9 Synthesis of $[UO_2(NO_3)_2(CH_2SCH_2CON\ (^iC_4H_9)_2)_2]$ (3): This was prepared similarly to **1** in 82% yield by using $\mathbf{L^3}$ (258 mg, 0.60 mmol) and $[UO_2(NO_3)_2 \cdot 6H_2O]$ (300 mg, 0.59 mmol). ^{1}H NMR (25 °C, $CDCl_3$): $\delta = 0.93$ (d, 12H, CH_3, ^{i}Bu J = 6.5 Hz), 1.21 (d, 12H, CH_3, ^{i}Bu J = 6.5 Hz), 2.28 (m, 2H, CH, ^{i}Bu), 2.46 (m, 2H, CH, ^{i}Bu), 3.43 (s, 4H, $-CH_2S-$), 3.44 (d, 4H, NCH_2, ^{i}Bu J = 6.8 Hz), 3.60 (8H, NCH_2 + $-SCH_2CO-$). IR (cm^{-1}): ν = 1570 (s) (C=O). Analysis (%): Calcd. for $C_{22}H_{44}N_4O_{10}S_2U$: C, 32.0; H, 5.4; N, 6.8; S, 7.8; Found: C, 31.9; H, 5.6; N, 6.9; S, 7.5.

2.2.10 Synthesis of $[UO_2(NO_3)_2(C_7H_6(SCH_2CON\ (^iC_4H_9)_2)_2)]$ (4): This was prepared similarly to **1** in 83% yield. by using $\mathbf{L^5}$ (250 mg, 0.50 mmol) and $[UO_2(NO_3)_2 \cdot 6H_2O]$ (251 mg, 0.50 mmol). ^{1}H NMR (25 °C, CD_3COCD_3): $\delta = 0.75$ (m, 12H, CH_3, ^{i}Bu), 1.21 (m, 12H, CH_3, ^{i}Bu), 2.00 (br, 4H, CH, ^{i}Bu), 2.28 (s, 3H, CH_3, tolyl), 3.60 (br , 4H, NCH_2 , ^{i}Bu), 3.96 (br , 4H, NCH_2, ^{i}Bu) , 4.48 (br, 4H, $-SCH_2CO-$), 7.07 (br, 1H, tolyl), 7.44 (br, 1H, tolyl), 7.46 (br, 1H, tolyl) . IR (cm^{-1}): ν =1570 (s) (C=O). Analysis (%): Calcd. for $C_{27}H_{46}N_4O_{10}S_2U$: C, 36.5; H, 5.2; N, 6.3; S, 7.2; Found: C, 36.4; H, 5.2; N, 6.1; S, 7.3.

2.2.11 Crystallography : Crystal data for **2** and **4** were measured on a Oxford Diffraction X-Calibur CCD System at 150(2)K with MoK_α radiation (λ = 0.71073 Å). The crystals were positioned at 50 mm from the CCD. 321 frames were measured for both the crystals with a counting time of 10 s. Data analyses were carried out with the CrysAlis program [111] for all compounds. The structures were solved using direct methods with the Shelxs97 program[112]. All non- hydrogen atoms were refined with anisotropic thermal parameters. The hydrogen atoms bonded to carbon atoms were included in the geometric positions and given thermal parameters equivalent to 1.2 times those of the atoms to which they attached. Empirical absorption corrections were carried out using the ABSPACK program [113] for all compounds.

The structures were refined to convergence on F^2 using Shelxl97[112]. Selected crystallographic data for complexes **2** and **4** are summarized in Table 2.1.

Table 2.1: Crystal refinement data of compounds 2 and 4

	2	**4**
Empirical Formula	$C_{22}H_{44}N_4O_{10}S_2U$	$C_{27}H_{46}N_4O_{10}S_2U$
Crystal system	monoclinic	Triclinic
Space group	P 2_1/n	P -1
a (Å)	17.0993(9)	10.8372(9)
b (Å)	10.1195(4)	17.3889(12)
c (Å)	19.1525(11)	19.3630(14)
α (°)	90.0	78.941(6)
β (°)	108.337(8)	89.383(6)
γ (°)	90.0	82.011(6)
V (cm^3)	3145.8 (3)	3545.9(5)
Z	4	4
ρ_{calcd} [g cm^{-3}]	1.746	1.665
μ [mm^{-1}]	5.347	4.750
Reflections collected/ unique	9116/7336	19262/10579
Data/restrains/parameters	7336/0/356	10579/65/793
Goodness of fit on F^2	1.116	0.962
Final R_1 indices [$I > 2\sigma(I)$]	0.0648	0.1085
wR_2 indices (all data)	0.0877	0.1675

$w = 1/[\sigma^2(Fo^2)+(0.0352P)^2+17.6598P]$ for **10**, $w = 1/[\sigma^2(Fo^2)+(0.1632P)^2+43.9344P]$ for **12** , where $P = (Fo^2 + 2Fc^2)/3$

2.2.12 Theoretical methods: Full geometry optimization for all the ligands and complexes has been carried out applying a popular non-local correlated hybrid density functional, namely, B3LYP. The crystal structures were taken as the initial geometry for optimization of the complexes for locating the minimum energy structure. Gaussian type atomic basis functions, 6-31 + G(d), were adopted for H, C, N, O and S atoms while for the U atom, SARC-ZORA [114] basis sets were used for all the calculations. SARC-ZORA basis sets are segmented all-electron scalar relativistic basis sets in which the coefficients of contracted GTOs have been optimized for use with the ZORA scalar relativistic Hamiltonian. This particular basis set for U was obtained from the Extensible Computational Chemistry Environment Basis Set Database, Pacific Northwest National Laboratory [115]. Geometry optimization to locate the minimum energy structure was carried out applying a quasi-Newton–Raphson based algorithm. The energy of the systems was further improved by performing single point calculations at the MP2 level, adopting the same set of basis functions. These calculations have been performed applying the GAMESS suit of ab initio programs on a LINUX cluster platform [116].

2.2.13 Solvent extraction studies: Distribution studies were performed using a solution of $\mathbf{L^4}$ in dodecane with the required aqueous phase spiked with ^{233}U , ^{239}Pu or ^{241}Am tracers in a thermostated water bath for 1 hour at 25 ± 0.1 C. Assays of organic and aqueous phases were done in duplicate by alpha counting using a dioxane based liquid scintillator for ^{233}U and ^{239}Pu and direct γ counting for ^{241}Am. The distribution ratio (D) is defined as the ratio of the concentration of uranium in the organic phase to that of the aqueous phase.

2.3 Results and discussion

2.3.1 Synthesis of dithiodiglycolamide ligands: These ligands $\mathbf{L^1}$-$\mathbf{L^5}$ were prepared by reacting 1,2 ethane dithiol or 5-methyl-1, 2-dithiophenol and *N,N'*-dialkyl carbamoyl chloride [117] (Scheme 2.1). The IR spectra of all ligands show the presence of carbamoyl groups in the synthesized ligands. The ^{1}H NMR spectra of all the ligands show the expected peaks and integrations. The CHN analyses support the expected stoichiometry for the newly prepared ligands.

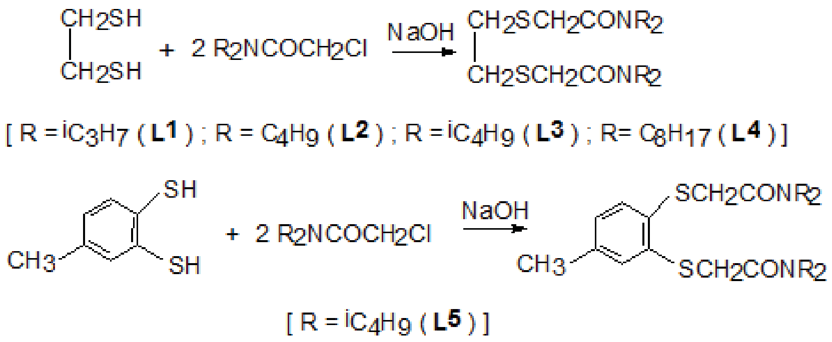

$$UO_2(NO_3)_2.6H_2O \quad + \quad L \longrightarrow \quad UO_2(NO_3)_2.L$$

Where L = L^1 (**1**), L^2 (**2**), L^3 (**3**), L^5 (**4**)

Scheme 2.1. Synthesis of dithidiglycolamide ligands and their complexes

2.3.2 Synthesis of 1, 2-ethylene bis (thioglycolamide) and 5-methyl- 1, 2- phenylene bis(thioglycolamide) uranyl nitrate complexes: The reaction of $[UO_2(NO_3)_2{\cdot}6H_2O]$ with the ligands **L^1-L^3 and L^5** yielded compounds **1-4** (Scheme 1). C, H and N analyses revealed that the ratio of uranyl nitrate to ligand is 1:1 in all compounds. The IR spectra of complexes **1-4** show that the water molecules from the starting compound $[UO_2(NO_3)_2{\cdot}6H_2O]$ are completely replaced by the ligand and that the ligand is bonded through the carbamoyl oxygen atom to the uranyl group. The observed frequency difference for a carbamoyl ($\Delta\nu_{CO}$ = 37-82 cm^{-1}, where $\Delta\nu_{CO} = \nu_{CO\ (free\ ligand\ )} - \nu_{CO(coordinated)}$) group shows that the carbamoyl group is bonded to the uranyl group directly (see Table 2.2). This difference is comparable in magnitude with those observed in $[UO_2(NO_3)_2$(*N*-cyclohexyl,2-pyrrolidone)$_2$ [118] and $[UO_2(NO_3)_2$(1,3-dimethyl,2-imidazolidone)$_2]$ [54], $[UO_2(NO_3)_2\{^{i}C_3H_7CON(^{i}C_4H_9)_2\}_2]$ [56], $[UO_2(NO_3)_2(^{i}C_3H_7)_2NCOCH_2CON\ (^{i}C_3H_7)_2]$ [58a] and $[UO_2(NO_3)_2(C_{15}H_{27}N_3O)]$ [119] . Moreover, the IR asymmetric stretch of OUO bond shifted to lower wavenumber (as shown in Table 2.2) as compared to that of $UO_2(NO_3)2.6H_2O$ (ν_{OUO} = 949 cm^{-1}) which further shows that the ligand is complexed to the uranyl centre

Table 2.2: IR frequencies for the uranyl (VI) complexes 1-4

S.No.	Compound	IR (ν_{CO} in cm^{-1})	$\Delta\nu_{CO} = \nu_{CO(Ligand)} - \nu_{CO(Complex)}$ cm^{-1}	Asymmetric Stretch (ν_{OUO} in cm^{-1}
1	$[UO_2(NO_3)_2(CH_2SCH_2CON\ (^iPr)_2)_2]$ (**1**)	1578	46	923
2	$[UO_2(NO_3)_2(CH_2SCH_2CON\ (Bu)_2)_2]$ (**2**)	1600	37	932
3	$[UO_2(NO_3)_2(CH_2SCH_2CON\ (^iBu)_2)_2]$ (**3**)	1570	74	930
4	$[UO_2(NO_3)_2(C_7H_6(SCH_2CON\ (^iBu)_2)_2)]$ (**4**)	1570	82	935

The ^1H NMR spectra of **1-4** show the expected peaks and integrations. All protons are deshielded with respect to the free ligand indicating that the bonding between the ligand and uranyl group persists in solution. The CH_2 adjacent to carbamoyl group is more deshielded (ca. 0.4 ppm) compared to that of the CH_2 attached to S atom. The ESI-MS spectrum of **2** in acetone shows the presence of peak at m/z of 764.2, indicating that the metal ligand bond retains in solution (Figure 2.2). The ESI-MS spectrum in positive mode of the compound **4** in acetone shows a molecular ion peak at m/z of 826.33 $[(UO_2L(NO_3)^+]$ indicating that the ligand remains bonded to uranyl nitrate in solution. This also shows further that the compound undergoes disproportionation in solution to give a mixture of $[UO_2L_2]$ (m/z = 629.3, $(UO_2L_2)^{2+}$) and $[UO_2L_3]$ (m/z = 876.4, $(UO_2L_3)^{2+}$) species (Figure 2.3). It is apparent from IR and NMR spectral results that the ligands act as bidentate chelating ligands and bonds through the carbamoyl groups to uranyl group. The structures of **2** and **4** have been determined by single crystal X-ray diffraction methods and confirm the spectral and analysis results.

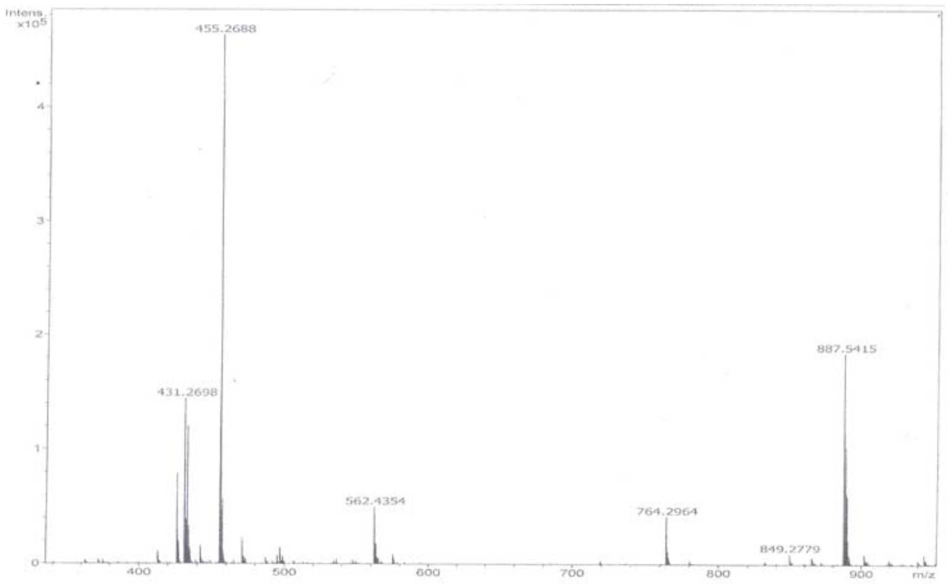

Figure 2.2: ESI-MS spectrum of complex 2 in acetone

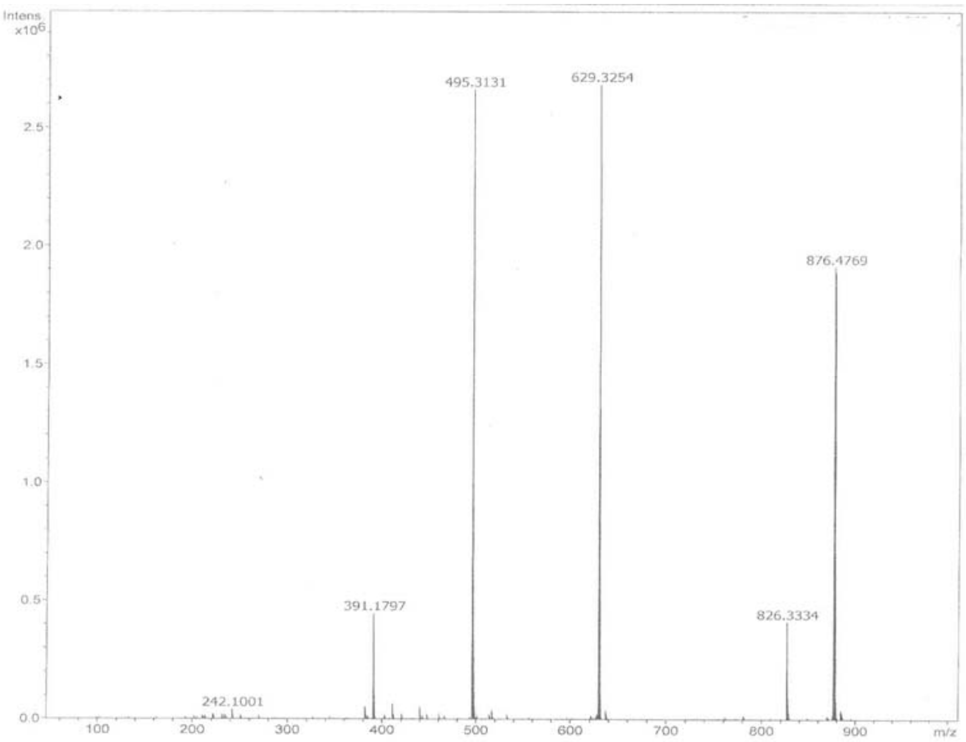

Figure 2.3: ESI-MS spectrum of complex 4 in acetone

2.3.3 Structure of [$UO_2(NO_3)_2(CH_2SCH_2CON\{C_4H_9\}_2)_2$] (2). The structure of **2** is shown in Figure 2.4, and selected bond distances and angles are given in Table 2.3. The structure of complex **2** shows that the uranium atom is surrounded by eight oxygen atoms to form a hexagonal bi-pyramidal geometry around the metal centre. Four oxygen atoms of the two bidentate nitrate groups, together with two oxygen atoms of the bidentate dithio glycolamide ligand form the equatorial hexagonal plane. The UO_6 atoms in the equatorial plane show an r.m.s deviation of 0.029 Å. The two uranyl oxygen atoms occupy the axial positions.

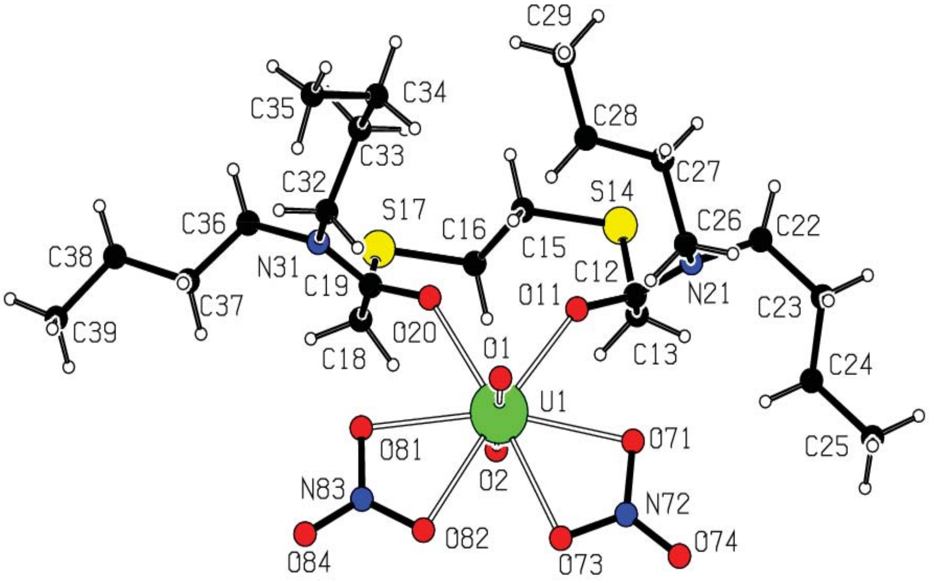

Figure 2.4: Structure of $[UO_2(NO_3)_2(CH_2SCH_2CON\{C_4H_9\}_2)_2]$ (2)

This type of coordination is similar to that observed in the compounds of the bi-functional ligands, malonamide, carbamoyl methyl phosphonate, carbamoyl methyl phosphine oxide, carbamoyl methyl sulfoxide and carbamoyl methyl pyrazole with uranyl nitrate such as, $[UO_2(NO_3)_2(\{({}^iC_3H_7)_2NCH_2CO\}_2]$ [58a], $[UO_2(NO_3)_2({}^iC_3H_7O)_2POCH_2CONEt_2]$, $[UO_2(NO_3)_2(C_6H_5)_2POCH_2CONEt_2]$ [62], $[UO_2(NO_3)_2.C_6H_5SOCH_2CONBu_2]$ [24], $[UO_2(NO_3)_2(C_{15}H_{27}N_3O)]$ [119] and $[UO_2(NO_3)_2(C_3H_3N_2CON\{C_2H_5\}_2)]$ [120]. The average U-O (amide) distance (2.361(4) Å) in **2** is comparable in magnitude with those of earlier reported uranyl nitrate-amide compounds such as, $[UO_2(NO_3)(DMF)_2]$ (2.397(6)Å) [121] $[UO_2(NO_3)_2(\text{tetrabutylglutaramide})_2]$ (2.378(6) Å [109], $[UO_2(NO_3)_2(\text{dibutyldecanamide})_2]$ (2.37(2) Å) [122], and $[UO_2(NO_3)_2(C_{15}H_{27}N_3O)]$ (2.364(7) Å) [119]. The observed average U-O

(NO_3) bond distance of 2.512(5) Å lies within the expected range [123] .The angles subtended at the metal atom show that the uranium atom has a slightly distorted hexagonal bi-pyramidal geometry.

Table 2.3: Important bond lengths (Å) and angles (°) for 2 and 4.

	2		
U1 – O1	1.748(5)	U1 – O71	2.507(5)
U1 – O2	1.746(5)	U1 – O73	2.489(5)
U1 – O11	2.341(4)	U1 – O81	2.534(5)
U1 – O20	2.382(5)	U1 – O82	2.518(5)
C12 – O11	1.256(8)	C19 – O20	1.263(8)
O1 – U1 – O2	177.7(2)	O11 – U1 – O20	69.75(16)
O11 – U1 – O71	64.73(15)	O71 – U1 – O73	50.72(15)
O73 – U1 – O82	60.46(16)	O81 – U1 – O20	64.55(16)
O82 – U1 – O81	49.93(16)	C12 – O11 – U1	142.5(4)
C19 – O20 – U1	136.0(4)		
	4		
U2 – O1B	1.774(11)	U2 – O71B	2.561(14)
U2 – O2B	1.751(11)	U2 – O72B	2.528(12)
U2 – O11B	2.336(11)	U2 – O81B	2.499(14)
U2 – O20B	2.342(10)	U2 – O82B	2.543(12)
C12B – O11B	1.26(2)	C19B – O20B	1.298(18)
O1B – U2 – O2B	176.8(5)	O11B – U2 – O20B	70.7(4)
O11B – U2 – O71B	63.2(4)	O71B – U2 – O72B	50.4(4)
O72B – U2 – O81B	59.4(4)	O82B – U2 – O20B	66.9(4)
O82B – U2 – O81B	49.7(4)	C12B – O11 – U2	144.0(10)
C19B – O20B – U2	145.0(10)		

2.3.4 Structure of $[UO_2(NO_3)_2C_7H_6(SCH_2CON\{C_4H_9\}_2)_2]$ (4): The crystal structure of complex **4** consists of two crystallographically independent molecules and the structure of one of the molecules is shown in Figure 2.5, and selected bond distances and angles are given in Table 2.3. The structure of complex **4** shows that the uranium atom is surrounded by eight oxygen atoms in a hexagonal bi-pyramidal geometry. Four oxygen atoms of the two bidentate nitrate groups, together with two oxygen atoms of the bidentate dithiodiglycolamide ligand form the equatorial hexagonal plane. The UO_6 atoms in the equatorial plane show an r.m.s deviation of 0.069 Å. The two uranyl oxygen atoms occupy the axial positions.

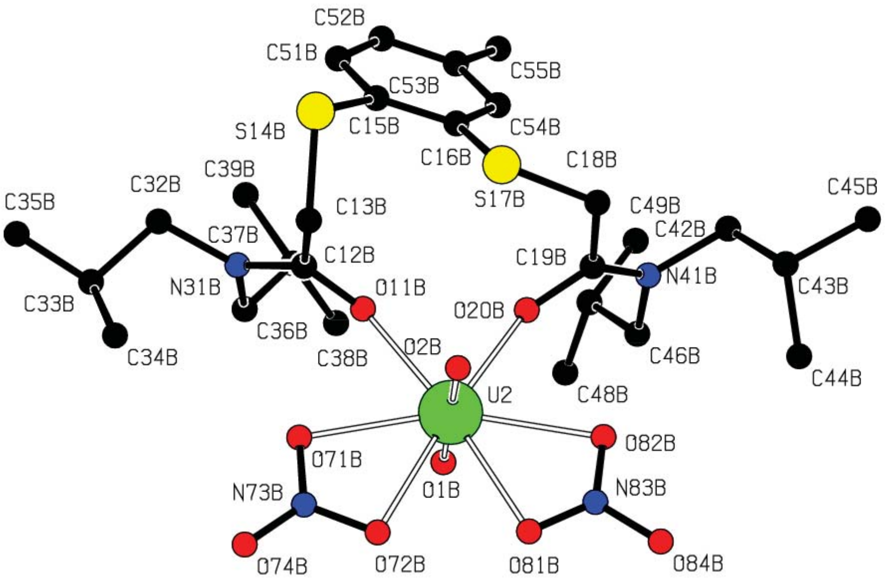

Figure 2.5: Structure of $[UO_2(NO_3)_2C_7H_6(SCH_2CON\{C_4H_9\}_2)_2]$ (**4**)

This type of co-ordination is similar to that observed in the compounds of the bi-functional ligands, carbamoyl methyl phosphonate, carbamoyl methyl phosphine oxide [59] malonamide [58a] and carbamoyl methyl pyrazole [119] . The average -O(amide) distance (2.339(11) Å) in **4** is comparable in magnitude with those of earlier reported uranyl nitrate-amide compounds [109, 119-120, 122]. The observed average U-O (NO_3) bond distance 2.533(13) Å lies within the expected range[123] . The angles subtended at the metal atom show that the uranium atom has a slightly distorted hexagonal bi-pyramidal geometry.

It is interesting to note from these structures that both these ligands act as bidentate chelating ligands, though both the carbamoyl groups are separated by six atoms. It is reported that when, the carbamoyl groups are separated by more than five atoms in a bridge, the ligands adopt energetically more favored bridging bidentate modes of bonding than the less favored bidentate chelating mode of bonding. The observed structures clearly reflect that the replacement of two of the CH_2 groups by two sulfur atoms in the present cases and two oxygen atoms in 1,2-phenylene bis(oxyacetamide) case changes the mode of bonding and hence the solid state structure. The uranyl (O=U=O) bond distances are 1.748 (5) Å and 1.746 (5) Å in complex **2** and 1.774 Å and 1.751 Å in complex **4**. The O=U=O bond angle in complex **2** is 177.7° (2) and 176.8 Å in complex **4**. These bond lengths and bond angles fall in the normal range of uranyl as earlier reported in the literature[124] .

2.3.5 Theoretical studies on dithio-diglycolamide uranyl nitrate compounds: Full geometry optimization of the four ligands (Fig. 2.6 (**a–d**)) and their corresponding complexes (Fig. 2.7 (**e–h**)) has been carried out applying the B3LYP correlated non-local hybrid density functional. SARC-ZORA basis sets for U and Gaussian type atomic basis functions, 6-31 + G(d) for the H, C, N, O and S atoms were applied in all the calculations. Both all-*cis* and all-*trans* conformers of ligand **a** (all CH2 group bridging), **b** (two of the CH_2 groups replaced with sulfur atoms), **c** (tolyl analogue of **a**) and **d** (tolyl analogue of **b**) were optimized to find the relative stability of the conformers. Note that even though the initial structures of the ligands considered were all *cis* or all *trans* conformers, after full optimization, the lowest energy structures turned out as shown in Fig. 2.6. It is predicted that in the case of ligand **a**, the all-*trans* conformer is more stable than the all-*cis* conformer by 5.5 kcal/mol, while for ligand **b**, the all-*trans* conformer is less stable by 7.5 kcal/mol. Note that for **c** and **d** invariably the *cis* conformers are the most stable structures. Based on the energies of the uranyl nitrate complexes with these four ligands (all-*cis* conformer of ligands **a–b** and ligands **c–d**) and the energy of these complexes at the dissociation limit, the binding energies of the complexes were calculated

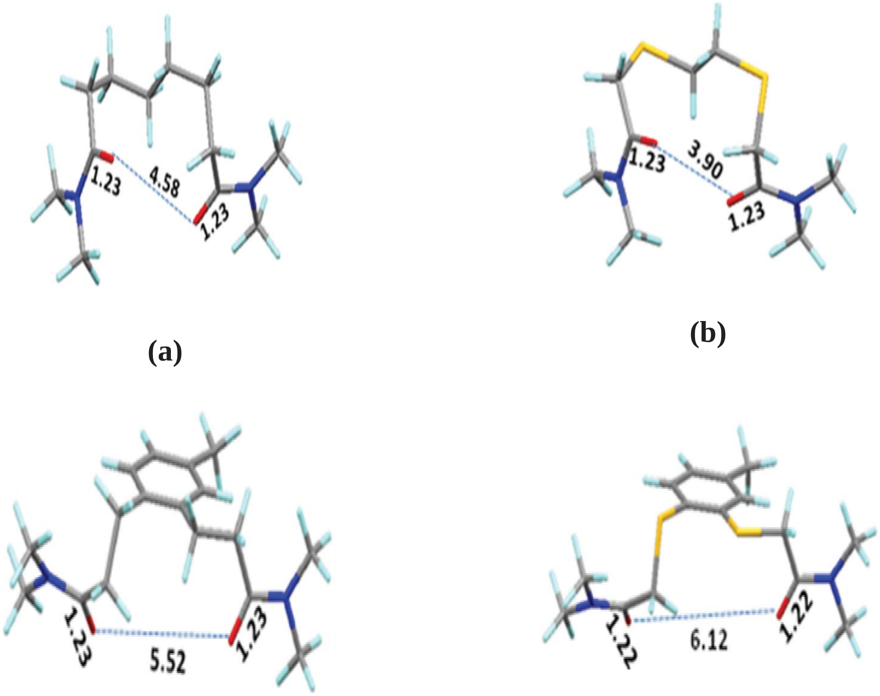

(a) **(b)**

(c) **(d)**

Figure 2.6: Optimized structure of the four ligands with selected distances in Å.

and these are listed in Table 2.4 together with selected geometrical parameters. It is observed that the binding energies of these complexes should be similar and that the complex with ligand **a** should be the least stable. However, it is to be noted that the all-*cis* conformer of ligand **a** is less stable than its all-*trans* conformer, making it difficult to form a complex with uranyl nitrate as for ligand **a** the formation of bidentate complexes is only possible if the ligand is in its all-*cis* conformation. It is possible that the ligand in its all-*trans* conformation forms a complex with uranyl nitrate as a monodentate ligand. Formation of such complexes has been explored and the optimized structure of such complexes with ligands **a** and **b** are displayed in Fig. 2.8 (**i–j**). To satisfy the coordination of uranyl nitrate and these monodentate ligands, a solvent H_2O molecule is added to complete the equatorial coordination sphere. It is calculated that the monodentate ligand **a** forms a more stable complex than ligand **b** by 5.0 kcal/mol. This study clearly shows that the chelating mode of bonding for dithio based ligands is more stable energetically than the corresponding all CH_2 bridged ligand with uranyl nitrate. However, this result is reversed when bridging or monodentate modes of bonding are considered.

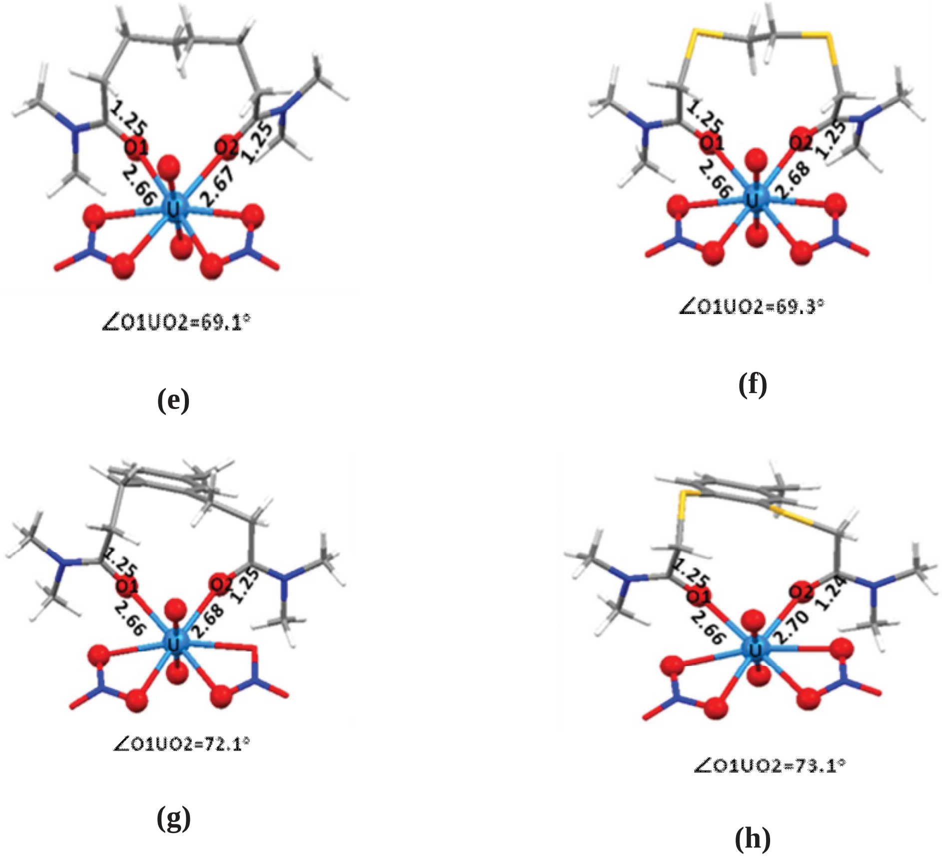

Figure 2.7: Optimized structures of four complexes of uranyl nitrate and bi-dentate ligands with selected bond distances in Å and bond angle in degrees.

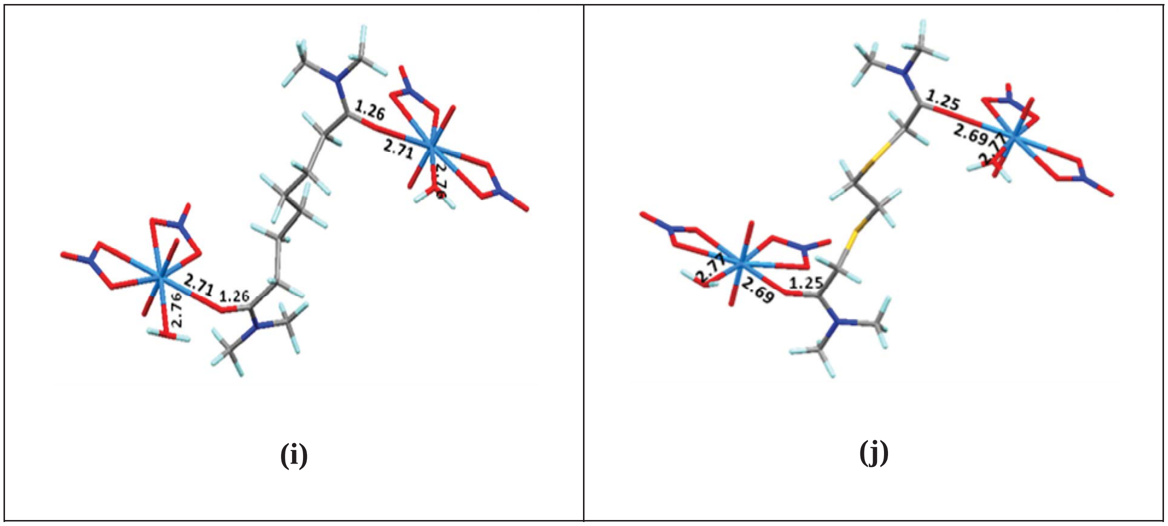

(i)

(j)

Figure 2.8: Optimized structures of two complexes of uranyl nitrate and mono-dentate ligands a and b with selected bond distances in Å.

Table 2.4: Relative stability of ligands and binding energy of complexes in kcal/mol

System	Relative Stability ($E_{\text{all trans}}$-$E_{\text{all cis}}$) in kcal/mol	Binding Energy ($E_{\text{complex at eqm}}$-$E_{\text{complex at diss limit}}$) in kcal/mol
Ligand **a**	5.5	-
Ligand **b**	-7.5	-
Complex **e**	-	57.25
Complex **f**	-	61.05
Complex **g**	-	59.7
Complex **h**	-	61.9
Complex **i**	-	42.8
Complex **j**	-	37.8

2.3.6 Extraction studies of U (VI), Pu (IV) and Am(III) with L^4 from nitric acid medium:

The extraction studies were carried out by using the ligand $\mathbf{L^4}$ in dodecane with UO_2(VI), Pu(IV) and Am(III) ions in tracer level (using the ^{233}U, ^{239}Pu and ^{241}Am tracers) from a nitric acid medium to assess the feasibility of using this ligand (0.2 M) for extraction purposes.Distribution ratios (D) for UO_2(VI), Pu(IV) and Am(III) as a function of nitric acid concentrations (Figure 2.9) clearly show that UO_2(VI) and Pu(IV) are extracted significantly from nitric acid at a concentrations of 1 to 7 M. However, Am(III) did not show appreciable extraction under the conditions studied. The observed distribution ratios follow the order of: $D_{Pu(IV)} >> D_{U(IV)} >> D_{Am\,(III)}$ and are similar to those observed for the malonamides, CMP, CMPO, CMSO or malonamide ligands with these metal ions [24, 125]. In order to establish the nature of species extracted during the solvent extraction process, the distribution ratios for UO_2(VI), were measured as a function of $\mathbf{L^4}$ concentrations. The log D_U vs. log [HNO_3] (Figure 2.10) shows a straight line with a slope close to two, indicating that two nitrate ions are involved in the extraction process. The plot of log D_U vs. log [$\mathbf{L^4}$] for UO_2(VI), shows a (Figure 2.11) straight line with a slope equal to 1.35, indicating that the species extracted under the solvent extraction conditions are a mixture of $UO_2(NO_3)_2.L$ and $UO_2(NO_3)_2.2L$ [126].

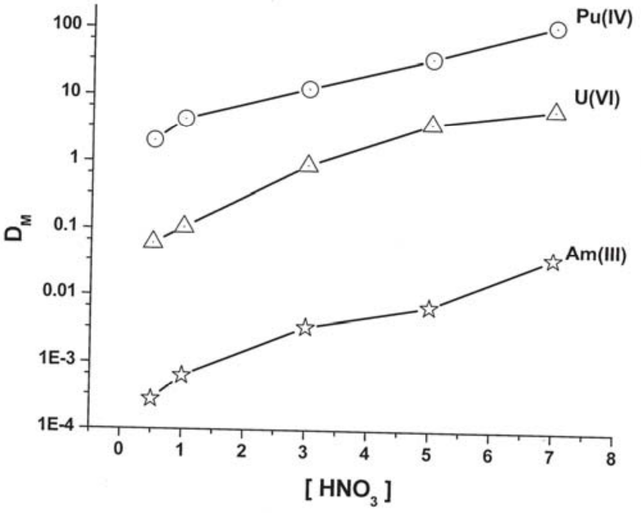

Figure 2.9: Distribution ratio vs. [HNO_3 for UO_2(VI), **Pu(IV) and Am(III) ions with 0.2M L^4 in dodecane .**

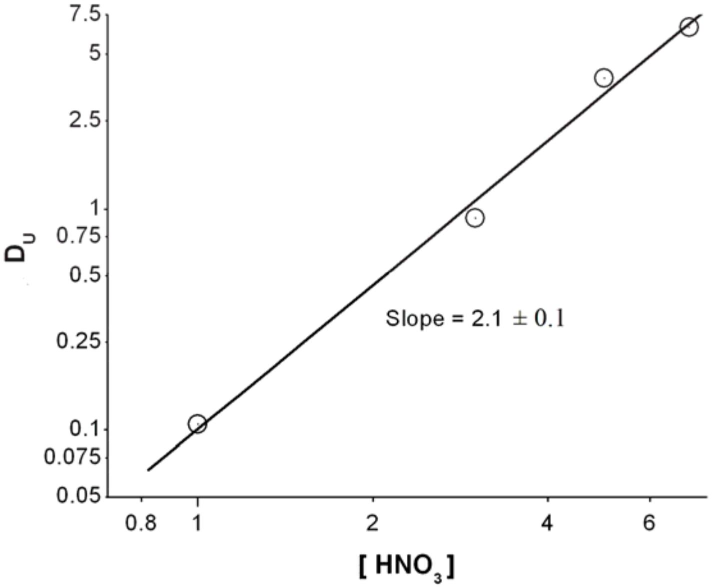

Figure 2.10: Variation of D_U with conc. of nitric acid [HNO_3]

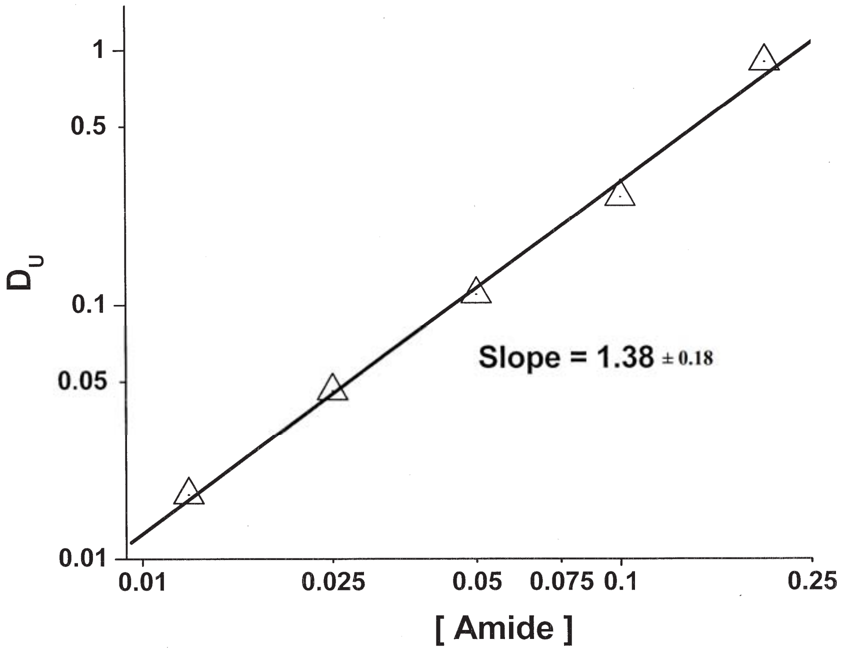

Figure 2.11: Variation of D_U with conc. of extractant [Amide]

2.4 Conclusions:

The coordination chemistry of dithio-diglycolamide ligands with uranyl(VI) nitrate show a chelating mode of bonding for these ligands. The dioctyl based ligand shows an appreciable extraction for uranyl and plutonium(IV) ions from the nitric acid medium. The extracted ions could be stripped back quantitatively using 0.5 M HNO_3 or a mixture of 0.5 M HNO_3 + 0.5 M $H_2C_2O_4$, respectively. Theoretical studies clearly revealed that the chelating mode of bonding for these ligands is more energetically favorable than monodentate or bridging bidentate modes of bonding.

Chapter 3

Synthesis, coordination, structural and extraction studies of α-hydroxyacetamide based ligands with lanthanide(III) and uranyl(VI) ions.

3.1 Introduction:

The prior separation of long lived trivalent actinides americium and curium from the HLLW (High Level Liquid Waste) solution is an important step to be focussed upon for the safe disposal of waste in vitrified form under deep geological repositories [127]. This method of disposal by separation of long-lived radionuclides followed by transmutation is being considered by several countries [128]. Due to the striking similarities in chemical properties, the selective extraction / separation of trivalent actinides (Am (III) and Cm (III)) from HLLW solution containing large excess of trivalent lanthanides is very difficult and challenging. Therefore, the co-extraction of An(III) and Ln(III) from HLLW solution followed by group separation of actinides from lanthanide is proposed [94b, 129] (SANEX process). Several reagents were synthesized in last two decades for this purpose and their extraction properties with trivalent actinides and lanthanides from HLLW solution studied. Among them, the carbamoyl methyl phosphine oxides, (TRUEX process) [130] trialkyl phosphine oxides (TRPO process) [131], di-isodecyl phosphoric acid (DIDPA process) [132] , malonamides (DIAMEX process) [49b, 125b, 133] and tetra alkyl diglycolamides (TODGA or TEHDGA) [58c, 134] have shown excellent extraction properties for actinide and lanthanide ions from the HNO_3 medium [129b, 135]. The major drawback of using organophosphorus extractants is the generation of a solid residue that results upon their incineration at the end of their useful life in addition to poor back extraction properties. The incinerable malonamide based extractants show better extraction and back extraction properties, but the distribution coefficients (D values) obtained for trivalent lanthanide and actinide ions are relatively very low (not more than 10 for An(III) at high ligand concentration ~1M)[136].The diglycolamide based extractants show better extraction properties as compared to malonamide based extractants due to their very high D values for Am(III) from 3-4 M HNO_3 (more than 100)[136]. The main disadvantage of these extractants is that, they extract Sr(II) ions from the HLLW solution [58c, 137] along with An(III) and Ln(III) ions, and therefore, needs additional steps during the stripping process. Several new extractants functionalized with carbamoyl methyl phosphine oxides, malanomides and glycolamides were explored [138] in recent years for the separation of lanthanide and actinide ions from a nitric acid medium. However, in most of the cases they show very high D values even in lower acidities (< 0.5M HNO_3) and therefore need very low acidities for stripping (which is not advisable in plant operation) or when using complexing agents. However, *N,N*-dioctyl-α-hydroxy acetamide is an important major radiation degradation product [139] as well as synthetic precursor [140] of the well known extractant tetra-octyl diglycolamide (TODGA), no work on the extraction and separation properties of this compound with trivalent actinides or lanthanides is reported so far. We report in this chapter herein, the extraction properties of *N,N*-dioctyl-α-hydroxy acetamide with Am(III), Eu(III), Sr(II), Cs(I), Pu(IV), Ru(III), Zr(IV) and U(VI) ions from HNO_3 medium and the structures of europium(III), samarium(III) and uranyl nitrates with analogous *N,N*-diisopropyl-α-hydroxy acetamide ligand.

3.2 Experimental:

3.2.1 General Considerations. All reagents and solvents were of analytical grades and used as received. IR spectra were recorded as nujol mulls using a JASCO-610 FITR spectrometer. ^{1}H NMR spectra were recorded using a Bruker AMX-300 spectrometer. The chemical shifts (δ) are reported in ppm and coupling constants (J) are reported in hertz. Electrospray ionization mass spectrometric detection of positive ions in CH_2Cl_2 or CH_3COCH_3 were recorded using a MicrOTOF Q-II instrument. The samples were introduced in to the source with the syringe pump. Nitrogen was employed as both the drying and spraying gas with a source temperature of 180° C. The cone voltage was set to 45V, the voltage applied on the capillary was 1162 kV and the sample solution flow rate was 5 μL min^{-1}. Spectra were recorded from m/z of 100 to 1000.

3.2.2 Synthesis of Ligand {(^{i}C$_3$H$_7$)$_2$NCOCH$_2$OH} (L^6): To a solution of glacial acetic acid (5.8 gm , 0.097 mol) in 1,2- dichloroethane (100 mL), triethyl amine (10 g, 0.099 mol) was added slowly with stirring. To this solution, $(^iC_3H_7)_2NCOCH_2Cl$ (17 g, 0.095 mol) and tetrabutyl ammonium bromide (200 mg, as a catalyst) was added and heated to reflux temperature for 50 h. The solution was treated with 200 mL of 5% HCl, the organic phase was separated, dried over anhydrous Na_2SO_4 and filtered. This solution on slow evaporation yielded an off white solid compound. To a solution of NaOH (3.4 gm, 0.085 mol) in methanol, the above solid (16 gm) was added slowly with stirring. The solution was allowed to stir for an hour, heated to reflux temperature for 30 min and treated with 200 mL of 10% HCl. The organic phase was extracted with di-isopropyl ether, dried over anhydrous Na_2SO_4 and filtered. The final product was obtained as off white crystalline solid in 85% yield. IR (nujol, ν cm^{-1}) : 3353 (br, OH); 1649 (s, CO). ^1H NMR ($CDCl_3$, 500 MHz, δ in ppm) : 1.21 (d, 6H, CH_3, J = 6.5 Hz); 1.42 (d, 6H, CH_3, J = 7.0 Hz) ; 3.50 (m, 1H, CH); 3.62 (m, 1H, CH) ; 3.92 (t, 1H, OH, J = 4.5 Hz); 4.09(s, 2H, CO-CH_2-O). Analysis (%): Calc. For. $C_8H_{17}NO_2$: C, 60.3; H, 10.8; N, 6.5. Found: C, 60.2; H; 10.6; N, 6.3.

3.2.3 Synthesis of (^{n}C$_8$H$_{17}$)$_2$NCOCH$_2$OCOCH$_3$: To a solution of glacial acetic acid (5.8 g, 0.097 mol) in 1,2- dichloroethane (100 mL), triethyl amine (10 gm, 0.099 mol) was added slowly with stirring. To this solution, $(C_8H_{17})_2NCOCH_2Cl$ (30 gm, 0.095 mol) and tetrabutyl ammonium bromide (200 mg, as a catalyst) was added and heated to reflux temperature for 50 h. The solution was treated with 200 mL of 5% HCl, the organic phase was separated, dried over anhydrous Na_2SO_4 and filtered. This solution on slow evaporation yielded 28 g, (87.5% based on ester) of a pale yellow liquid. IR (nujol, ν cm^{-1}) : 1753 (s) (CO, ester); 1668 (s) (CO, amide); ^1H NMR ($CDCl_3$, 500 MHz, δ in ppm): 0.88 (m, CH_3); 1.28 (br, CH_2); 1.55 (m, CH_2); 2.10 (s, CH_3, ester); 3.14 (t, NCH_2, J = 7.5 Hz); 3.30 (t, NCH_2, J = 7.5 Hz); 4.70 (s,

OCH_2CO). Spectra show that the product is a mixture of acetate ester and the final hydroxo compound.

3.2.4 Synthesis of Ligand {($^n C_8H_{17})_2NCOCH_2OH$} (L^7) : To a solution of NaOH (3.4 g, 0.085 mol) in methanol, the above mixture (27 g) was added slowly with stirring. The solution was allowed to stir for an hour, heated to reflux temperature for 30 min and treated with 200 mL of 10% HCl. The organic phase was extracted with di-isopropyl ether, dried over anhydrous Na_2SO_4 and filtered. This solution on evaporation yielded (22 gm, 95% based on ester) the desired product. IR (nujol, ν cm^{-1}): 3411 (br, OH); 1652 (s, CO). ^{1}H NMR ($CDCl_3$, 300 MHz, δ in ppm): 0.84 (br, 6H, CH_3); 1.25 (br, 20H, CH_2); 1.50 (br, 4H, CH_2); 3.01 (t, 2H, NCH_2, J = 7.2 Hz) ; 3.32 (t, 2H, NCH_2, J = 7.2 Hz) ; 3.49 (br, 1H, OH); 4.10 (s, 2H, CO-CH_2-O). ES-MS (CH_2Cl_2, m/z) : 300 ({LH}$^+$, 100%); 322 ({L+Na}$^+$, 22%); 621 ({2L+Na}$^+$, 18%). Analysis (%): Calc. For. $C_{18}H_{37}NO_2$: C, 72.2; H, 12.5; N, 4.7. Found: C, 72.1; H; 12.2; N, 4.6.

3.2.5 Synthesis of [$Eu(NO_3)_3(H_2O)\{(^iC_3H_7)_2NCOCH_2OH\}_3$](5): To a solution of $(^iC_3H_7)_2NCOCH_2OH$ (370 mg, 2.3 mmol) in CH_2Cl_2, solid $Eu(NO_3)_3.6H_2O$ (200 mg, 0.45 mmol) was added and stirred (about 10 min) until all europium salts dissolved to give a clear solution. The solution on further stirring deposited white powder and the whole solution was allowed to stir for further 3 hr. The resultant powder was filtered and washed with CH_2Cl_2 (about 5 ml) and dried. This powder was recrystallized from acetone/$ClCH_2CH_2Cl$ mixture to give crystalline solid in 85% yield. IR (nujol, ν cm^{-1}) : 3437 - 3000 (br, OH); 1613 (s, CO). ^{1}H NMR (CD_3COCD_3, 300 MHz, δ in ppm) : 0.25 (br); 0.5 (br) ; 2.65 (br): (broad peaks due to paramagnetic nature). Analysis (%): Calc. For. $C_{24}H_{53}N_6O_{16}Eu$: C, 34.6; H, 6.4; N, 10.1. Found: C, 34.8; H; 6.1; N, 9.8.

3.2.6 Synthesis of [$Sm(NO_3)_3(H_2O)\{(^iC_3H_7)_2NCOCH_2OH\}_3$](6) : To a solution of $(^iC_3H_7)_2NCOCH_2OH$ (370 mg, 2.3 mmol) in chloroform, solid $Sm(NO_3)_3.6H_2O$ (200 mg, 0.45 mmol) was added and stirred (about 10 min) until all samarium salts dissolved to give a clear solution. The solution on further stirring deposited white powder and the whole solution was allowed to stir for further 3hr. The resultant powder was filtered and washed with CH_2Cl_2 (about 5 ml) and dried. This powder was recrystallized from acetone/ $ClCH_2CH_2Cl$ mixture to give crystalline solid in 90% yield. IR(nujol, ν cm^{-1}) : 3430 - 3000 (br, OH); 1603 (s, CO). ^1H NMR (CD_3COCD_3, 300 MHz, δ in ppm) : 1.34 (br, 6H, CH_3); 1.57 (br, 6H, CH_3); 3.81 (m, 1H, CH); 3.98 (m, 1H, CH); 4.6 (s, 2H, CO-CH_2-O). Analysis (%): Calc. For. $C_{24}H_{53}N_6O_{16}Sm$: C, 34.6; H, 6.4; N, 10.1. Found: C, 34.5; H; 6.2; N, 9.9.

3.2.7 Synthesis of $[UO_2(NO_3)_2\ \{(^iC_3H_7)_2NCOCH_2OH\}_2](7)$: This was prepared by taking $(^iC_3H_7)_2NCOCH_2OH$ (370 mg, 2.3 mmol) and $UO_2(NO_3)_3.6H_2O$ (387 mg, 0.77 mmol) in 20 ml of chloroform.The mixture is stirred till all uranium salt is dissolved to give a clear solution. After further stirring for about half an hour, the solution is evaporated to dryness and washed with hexane. Crystallization from acetonitrile and chloroform (1:1) gave crystals of compound **7** in 70% yield. IR(nujol, ν cm^{-1}) : 3430 - 3000 (br, OH); 1604 (s, CO). ^1H NMR (CD_3COCD_3, 300 MHz, δ in ppm): 1.45 (br, 6H, CH_3); 1.81 (br, 6H, CH_3); 3.59 (m, 1H, CH); 3.76 (m, 1H, CH); 4.06 (s, 2H, CO-CH_2-O). Analysis (%): Calc. For. $C_{16}H_{34}N_4O_{12}U$: C, 27.0; H, 4.8; N, 7.9. Found: C, 26.5; H; 4.6; N, 7.6.

3.2.8 Crystallography: Crystal data for compound **5**, **6** and **7** were measured on a Agilent SuperNova system equipped with Titan CCD detector at 293(2) K using CuK_α radiation (λ = 1.5418 Å).The crystals were positioned at 101 mm from the CCD. 1481, 1486 and 591 frames were measured respectively for compound **5**, **6** and **7** with an integration time of 1 s.Data analysis were carried out with the CrysAlis program [111] . The structure was solved using direct methods with the Shelxs97 program [112]. All non- hydrogen atoms were refined with anisotropic thermal parameters. The hydrogen atoms bonded to carbon atoms were included in geometric positions and given thermal parameters equivalent to 1.2 times those of the atoms to which they attached. Empirical absorption corrections were carried out using the ABSPACK program [113]. The structures were refined to convergence on F^2 using Shelxl97 [112]. Selected crystallographic data for complexes **5**, **6** and **7** are summarized in Table 3.1.

Table 3.1: Crystallographic data for complex 5, 6 and 7

	5	**6**	**7**
Empirical Formula	$C_{24}H_{53}N_6O_{16}Eu$	$C_{24}H_{53}N_6O_{16}Sm$	$C_{16}H_{34}N_4O_{12}U$
Crystal system	monoclinic	monoclinic	monoclinic
Space group	$P\ 2_1/c$	$P\ 2_1/c$	$P\ 2_1/n$
a (Å)	10.9253(2)	10.9512 (4)	6.0207 (4)
b (Å)	26.9890(5)	27.0203 (9)	16.3600 (9)
c (Å)	13.0207(3)	13.0160 (4)	14.3234 (6)
α (°)	90.0	90.0	90.0
β (°)	101.530(2)	101.549 (3)	100.113(5)
γ (°)	90.0	90.0	90.0
V (cm^3)	3761.85(14)	3773.5 (2)	1388.92 (13)
Z	4	4	2
ρ_{calcd} [$g\ cm^{-3}$]	1.472	1.463	1.699
μ [mm^{-1}]	12.557	12.306	16.963
Reflections collected/ unique	23590/7093	23645/7091	5147/2704
Data/restrains/parameters	7093/9/446	7091/9/446	2704/117/176
Goodness of fit on F^2	1.109	1.062	1.339
Final R_1 indices [$I > 2\sigma(I)$]	0.0656	0.0774	0.1274
wR_2 indices (all data)	0.1851	0.2243	0.3405

$w = 1/[\sigma^2(Fo^2)+(0.1000P)^2]$ for **5**, $w = 1/[\sigma^2(Fo^2)+(0.0987P)^2+16.3796P]$ for **6,**
$w = 1/[\sigma^2(Fo^2)+(0.2000P)^2]$ for **7** , where $P = (Fo^2 + 2Fc^2)/3$

***3.2.9 Solvent extraction experiment*:** Distribution studies were performed by using a 0.2 M solution of $(C_8H_{17})_2NCOCH_2OH$ in dodecane with the aqueous phases spiked with ^{233}U, ^{239}Pu, ^{241}Am, ^{152,154}Eu, ^{137}Cs or ^{88,89}Sr tracer in a thermostated water bath for 30 min at 25 ± 0.1 °C. Assays of organic and aqueous phases were done in duplicate by alpha counting using dioxane based scintillator for ^{233}U and ^{239}Pu and gamma counting directly for ^{241}Am, $^{152,154}Eu$, ^{137}Cs and $^{85,89}Sr$. The distribution ratio (D) is defined as the ratio of the concentration of metal ion in organic phase to that of the aqueous phase.

3.3 Results and discussions:

3.3.1 Synthesis of α-hydroxy acetamide ligands: The ligands were prepared by the reaction of R_2NCOCH_2Cl with Et_3N and CH_3COOH in 1,2-dichloroethane followed by hydrolysis using NaOH in near quantitative yields (Scheme 1).

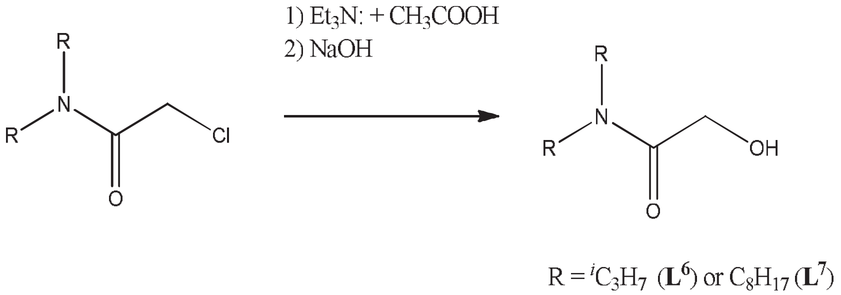

$$Ln(NO_3)_3.\,5H_2O \;+\; 3\,\mathbf{L^6} \xrightarrow{CHCl_3} Ln(NO_3)_3.\,3\,\mathbf{L^6}$$

Ln = Eu (**5**)
= Sm (**6**)

$$UO_2(NO_3)_2.6H_2O \;+\; 2\,\mathbf{L^6} \xrightarrow{CHCl_3} UO_2(NO_3)_2.2\,\mathbf{L^6}$$

(**7**)

Scheme 3.1. Synthesis of *α*-Hydroxy Acetamide Ligands and their Complexes

The IR spectra of the ligands showed the presence of hydroxo and carbamoyl groups. The ^1H NMR spectra showed the expected peaks for the desired compounds and the octyl ligand shows the presence of some un-reacted starting chloro compound (< 2-3 %). The ESI-MS spectrum of the octyl ligands shows the molecular ion peaks at m/z values of : 300 ($\{LH\}^+$, 100%); 322 ($\{L+Na\}^+$, 22%); 621 ($\{2L+Na\}^+$, 18%).

3.3.2 Synthesis of complexes of α-hydroxy acetamide ligands with lanthanides and uranyl ions: In order find out the nature bonding between the ligand and metal, the compounds of

Eu(III) Sm(III) and uranyl (UO_2^{2+}) nitrates with *N*,*N*-diisopropyl-α-hydroxy acetamide were synthesized and characterized. IR spectra of the compounds shows that there is significant downfield shift in the C=O frquency of the ligand when complexed with the metal ions as shown in Table 3.2. This down field shift shows that there is metal ligand bonding through the carbamoyl C=O groups. These type of downfield shift in carbamoyl frequency has also been reported for the complexes $Ln(NO_3)_3(TEMA)_2$ [141], $[La(L)_3][La(NO_3)_6]$ and $UO_2(NO_3)_2L$ (where L= diglycolamide)[58d].

Table 3.2: IR frequencies for Ln(III) and uranyl(VI) complexes

S.No.	Compound	IR (ν_{CO} in cm^{-1})	$\Delta\nu_{CO} = \nu_{CO(Ligand)} - \nu_{CO(Complex)}$ cm^{-1}
1	$[Eu(NO_3)_3(H_2O)\{(^iC_3H_7)_2NCOCH_2OH\}_3]$ (**5**)	1613	36
2	$[Sm(NO_3)_3(H_2O)\{(^iC_3H_7)_2NCOCH_2OH\}_3]$ (**6**)	1603	46
3	$[UO_2(NO_3)_2\,(^iC_3H_7)_2NCOCH_2OH]$(**7**)	1604	45

The ^1H NMR chemical shifts for complexes are somewhat downfield shifted as compared to the uncomplexed ligand, which confirms that the bonding of the ligand to the metal also exists in the solution phase. The molecular structures of **5, 6** and **7** have been determined by single crystal X-ray diffraction methods and confirms the spectral and analysis results.

3.3.3 Structure of $[Eu(NO_3)_3(H_2O)\{(^iC_3H_7)_2NCOCH_2OH\}_3]$(5) and $[Sm(NO_3)_3(H_2O)\{(^iC_3H_7)_2NCOCH_2OH\}_3]$: The structures for the Sm(III) and Eu(III) complexes (Fig 3.1 and 3.2) show that both are iso-structural with the metal ion surrounded by three of the ligands, one nitrate and one water molecule to give distorted tricapped trigonal prismatic geometry. Two of the nitrates are outside the primary coordination sphere and are hydrogen bonded to the water molecule and ligand. The important bond lengths and bond angles are listed in Table 3.3. The ligand acts as a neutral bidentate chelating ligand and bonds through the hydroxyl and carbamoyl oxygen atoms to metal center similar to that reported in the literature [142]. It is worthy to note here that there is always a difference between the number of ligands involved during the solvent extraction process (tracer) to that involved in the solid state compounds (bulk). The number of ligands involved during the extraction of Ln(III) with carbamoyl methyl phosphine oxides, malonamides and tetra alkyl diglycolamide are three, three and four respectively. However, the solid state structures show two, two and three ligands respectively for carbamoyl methyl phosphine oxides [62, 143], malonamides[144] and tetra alkyl diglycolamide.[58d]

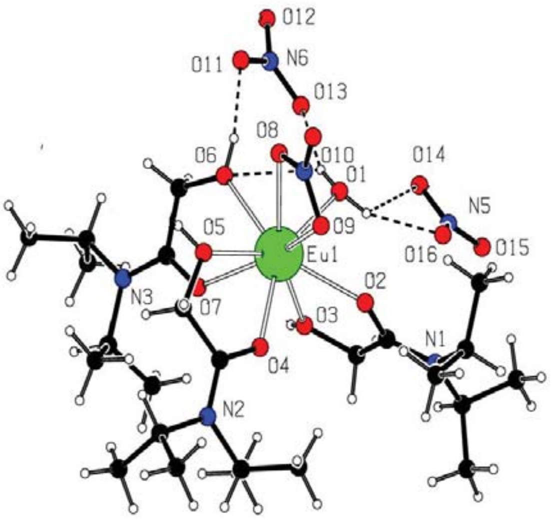

Figure 3.1: Molecular structure of $[Eu(NO_3)_3(H_2O)\{(^iC_3H_7)_2NCOCH_2OH\}_3]$ (5)

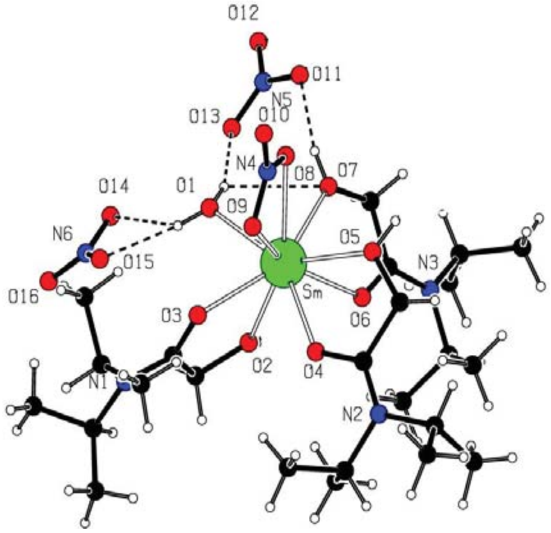

Figure 3.2: Molecular structure of $[Sm(NO_3)_3(H_2O)\{(^iC_3H_7)_2NCOCH_2OH\}_3]$ (6).

3.3.4 *Molecular Structure of $[UO_2(NO_3)_2\{(^iC_3H_7)_2NCOCH_2OH\}_2]$ (7):* The structure of complex **7** is shown in Fig. 3.3 and selected bond lengths and angles are given in Table 3.4. The structure of complex **7** shows that the uranium atom is surrounded by eight oxygen atoms to form a hexagonal bi-pyramidal geometry around the metal centre. Four oxygen atoms, from the two bidentate ligand (**L**^{6}), and the two oxygen atoms, from a bidentate nitrate ligand, form the equatorial hexagonal plane. The two uranyl oxygen atoms occupy the axial positions. One of the nitrate groups is outside the coordination sphere of the uranium ion.

Table 3.3: Important bond lengths (Å) and angles (°) for $[Eu(NO_3)_3(H_2O)\{(^iC_3H_7)_2NCOCH_2OH\}_3]$ (5) and $[Sm(NO_3)_3(H_2O)\{(^iC_3H_7)_2NCOCH_3]$ (6)

	5	**6**
M – O1	2.422(5)	2.430(8)
M – O2	2.380(4)	2.458(7)
M – O3	2.451(4)	2.401(6)
M – O4	2.368(5)	2.398(7)
M – O5	2.514(5)	2.527(7)
M – O6	2.457(5)	2.409(7)
M – O7	2.400(5)	2.464(7)
M – O8	2.500(5)	2.531(7)
M – O9	2.531(5)	2.535(8)
O9 – M – O8	50.2(2)	50.41(16)
O2 – M – O3	63.2(2)	63.18(15)
O4 – M – O5	62.4(2)	63.02(14)
O6 – M – O7	62.6(2)	62.49(15)

Table 3.4: Important bond lengths (Å) and angles (°) for $[UO_2(NO_3)_2\{(^iC_3H_7)_2NCOCH_2OH\}_2]$ (7)

		7	
U1 – O1	1.73 (3)	O1 – U1 – O4	90.3 (10) x 2
U1 – O2	2.53 (2)	O1 – U1 – O3	93.0 (9) x 2
U1 – O3	2.40 (2)	O1 – U1 – O2	91.8 (9) x 2
U1 – O4	2.47 (2)	O1 – U1 – O4	94.0 (10) x 2
C1 – O3	1.26 (3)	O1 – U1 – O3	87.2 (9) x 2
		O1 – U1 – O2	84.0 (9) x 2

O1 – U1 – O1	175.2 (14)

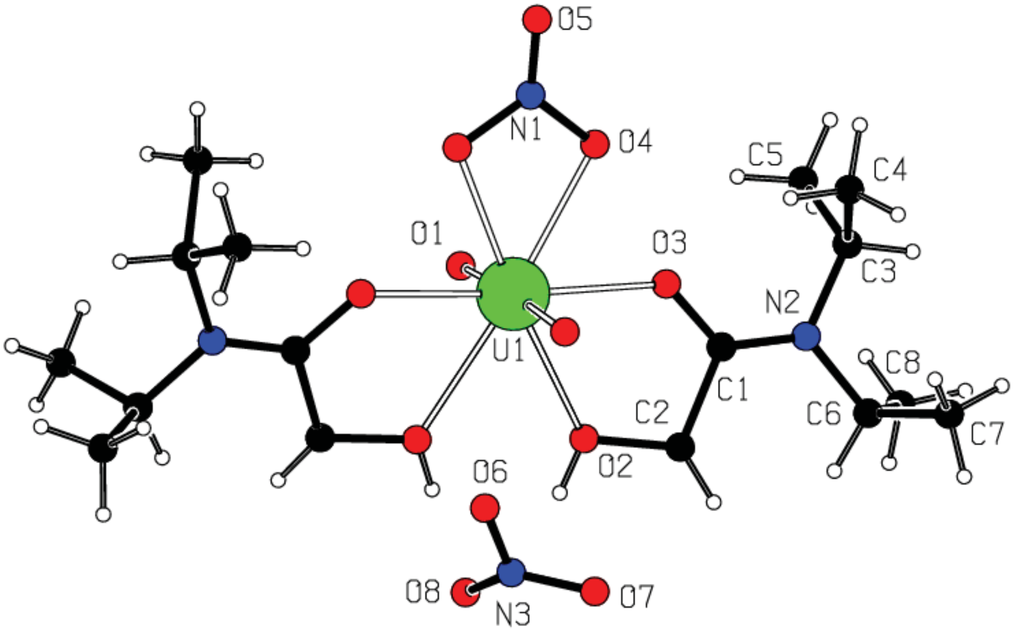

Figure 3.3: Molecular Structure of $[UO_2(NO_3)_2\{(^iC_3H_7)_2NCOCH_2OH\}_2]$ ***(7)***

3.3.5 Extraction studies of Lanthanides and Actinides with ligand L^7:

3.3.5.1 Time of equilibration**:** The time of equilibration for Am(III) and Pu(IV) ions from 4M HNO_3 using 0.2 M of Ligand $\mathbf{L^7}$ in dodecane was studied (Fig. 3.4). This study shows clearly that the extraction process is completed in less than 10 minutes in both cases. Therefore, all other experiments were carried out by performing the extraction after about 30 minutes of contact time.

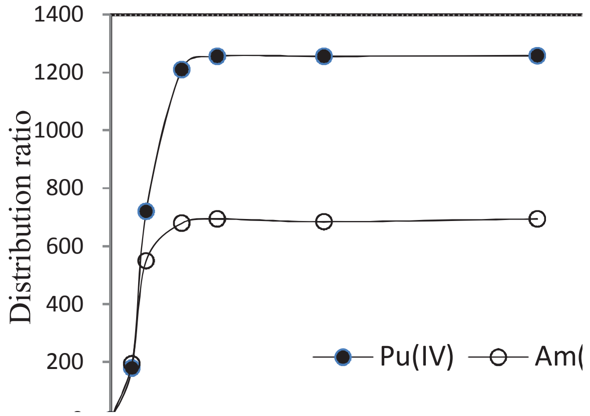

Figure 3.4 : Distribution ratios of Pu(IV) and Am(III) as a function of time

***3.3.5.2 The distribution ratio for different metal ions*:** The extraction studies of Am(III), Pu(IV), UO_2(VI), Eu(III), Sr(II), and Cs(I) ions from different concentrations of HNO_3 using 0.2 M solution of *N,N*-dioctyl-α-hydroxyl acetamide (**L^7**) in dodecane diluent were carried out. The data on D_M vs. [HNO_3] are shown Fig. 3.5. These graphs show clearly that the data on D_M follows the order $D_{Pu} >> D_{Am} > D_{Eu} >> D_U$ above 3M HNO_3 (D_{Sr} and D_{Cs} are negligible at all acidities studied and therefore not included in the Figure). The observed D values for Am(III) and Eu(III) are higher than the values reported for any of the monoamides and malonamides [49b, 129b] and lower than that of tetra-alkyl diglycolamide[58c, 134, 135b]. The D value for uranyl(VI) is much less and comparable to that of the values obtained with the diglycolamide based extractants. The interesting observation is that the D value for Sr(II) ion is negligible ($< 10^{-4}$) as compared to that observed for diglycolamide based extractants (D_{Sr} ~5) [58c, 137].

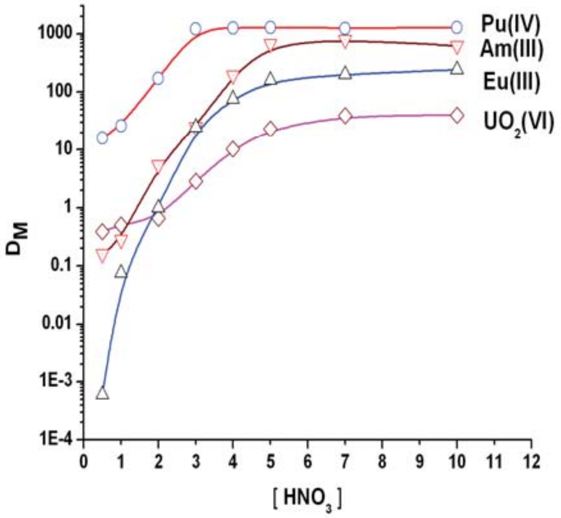

Figure 3.5: Distribution ratios for Pu(IV), Am(III), Eu(III) and UO_2(VI) vs. [HNO_3]

3.3.5.3 The stripping of metal ions: Stripping studies on the extracted metal ions were performed using 0.5 M HNO_3 solution. The Am(III), Eu(III) and UO_2(VI) ions could be back extracted almost quantitatively (99.0 %) from the loaded organic phase in a single contact. The Pu(IV) could be back extracted quantitatively using a mixture of 0.5 M HNO_3 and 0.2 M oxalic acid.

3.3.5.4 Variation of extractant and nitrate concentration on Am(III) extraction**:** In order to find out the nature of species extracted during the extraction of Am(III) (as a tracer) the D_{Am} value was measured as a function of amide concentrations at a constant HNO_3 concentration. The log-log plot of D_{Am} vs. [amide] (Fig. 3.6) shows a straight line with a slope close to 6. This indicates that there are six molecules of amide involved in the extraction process. Similarly, the log-log plot of D_{Am} vs. [NO_3^-] plot (Fig. 3.7) shows a straight line with slope close to 3, indicating that there are three molecules of NO_3 involved in the extraction process.

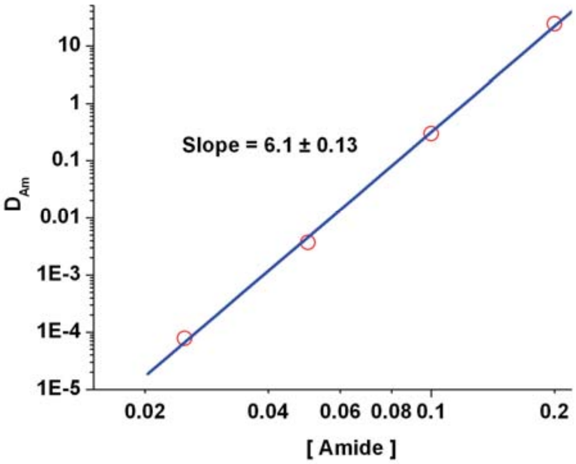

Figure 3.6 : Graph showing the variation of D_{Am} with different concentrations of extractant L^7 in dodecane at room temperature; D_{Am} vs. [amide]

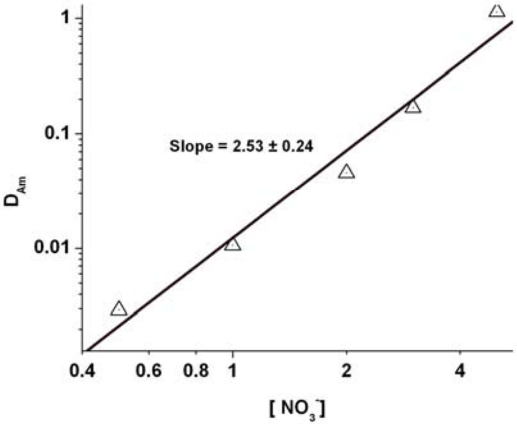

Figure 3.7: Graph showing the variation of D_{Am} with different concentrations of extractant in dodecane at room temperature D_{Am} v.s $[NO_3]^-$

From these studies, the nature of species extracted during extraction process (using tracer) could be written as $[Am(NO_3)_3\mathbf{L}^7]$.

3.3.5.5 Variation of extractant concentration on Pu(IV) extraction: Variation of extractant concentration on D of Pu(IV) was studied at a fixed concentration of 3M nitric acid. As the concentration was varied from 0.2 M to 0.004 M, the D value decreased drastically from

6900 to 0.00034. Figure 3.8 shows D vs [Extractant] (log-log plot) and it gave a slope of 4.4. This indicates that the extraction process involves 4 to 5 molecules of the ligand.

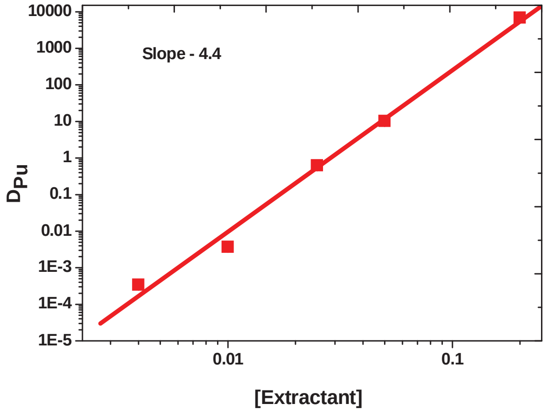

Figure 3.8: Graph showing the variation of D_{Pu} with different concentrations of the extractant L^7 in dodecane at room temperature at 3M HNO_3

3.3.5.6 Extraction of plutonium and americium from different acids: Table 3.5 shows D values for Pu(IV) and Am(III) from different non complexing as well as complexing acids. It is seen that the acid with least complexing anion,(ClO_4^-) showed the highest D value for both Pu(IV) as well as Am(III) and the acid with most complexing anion (PO_4^{3-}) gave minimum D value for Pu(IV) and Am(III). The order of extraction is similar for both metal ions. The strong complexing nature of these anions with Pu(IV) may be adversely affecting the metal ligand complexation which is essential for the extraction process. When considering HCl and HF, even though F^- is more complexing than Cl^- both Pu(IV) as well as Am(III) are better extracted from HF than HCl, which is an unexpected order. However, the fact that F^- is very small ligand as compared to Cl^-, means that more of the ligand molecule may have access to the primary coordination sphere of metal ion which in turn increases the solubilty in the organic phase, hence, the order of extraction.

Table 3.5: Distribution coefficients of Pu(IV) (D_{Pu}) and Am(III) (D_{Am}) in dodecane from 3M of different acids at room temperature (values are within ± 5%)

Medium (3M)	D_{Pu}	D_{Am}
$HClO_4$	7000	8257
HNO_3	6900	16
HF	81	1.38×10^{-3}
HCl	3.35	1.09×10^{-3}
H_2SO_4	0.0048	2.3×10^{-4}
H_3PO_4	0.0018	2.15×10^{-4}

3.3.5.7 Effect of different anions on the extraction of Am(III) from nitric acid: Figure 3.9 shows the effect of different anions on the extraction of Am(III) from 1 M nitric acid into a solution of 0.2 M ligand in dodecane. In the absence of any anion, the D value is very low at 0.016. On adding anions such as I^-, SCN^- ClO_4^- and Br^-, the extraction improved drastically, while addition of anions such as PO_4^{3-} and $C_2O_4^{2-}$ decreased the extraction efficiency. The presence of highly complexing anions like PO_4^{3-} and $C_2O_4^{2-}$ which form strong complexes with Am(III), may prevent complex formation with the ligand, making extraction difficult. However, weakly complexing and less hydrated ions such as I^-, SCN^-, ClO_4^- considerably enhance the extraction process as evidenced from the high extraction efficiency in the presence of these anions. From the single crystal structure of the europium(III) complex with the ligand $\mathbf{L}^6$ (Fig 3.1), which is considered a surrogate for Am(III), it has been shown that the metal ion is surrounded by three ligands, one nitrate group and one water molecule in the primary coordination sphere and two of the nitrate ions are outside the coordination sphere as the charge neutralizing anions. It is very difficult for the weakly complexing anions to change the primary coordination sphere of the metal ions, but these anions can very well be exchanged with the charge neutralizing nitrate ions which are outside the primary coordination sphere. The extraction of cations into a non-polar medium by a neutral extractant, involves neutralizing the charge of the metal ion by an anion and also complexation of the metal ion with the neutral ligand before extraction. If the anion which neutralizes the charge of the metal ion has less hydration around it, then extraction to the non-polar solvent would be easier as shown in Scheme 3.2. This may be the reason for the enhanced extraction of americium(III) when non complexing and less hydrated ions are added to nitric acid medium.

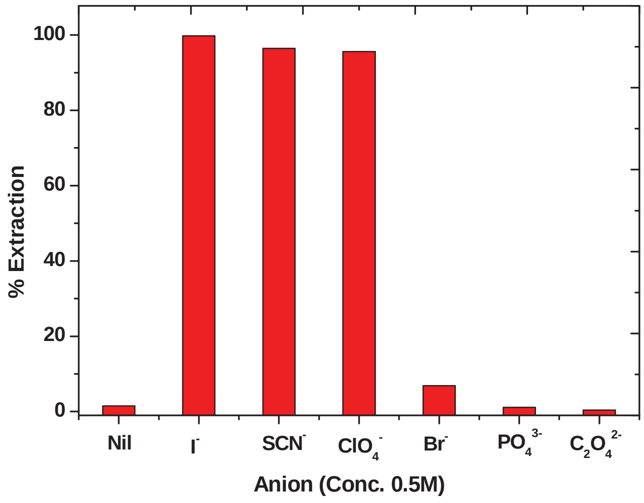

Figure 3.9. **Extraction efficiency of Am(III) in 0.2 M extractant (in dodecane) from 1 M nitric acid in the presence of different anions at room temperature**

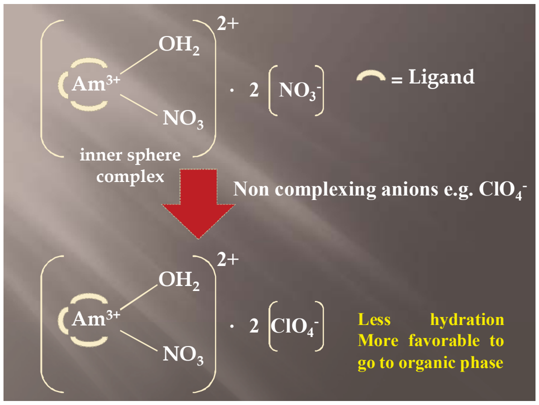

Scheme 3.2 Proposed mechanism for the action of weakly complexing anions on the extractable species in the organic phase.

3.3.5.8 Effect of different anions on the extraction of Pu(IV) from nitric acid: Figure 3.10 shows the effect of the addition of various anions to a 0.5M HNO_3 medium on the percentage extraction of Pu(IV) by the extractant $\mathbf{L^7}$. The results show that the least complexing and less hydrated anions such as I^-, SCN^-, ClO_4^-, Br^- showed positive contributions to the extraction of of Pu(IV). The strongly complexing anions PO_4^{3-} and $C_2O_4^{2-}$, showed a strong negative impact on the extraction of Pu(IV), as these anions may be interfering with the extraction process by forming unextractable complexes with Pu(IV). These findings are coherent with the findings with Am(III) and supports the idea that some of the nitrate groups are outside the coordination sphere of Pu(IV) as well.

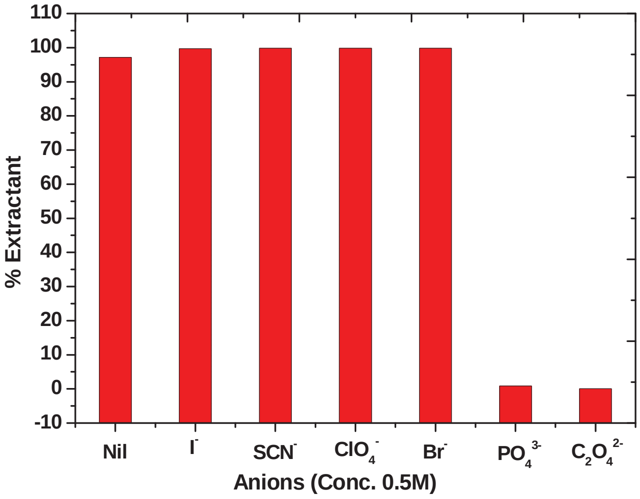

Figure 3.10. Extraction efficiency of Pu(IV) in 0.2 M extractant L^7 (in dodecane) from 0.5 M nitric acid in the presence of different anions at room temperature

3.3.5.9 Effect of non complexing anions on the extraction of Pu(IV) from phosphoric acid medium: Uranium analysis of plutonium bearing fuel samples by the method of Davis and

Gray leads to the generation of aqueous waste containing plutonium in phosphoric acid medium [145]. Recovery of plutonium for its recycling and removal of accompanying Am(III) from the waste is essential for the safe disposal of the effluents. Experiments were carried out to investigate the possibility of extracting plutonium using this extractant (**L**^{7}), from media containing complexing ions like phosphate from which extraction is generally very difficult. Figure 3.11 shows the effect of adding non complexing anions iodide (I^-) and perchlorate (ClO_4^-) on the extraction of plutonium from 1M nitric acid plus 1M $NH_4H_2PO_4$. Pu(IV) exhibited a D value of 155 from 1M HNO_3 and the calculated percentage extraction is 99.36%. As shown in Fig. 3.10, on adding 1M $NH_4H_2PO_4$, the percentage extraction reduced drastically to close to zero. To this medium, when ClO_4^- ion was introduced, the D value and percentage extraction increased rapidly. As evidenced by Fig. 3.11**,** on introducing 0.5M of ClO_4^-, the percentage extraction of plutonium(IV) increased to 97.5%. This showed that, the adverse effect of complexing anion on extraction could be compensated for by the introduction of non-complexing anion such as ClO_4^-. A similar trend was observed when iodide was introduced in 1M HNO_3 plus 1M $NH_4H_2PO_4$. However, in this medium there is gradual oxidation of I^- to I_2 and iodine is extracted to the organic medium interfering with extraction process of Pu IV). Because of this reason, only experiments with lower concentrations of I^- were carried out.

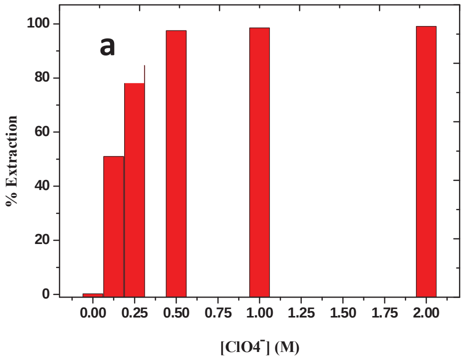

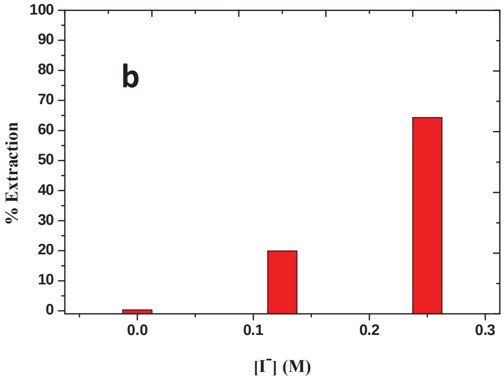

Figure 3.11. Effect of addition of non-complexing anions (a) ClO_4^- ion; (b) I^- ions on the extraction efficiency of Pu(IV) from phosphate medium at room temperature in 1M HNO_3

3.3.5.10 Effect of perchloric acid on extraction of Pu(IV) from different acids: As observed in Table 3.5, Pu(IV) is poorly extracted from H_2SO_4 and H_3PO_4 medium and the percentage extraction is less than 1%. Experiments were carried out to extract plutonium from these media after introduction of acid containing the non-complexing anion ClO_4^-. Fig. 3.12 shows that, by introducing $HClO_4$ to these media, Pu(IV) could be effectively extracted using this extractant, opening a novel procedure to extract plutonium from such media. These results once again confirmed the enhancing effect of non-complexing anions on the extraction of plutonium(IV).

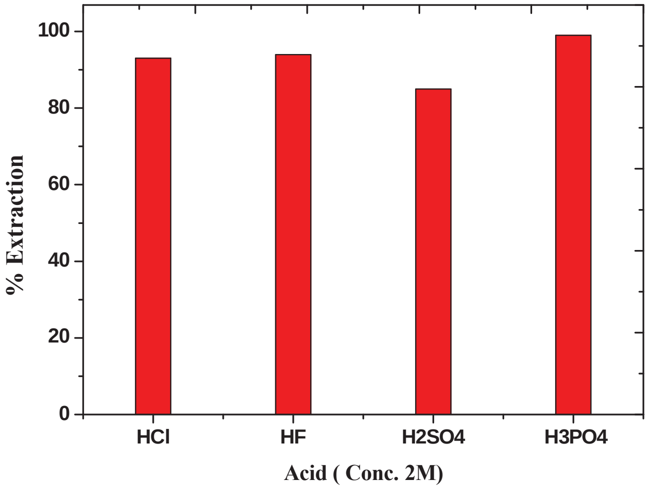

Figure 3.12. Extraction efficiency of Pu(IV) in 0.2M extractant L^7 (in dodecane) from different complexing acids in presence of 3M $HClO_4$ at room temperature

3.3.5.11 Studies on mutual separation of Am(III) and Pu(IV): Solutions containing plutonium(IV) and americium(III) in nitric acid are frequently encountered because of the continuous formation of ^{241}Am by the beta decay of ^{241}Pu. It would be useful if they can be separated during solvent extraction. Table 3.6 gives $D_{Pu(IV)}$, $D_{Am(III)}$ and corresponding separation factors calculated as the ratio of $D_{Pu(IV)}$ and $D_{Am(III)}$. At higher nitric acid concentrations, both cations are extracted and the separation factor is poor. At 0.5 M HNO_3, mainly plutonium is extracted and americium is poorly extracted by $\mathbf{L}^7$ and the separation factor is very high. The data in the Table shows that after removal of Pu(IV) at lower concentration, the nitric acid concentration can be increased by introduction of concentrated nitric acid and americium(III) also can be separately extracted.

Table 3.6. Separation Factor for Am(III) / Pu(IV) from different nitric acid concentrations

[HNO$_3$], M	D$_{Am}$	D$_{Pu}$	S.F. (D$_{Pu}$/D$_{Am}$)
0.5	0.00292	103	35273
1.0	0.016	155	9687
3.0	9.07	6896	760
5.0	543	6814	12.5
7.0	4610	5127	1.11
9.0	6190	4764	0.769

3.3.5.12 Stripping of plutonium from loaded extractant: Studies were carried out on stripping of plutonium(IV) from loaded extractant by reductive stripping (to Pu(III) as well as complexation stripping methods. Am(III) can be easily stripped at low nitric acid concentrations whereas, Pu(IV) showed fairly high D values even at lower concentrations of nitric acid and as expected, the stripping by 0.5M and 0.2M nitric acid was poor. Fig. 3.13 gives the percentage stripping obtained by a single step stripping with different media at an organic to aqueous ratio of 1. Reductive stripping using mixture of nitric acid and hydroxylamine hydrochloride yielded >90% stripping in single step. Reductive stripping using 0.5M HNO$_3$ + 0.1M Fe(II) sulphate yielded a better stripping of 99.5%, probably because Fe(II) is a better reducing agent. Complexation stripping using citric acid or sodium bicarbonate showed partial stripping, whereas complexation stripping using at 0.2M oxalic acid in 0.5M HNO$_3$ yielded near quantitative stripping of 99.97%, but at higher nitric acid concentrations, stripping is not effective.

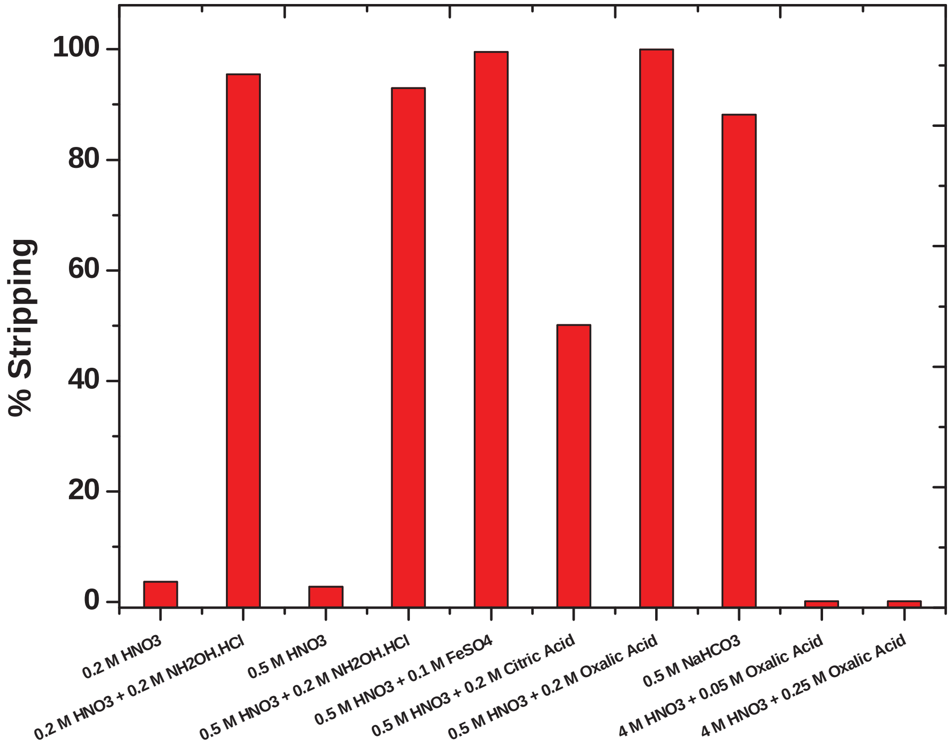

Figure 3.13. Stripping of Pu(IV) from oraganic phase (0.2 M L^7 extractant in dodecane) to aqueous medium using different stripping agents at room temperature.

Very high extraction behavior for trivalent lanthanide and actinide ions from 3-4M HNO_3 and quantitative back extraction by 0.5M HNO_3 showed the potential nature of this novel monoamide extractant (which is ideally suited for the real HLLW solution). This is the first monoamide which shows such an unusual and interesting extraction property with high D values for trivalent lanthanide and actinide ions from 3-4M HNO_3 medium. Poor extraction for the Sr(II) ion from 3-4M HNO_3 solutions reduces one extra step needed during the back extraction process. Due to the promising behaviour for this extractant, we next tried the extraction from simulated HLLW.

3.3.5.13 Extraction of metal ions from simulated HLLW: An extraction study using 0.2M of Ligand $\mathbf{L}^7$ in dodecane with 100 times diluted simulated HLLW solution from 4M HNO_3 was carried out. The preliminary results of this study are given in Table 3.7. These results show that more than 99% of α , 64% of β and 47% of γ activities could be extracted in a single contact. The Cs(I) and Ru(III) ions show either negligible or poor extraction under the conditions studied. The extracted activities (α, β, and γ) could be back extracted using 0.5M HNO_3 or a mixture of 0.2M oxalic acid and 0.5M HNO_3 quantitatively (Table 3.8).

Table 3.7. Extraction data for fission products and alpha emitters by 0.2M L^7 in dodecane from 4.0M HNO_3 having 100 times diluted (simulated) high level active waste

.

	Alpha α mg/L	Beta β mCi/L	Gamma γ mCi/L	^{144}Ce mCi/L	^{106}Ru mCi/L	^{137}Cs mCi/L	^{125}Sb µCi/L	^{95}Nb µCi/L
Feed	98.95	57.71	20.15	10.21	5.66	8.43	2.45	13.78
Raffinate (Aqueous)	<0.2	20.83	10.43	22.0	5.58	8.40	-	-
Loaded Organic	98.7	36.84	9.57	10.2	214µCi/L	-	1.94	11.4

***Extraction Parameters* :** Aqueous feed: 100 times diluted HAW-1 solution in 4.0M HNO_3**;** Conc. of extractant: 0.2M amide in *n*-dodecane**;** Organic to aqueous phase ratio: 1:1, volume of each phase: 4 mL, contact time: 30 min.

Table 3.8. Stripping of fission products and alpha emitters from loaded organic solvent using 0.2M oxalic acid in 0.5M nitric acid

	Alpha A mg/L	Beta β mCi/L	Gamma γ mCi/L	^{144}Ce mCi/L	^{106}Ru µCi/L	^{137}Cs mCi/L	^{125}Sb µCi/L	^{95}Nb µCi/L
Feed (Loaded	92.33	28.84	9.57	10.39	214	-	1.94	11.4

Organic)								
Raffinate-1 (Aqueous Phase)	92.1	-	8.96	9.90	17.8	-	1.94	10.0
Organic Phase	<0.2	-	86.07 µCi/L	94.0µCi/L	196	-	-	1.43

Extraction Parameters: Feed: Loaded organic; Strippant: 0.2M oxalic acid in 0.5M nitric acid; Conc. of extractant: 0.2M amide in *n*-dodecane; Organic to aqueous phase ratio: 1:1 volume of each phase: 1mL, contact time: 30 min.

Advanced fuel reprocessing consists of pyrochemical processes involving molten salts[146]. Ionic liquids, organic salts having melting points below an arbitrary temperature, (for example 150 °C), are considered viable alternatives in view of their wide electrochemical window and also in view of the possibility of working at a much lower temperatures as compared to the molten salts [147]. RTILs (Room Temperature Ionic Liquids) are ionic liquids which exist in the liquid state at room temperature and generally have low vapor pressures, high boiling points, and an ability to exist in the liquid state over a wide range of temperatures and are considered to be green alternatives to the VOC (Volatile Organic Compounds) based diluents like dodecane for metal ion separations [148]. One of the first reports on actinide extraction was by Visser et al., who used solutions of CMPO in ionic liquids. [C_4-mim][PF_6] to extract actinide ions Am^{3+}, Th^{4+}, Pu^{4+} and UO_2^{2+} from nitric acid feeds [149]. Dai et al. reported very high enhancement in metal ion extraction (about four orders of magnitude) in ionic liquids vis – à – vis those observed in molecular diluents [150]. Hence, we studied the extraction behaviour of the ligand $\mathbf{L}^{7}$ in the ionic liquid [C_8-mim][NTf_2].

3.3.5.14 Extraction studies of lanthanides and actindes in ionic liquid: Extraction studies of actinides (UO_2(VI), Pu(VI) and Am(III)) and Eu(III) was carried out with 0.2 M Ligand $\mathbf{L}^{7}$ in the ionic liquid [C_8-mim][NTf_2]. The D values for the extraction of the above ions into the ionic liquid have been calculated from the varying concentrations of HNO_3 (1M-7M) medium. All the above stated ions have very high D values for the extraction in ionic liquid as compared to the molecular diluent (Fig. 3.14). The interesting thing we observed from this study that Eu(III) and Am(III) follows a cation exchange mechanism (D values decreasing with increasing the concentration of HNO_3) while UO_2(VI) and Pu(IV) follows a solvation mechanism.

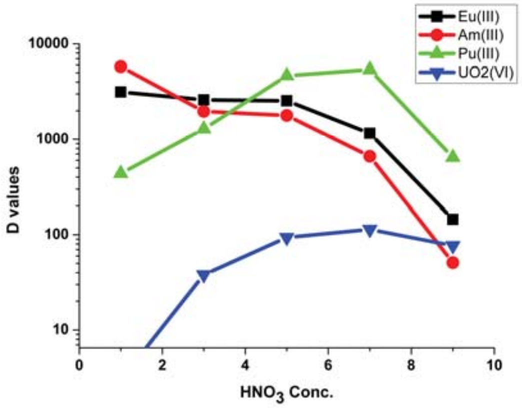

Figure 3.14. Distribution ratios for Pu(IV), Am(III), Eu(III) and UO_2(VI) vs. [HNO_3] at room temperature

In our earlier studies, we have seen that all the metal ions follow the solvation mechanism in dodecane. To confirm the species in molecular solvent as well as in the ionic liquid we have recorded the UV-visible spectra for the complexes of uranyl(VI) and Eu(III)with ligand $\mathbf{L}^7$ in $CHCl_3$ and the ionic liquid. The UV-visible spectra for uranyl(VI) and Eu(III) complexes with ligand $\mathbf{L}^7$ is similar in terms of position of absorption bands in both the solvents as shown in Fig. 3.15 and 3.16. So, this very preliminary study shows that the species in molecular diluents as well as in ionic liquid may be the same.

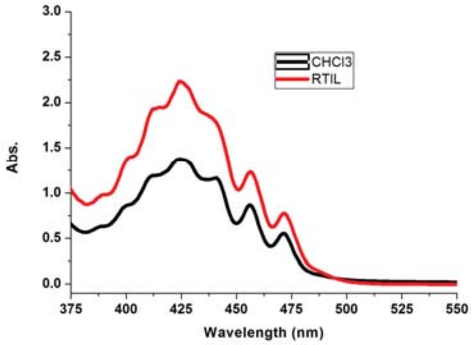

Figure 3.15: UV-vis spectra of uranyl complex in $CHCl_3$ and RTIL

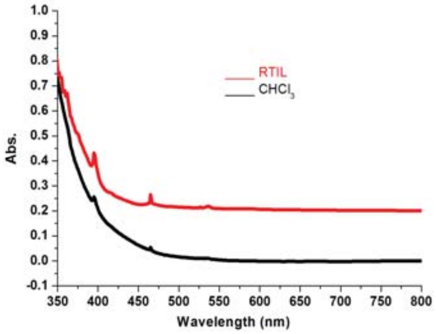

Figure 3.16: UV-vis spectra of europium complex in $CHCl_3$ and RTIL

This study confirms that the extraction of metal ions are far better in the ionic liquid as compared to the molecular diluent with this ligand and hence, it points to the applicability of this ligand system in actinide and lanthanide extractions from the nitric acid medium.

3.4: Conclusions:

High extraction behavior for trivalent lanthanide and actinide ions above 3M HNO_3 and quantitative back extraction by 0.5M HNO_3 showed the potential nature of the novel monoamide extractant $\mathbf{L}^7$. Poor extraction for Sr(II) ions from 3-4 M HNO_3 and Ru(III) from real HLLW solution makes it advantageous over other extractants by reducing extra steps needed during the back extraction process. The structures of the Eu(III), Sm(III) and UO_2(VI) nitrates with $\mathbf{L}^6$ show the ligands acts as a neutral bidentate chelating ligands and bind through the hydroxyl and carbamoyl oxygen atoms to the metal centers. The present investigation has also shown that a newly synthesized, completely incenerable amide based extractant, *N,N'*-dioctyl-α-hydroxy acetamide ($\mathbf{L}^7$) in *n*-dodecane and in the ionic liquid [C_8-mim][NTf_2], extracted both Am(III) and Pu(IV) strongly from acids with anions of low complexing nature such as HNO_3 and $HClO_4$. It also has been concluded that extraction of Am(III) and Pu(IV) is difficult from complexing media such as phosphoric acid, oxalic acid and sulphuric acid with this ligand. However, it was observed that from these complexing acids, Pu(IV) and Am(III) could be extracted by this extractant, after adding less complexing and less hydrated anions such as ClO_4^-, I^- or SCN^- to this medium. This novel observation opens up a new procedure for extraction of metal ions from difficult to extract media. This was confirmed by extracting plutonium(IV) from phosphoric acid medium after adding perchloric acid.

Chapter-4

Synthesis, coordination, and photoluminescence studies of (diphenyl-(2-pyridyl) phosphine oxide and diphenyl-(2-pyridyl-N-oxide) phosphine oxide) with lanthanides and uranyl nitrate

4.1 Introduction:

The basic understanding of complex chemistry of the uranyl ion is very important to design new ligands for the selective separation of this ion from irradiated nuclear fuel, seawater, nuclear plant effluents, biological and environmental samples[151]. Many multifunctional phosphine oxide based ligands have been examined for the separation of actinides and lanthanides from high level nuclear waste solutions [125a, 135a, 152] and their structures with actinide and lanthanide compounds have also been reported [62, 143, 153]. The chemistry of mono and bi functional phosphine oxides with the uranyl ion is well documented. In all cases the phosphine oxide bonds through the oxygen atom to uranyl ion.[61, 102, 154] The chemistry of bi-functional phosphine oxides with the uranyl ion shows different modes of bonding for the ligand depending upon the stoichiometry and nature of ligands around the uranyl group[102]. Recently, there is renewed interest in the coordination and structural chemistry of bi-functional ligands containing soft nitrogen and hard oxygen donor atoms with uranyl(VI) and lanthanide ions.[106, 119-120] Our group's recent studies [120] supports the earlier observations that the complexation reaction of the ligands that form a five membered metallocyclic ring with the metal ion is sterically controlled, compared to that of the corresponding ligands that form six membered metallocyclic rings [155]. Diphenyl (2-pyridyl) phosphine oxide (PON) is a bi-functional ligand having soft pyridine nitrogen and hard phosphine oxide groups. The chemistry of this ligand with transition metal ions has been reported [156]. In all the compounds reported, this ligand acts either as a monodentate ligand *via* the phosphine oxide, or as a chelating ligand *via* both the phosphine oxide and pyridyl nitrogen atoms. Similarly, the diphenyl (2-pyridyl-*N*-oxide) phosphine oxide (PONO) ligand system has also been explored with uranyl(VI) and lanthanide(III) nitrates in view of the potential of this ligand for separations.[157].Due to their f-orbital configurations, lanthanides possess peculiar properties including optically pure emissions and excellent magnetic properties. Their optical properties are utilized in many fields including anion sensing, luminescent devices, temperature sensing and cell imaging [158]. Lanthanides possess good emission properties, but the absorption of light is very weak because of the formally Laporte forbidden f-f transitions. In most of the above stated applications an antenna molecule [159] is needed to pump harvest and transfer the energy into the emissive levels of lanthanides. In some cases, excellent quantum yields up to more than 80% can be achieved [160]. The intrinsic quantum yields are highly dependent on the non radiative processes and are affected by the ligand geometry around the lanthanide ions. Recently, it has been shown that anisotropy in the ligand field around the lanthanide center can have an impact on the emission quantum yield [161]. Lima et al. stated this phenomenon as ECA (Escalating Coordination Anisotropy). Due to increasing anisotropy around lanthanide centers, the Laporte forbidden f-f transitions become less forbidden and hence luminescent quantum yield can be increased significantly. Many antenna molecules are reported in the literature such as β-diketones [162], Schiff bases [163], pyridine carboxylic acids [163b] etc. Of these molecules, the widely studied antenna molecules for optical properties with Eu^{3+} are β-diketones like 1-(2-thenoyl) 3,3,3-trifluoroacetone (HTTA)[164], dibenzoylmethane (HDBM) [165] and 4,4,4-trifluoro-1-phenyl-1,3-butanedione (HBTFA)[166] etc. These antenna molecules efficiently transfer energy to the lanthanide centers, in particular to Eu^{3+}. These β-diketones make neutral tris and anionic tetra complexes with lanthanides [167]. In tris complexes of the above stated β-diketones, auxiliary ligands are necessary to satisfy cordination of lanthanides (8 or 9 coordination). Triphenylphosphineoxide (TPPO) [168], dibenzylsulphoxide (DBSO)[169], 1,10-phenanthroline (phen) [170] and bipyridine (Bipy)[38] are the common auxilliary ligands which are used in preparation of luminescent lanthanide complexes. To the best of our knowledge, diphenyl-(2-pyridyl)-phosphine oxide (PON) and diphenyl-(2-pyridyl-*N*-oxide)-phosphine oxide (PONO) have not been used as the auxiliary ligands in lanthanide tris-(β-diketonate) system. However, no report on the chemistry of the PON ligand with any of the 4f or 5f elements is reported in the literature.

We report herein the coordination chemistry of diphenyl-(2-pyridyl)-phosphine oxide with uranyl(VI) nitrate and uranyl(VI) bis-(β-dibenzoylmethanates). Similarly, the coordination as well as photoluminescent properties of lanthanide β-diketonates with PON and PONO ligands were also explored.

4.2 Experimental:

4.2.1 General Consideration: All reagents and solvents were of analytical grades and used as received. IR spectra were recorded using a Bruker Platinum ATR-FTIR spectrometer. ^{1}H and ^{31}P NMR spectra were recorded using a Bruker AMX-300Mhz spectrometer. The chemical shifts (δ) are reported in ppm. Mass spectra were recorded on Advion Mass Spectrometer, USA using electron spray ionization (ESI) in positive mode. All luminescence measurements were carried out using an Edinburgh Instruments FLSP 920 system equipped with 450W Xe lamp, 60W microsecond flash lamp and a hydrogen nanosecond flash lamp as excitation sources.

4.2.2 Synthesis of ($\{C_6H_5\}_2POC_5H_4N$) (L^8): 5 g (19 mmol) of diphenyl-2-pyridyl phosphine was taken in 50mL of benzene. 2 mL of 30% H_2O_2 was added into it and stirred for 5 hours. The mixture was dried over sodium sulphate and after evaporation of benzene, a light yellow powder was obtained. This was then washed with hexane and dried. Yield – 85 %. ^{31}P {^{1}H} NMR (25 °C, $CDCl_3$, δ in ppm): 21.28 ^{1}H NMR (25 °C, $CDCl_3$, δ in ppm): 7.40 -7.88 (m, 14H, Aromatic). IR (cm^{-1}): ν = 1189 (m, P=O). ESI-MS, *m/z*: 279.7 [M-H]$^+$ Elemental analysis (%): Calcd for $C_{17}H_{14}NOP$ (279): C, 73.11; H, 5.05; N, 5.02. Found: C, 73.15; H, 5.09; N, 4.98

4.2.3 Synthesis of ($\{C_6H_5\}_2POC_5H_5NO$) (L^9): 2 g (~7 mmol) of ligand L^8 is taken in chloroform and 1.2 g (~7mmol) *m*-CPBA (*m*-chloroperbenzoic acid) were added to the solution at 0°C. The mixture was stirred for 4 hrs washed with $NaHCO_3$ and dried over sodium sulphate after evaporation; a white product is obtained. Yield: 72%. .^{31}P $\{^1H\}$ NMR (25 °C, $CDCl_3$, δ in ppm): 23.59 ^1H NMR (25 °C, $CDCl_3$, δ in ppm): 7.45 -8.37 (m, 14H, Aromatic). IR (cm^{-1}): ν = 1180 (m, P=O), 1271 (N-O). ESI-MS *m/z*: 295.7, $[M-H]^+$: Elemental analysis (%): Calcd for $C_{17}H_{14}NO_2P$ (295): C, 69.15; H, 4.78; N, 4.74. Found: C, 69.29; H, 4.69; N, 4.62.

4.2.4 Synthesis of [$UO_2(NO_3)_2(\{C_6H_5\}_2POC_5H_5N)$] (8) : To a solution of $\mathbf{L^8}$ (112 mg, 400 mmol) in methanol (20 mL), solid [$UO_2(NO_3)_2{\cdot}6H_2O$] (100 mg, 200 mmol) was added and stirred for few minutes until all [$UO_2(NO_3)_2{\cdot}6H_2O$] dissolved to give a clear solution. This solution was filtered and layered with *iso*-octane. The solution on slow evaporation yielded yellow crystalline solid, which was filtered, washed with hexane, and dried. Yield: - 84 %. $^{31}P\{^1H\}$ NMR (25 °C, $CDCl_3$), δ in ppm): 36.73 . IR (cm^{-1}): ν = 1161 (m, P=O). Elemental analysis (%): Calcd for $C_{34}H_{28}N_4O_{10}P_2U$: C, 42.9; H, 3.0; N, 5.9. Found: C, 42.7; H, 2.9; N, 5.8

4.2.5 Synthesis of [$UO_2(DBM)_2(C_6H_5\}_2POC_5H_5N)$] (9): To a solution of $\mathbf{L^8}$ (57 mg, 200 mmol) in methylene chloride (20 mL), solid [$UO_2(DBM)_2{\cdot}H_2O$] (150 mg, 200 mmol) was added and stirred for few minutes until all [$UO_2(DBM)_2{\cdot}H_2O$] dissolved to give a clear solution. This solution was filtered and layered with *iso*-octane. The solution on slow evaporation yielded orange crystalline solid, which was filtered, washed with hexane and dried. Yield: - 90 %. $^{31}P\{^1H\}$ NMR (25 °C, $CDCl_3$): δ = 31.80 ppm. . IR (cm^{-1}): ν = 1171 (m. P=O). Elemental analysis (%): Calcd for $C_{64}H_{50}N_2O_8P_2U$: C, 60.3; H, 3.9; N, 2.2. Found: C, 60.2; H, 2.0; N, 2.1

4.2.6 General Synthesis of Ln(β-diketonate)$_3$.2H$_2$O: Sodium hydroxide (3mmol) is taken in methanol and stirred for an hour, when all sodium hydroxide dissolved, β-diketone (3 mmol) was added into it and stirred for 15 minutes. $LnNO_3.5H_2O$ (1 mmol) is added into the solution, immediately a white precipitate is observed. The solution is stirred for another two hours, filtered through celite and the filtrate is evaporated to dryness. The residue obtained is redissolved in chloroform and filtered. The filtrate on evaporation yielded a white solid of desired compound. [Sm(TTA)$_3$.2H$_2$O]: Yield (85%); [Sm(DBM)$_3$.2H$_2$O]: Yield (83%); [Eu(TTA)$_3$.2H$_2$O]: Yield (85%) and [Eu(DBM)$_3$.2H$_2$O]: Yield (83%).

4.2.7 Synthesis of [Eu(TTA)$_3$.({C$_6$H$_5$}$_2$POC$_5$H$_5$N)$_2$] (10): Eu(TTA)$_3$.2H$_2$O (0.5 mmol) was taken in $CHCl_3$ and Ligand **L^8** (1mmol) is added to the solution and stirred for 4 hours. After evaporation of the solvent, white product is obtained. (Yield 79%). IR (cm^{-1}): ν = 1158 (P=O). Elemental analysis (%): Calcd for $C_{58}H_{40}EuF_9N_2O_8P_2S_3$ (1374.06): C, 50.7; H, 2.93; N, 2.04. Found: C, 50.8; H, 2.82; N, 2.10. ESI-MS: m/z = 1373.9 , [M]$^+$

4.2.8 Synthesis of [Eu(DBM)$_3$.({C$_6$H$_5$}$_2$POC$_5$H$_5$N)$_2$] (11): Eu(DBM)$_3$.2H$_2$O (0.5 mmol) was taken in $CHCl_3$ and Ligand L^8(1mmol) is added to the solution and stirred for 4 hours. After evaporation of the solvent, white product is obtained. (Yield 76%). IR (cm^{-1}): ν = 1153 (P=O). Elemental analysis (%): Calcd for $C_{79}H_{61}EuN_2O_8P_2$ (1380.27): C, 68.74; H, 4.45; N, 2.03. Found: C, 68.2; H, 4.72; N, 2.11. ESI-MS: m/z = 1380.22, [M]$^+$

4.2.9 Synthesis of [Sm(TTA)$_3$.({C$_6$H$_5$}$_2$POC$_5$H$_5$N)$_2$] (12): Sm(TTA)$_3$.2H$_2$O (0.5 mmol) was taken in $CHCl_3$ and Ligand L^8 (1mmol) is added to the solution and stirred for 4 hours. After evaporation of the solvent, white product is obtained. (Yield 81%).^{31}P{^{1}H} NMR (25 °C, $CDCl_3$): δ = 28.46 ppm. IR (cm^{-1}): ν = 1159 (P=O). Elemental analysis (%): Calcd for $C_{58}H_{40}F_9N_2O_8P_2S_3Sm$ (1372.46): C, 50.76; H, 2.94; N, 2.04. Found: C, 50.52; H, 2.78; N, 2.11. ESI-MS: m/z = 1372.5, [M]$^+$

4.2.10 Synthesis of [Sm(DBM)$_3$.({C_6H_5}$_2$POC$_5$H$_5$N)$_2$] (13): Sm(DBM)$_3$.2H$_2$O (0.5 mmol) was taken in CHCl$_3$ and Ligand L$^{\mathbf{8}}$ (1mmol) is added to the solution and stirred for 4 hours. After evaporation of the solvent, white product is obtained. (Yield 71%).^{31}P{^{1}H} NMR (25 °C, CDCl$_3$): δ = 22.71 ppm. IR (cm^{-1}): ν = 1154 (P=O).Elemental analysis (%): Calcd for $C_{79}H_{61}N_2O_8P_2Sm$ (1378.67): C, 68.82; H, 4.46; N, 2.03. Found: C, 68.10; H, 4.62; N, 2.16. ESI-MS: m/z = 1377.1[M-H].

4.2.11 Synthesis of [Eu(TTA)$_3$. ({C_6H_5}$_2$POC$_5$H$_5$NO)] (14): Eu(TTA)$_3$.2H$_2$O (0.5 mmol) was taken in CHCl$_3$ and Ligand L$^{\mathbf{9}}$ (1mmol) is added to the solution and stirred for 4 hours. After evaporation of the solvent, white product is obtained. (Yield 75%). IR (cm^{-1}): ν = 1164 (P=O), 1228 (N-O). Elemental analysis (%): Calcd for $C_{41}H_{26}EuF_9NO_8PS_3$ (1110.78): C, 44.33; H, 2.36; N, 1.26. Found: C, 45.4; H, 2.30; N, 1.19. ESI-MS: m/z = 1110.6, [M]$^+$.

4.2.12 Synthesis of [Eu(DBM)$_3$.({C_6H_5}$_2$POC$_5$H$_5$NO)] (15): Eu(DBM)$_3$.2H$_2$O (0.5 mmol) was taken in CHCl$_3$ and Ligand L$^{\mathbf{9}}$ (1mmol) is added to the solution and stirred for 4 hours. After evaporation of the solvent, white product is obtained. (Yield 79%). IR (cm^{-1}): ν = 1155 (P=O), 1219 (N-O). Elemental analysis (%): Calcd for $C_{62}H_{47}EuNO_8P$ (1117): C, 66.67; H, 4.24; N, 1.25. Found: C, 65.23; H, 4.33; N, 1.36. ESI-MS: m/z = 1120.2, [M+3H]$^+$.

4.2.13 Synthesis of [Sm(TTA)$_3$.({C_6H_5}$_2$POC$_5$H$_5$NO)] (16) : Sm(TTA)$_3$.2H$_2$O (0.5 mmol) was taken in CHCl$_3$ and Ligand L$^{\mathbf{9}}$ (1mmol) is added to the solution and stirred for 4 hours. After evaporation of the solvent, white product is obtained. (Yield 72%).^{31}P{^{1}H} NMR (25 °C, CDCl$_3$): δ = 24.84 ppm. IR (cm^{-1}): ν = 1125 (P=O), 1228 (N-O). Elemental analysis (%): Calcd for $C_{41}H_{26}F_9NO_8PS_3Sm$ (1109.18): C, 44.4; H, 2.36; N, 1.26. Found: C, 45.9; H, 2.50; N, 1.29. ESI-MS: m/z = 1109.1, [M]$^+$.

4.2.14 Synthesis of [Sm(DBM)$_3$.({C_6H_5}$_2$POC$_5$H$_5$NO)](17): Sm(DBM)$_3$.2H$_2$O (0.5 mmol) was taken in CHCl$_3$ and Ligand L^9 (1mmol) is added to the solution and stirred for 4 hours. After evaporation of the solvent, white product is obtained. (Yield 82%).^{31}P{^{1}H} NMR (25 °C, CDCl$_3$): δ = 24.80 ppm. IR (cm^{-1}): ν = 1157 (m, P=O), 1217 (m, N-O). Elemental analysis (%): Calcd for $C_{62}H_{47}NO_8PSm$ (1115.39): C, 66.76; H, 4.25; N, 1.26. Found: C, 66.00; H, 4.19; N, 1.33. ESI-MS: m/z = 1114.6, [M-H]$^+$.

4.2.15 Crystallography: Crystal data for **8, 9 and 12** were measured on a Oxford Diffraction X-Calibur CCD System at 150(2)K with the MoK$_\alpha$ radiation (λ = 0.71073 Å). The crystals were positioned at 50 mm from the CCD. 321 frames were measured with a counting time of 10 s. For complex **17,** the data was collected on an Agilent SuperNova system equipped with a Titan CCD detector at 293(2) K using CuKα radiation (λ = 1.5418 Å). The crystals were positioned at 101 mm from the CCD. 925 frames were measured with a counting time of 1s. Data analyses for all the crystals were carried out with the CrysAlis program [111]. The structures were solved using direct methods with the Shelxs97 program [112]. All non-hydrogen atoms were refined with anisotropic thermal parameters. The hydrogen atoms bonded to carbon atoms were included in the geometric positions and given thermal parameters equivalent to 1.2 times those of the atoms to which they attached. Empirical absorption corrections were carried out using the ABSPACK program [113]. The structures were refined to convergence on F^2 using Shelxl97 [18b.] Selected crystallographic data for **8, 9, 12 and 17** are summarized in Table 4.1a and 4.1b.

Table 4.1a: Crystal refinement data of compounds 8 and 9,

	8	**9**
Empirical Formula	$C_{34}H_{28}N_4O_{10}P_2U$	$C_{47}H_{36}NO_7PU$
Crystal system	monoclinic	monoclinic

Space group	P 2_1/n	P 2_1/c
a (Å)	9.726(3)	17.9927(6)
b (Å)	11.074(3)	11.1401(3)
c (Å)	15.9365(14)	20.5688(6)
β (°)	93.180(19)	101.982(3)
V (cm^3)	1713.9(7)	4033.0(2)
Z	2	4
ρ_{calcd} [g cm^{-3}]	1.846	1.640
μ [mm^{-1}]	4.893	4.118
Reflections collected/ unique	4935/3357	11019/7975
Data/restrains/parameters	4935/0/233	11019/0/422
Goodness of fit on F^2	1.011	1.138
Final R_1 indices [I > 2σ(I)]	0.0606	0.0757
wR_2 indices (all data)	0.1080	0.1097

w = 1/[$\sigma^2(Fo^2)+(0.0062P)^2+0.000P$] for **8**, w = 1/[$\sigma^2(Fo^2)+(0.0252P)^2+19.3201P$] for **9** , where P = (Fo^2 +2Fc^2)/3

Table 4.1b: Crystal refinement data of compounds 12 and 17

	12	**17**
Empirical Formula	$C_{58}H_{40}F_9N_2O_8P_2S_3Sm$	$C_{62}H_{47}NO_8PSm$
Crystal system	triclinic	monoclinic
Space group	P -1	P 2_1/c
a (Å)	11.0848(4)	10.0703 (2)
b (Å)	11.8351(5)	22.3352 (4)
c (Å)	23.1047 (9)	27.7005 (6)
α (°)	81.285 (3)	--------
β (°)	76.852 (3)	97.987 (2)
γ (°)	70.690 (4)	--------
V (cm^3)	2776.0 (2)	6170.0 (2)
Z	2	4
ρ_{calcd} [g cm^{-3}]	1.642	1.201
μ [mm^{-1}]	1.316	7.785

Reflections collected/ unique	15534/13697	12019/8925
Data/restraints/parameters	15534/0/749	12019/180/658
Goodness of fit on F^2	1.052	0.981
Final R_1 indices [$I > 2\sigma(I)$]	0.0449	0.0788
wR_2 indices (all data)	0.0979	0.2194

$w=1/[\sigma^2(Fo)^2+(0.0331P)^2+2.4396P]$ for **12** and $w=1/[\sigma^2(Fo)^2+(0.1469P)^2]$ for **17** where $P=(Fo^2+2Fc^2)/3$

4.2.16 Theoretical methods: Full geometry optimization for all the ligand PON and uranyl nitrate complexe has been carried out applying a popular non-local correlated hybrid density functional, namely, B3LYP. The crystal structures were taken as the initial geometry for optimization of the complexes for locating the minimum energy structure. Gaussian type atomic basis functions, 6-31 + G(d), were adopted for H, C, N, O and S atoms while for the U atom, SARC-ZORA [114] basis sets were used for all the calculations. SARC-ZORA basis sets are segmented all-electron scalar relativistic basis sets in which the coefficients of contracted GTOs have been optimized for use with the ZORA scalar relativistic Hamiltonian. This particular basis set for U was obtained from the Extensible Computational Chemistry Environment Basis Set Database, Pacific Northwest National Laboratory [115]. Geometry optimization to locate the minimum energy structure was carried out applying a quasi-Newton–Raphson based algorithm. The energy of the systems was further improved by performing single point calculations at the MP2 level, adopting the same set of basis functions. These calculations have been performed applying the GAMESS suit of ab initio programs on a LINUX cluster platform [116].

4.3 Results and discussion:

4.3.1 Synthesis of (L^8): This ligand was prepared by the oxidation of corresponding phosphine with H_2O_2 in benzene (Scheme-4.1). The IR spectrum of the ligand shows the presence of P=O (1190 cm^{-1}) group in the synthesized ligand. ^{31}P NMR spectroscopy shows a single resonance at δ = 21.6 ppm, which is 25.5 ppm downfield as compared to starting phosphine (δ = -3.9 ppm). The ^{1}H NMR spectrum shows the expected peaks and integrations. The CHN analyses support the expected stoichiometry for the prepared ligand. The positive ESI-MS spectrum of the ligand clearly shows the molecular ion peak at m/z :279.7.

4.3.2 Synthesis of (L^9): **L^9** was prepared by the oxidation of pyridine group of **L^8** by *m*-chloroperbenzoic acid in dichloromethane (scheme- 4.1). The IR spectrum of the ligand shows the presence of *N*-oxide (1271 cm^{-1}) and P=O groups (1180 cm^{-1}). ^{31}P NMR spectroscopy shows a single resonance at δ = 23.6 ppm, which is ~2 ppm downfield as compared to **L^8** ligand. The ^{1}H NMR shows the expected peaks and integrations. The CHN analyses support the expected stoichiometery for the prepared ligand. The positive ESI-MS spectrum of the ligand clearly shows the molecular ion peak at m/z = 295.7.

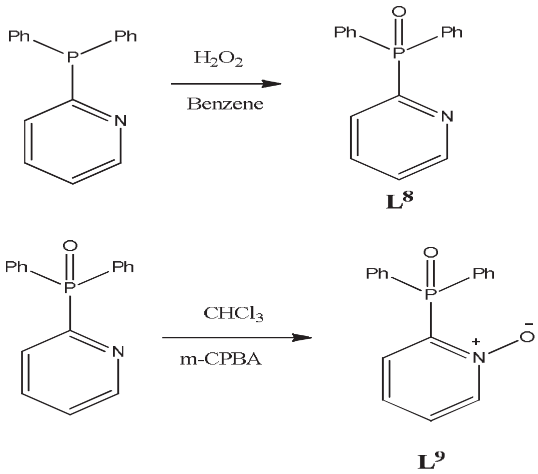

Scheme-4.1: Synthesis of ligands (diphenyl, (2-pyridyl) phosphine oxide (L^8) and diphenyl-(2-pyridyl-N- oxide) phosphine oxide) (L^9)

4.3.3 Synthesis of diphenylphosphino pyridine oxide uranyl nitrate complex. The reaction of [$UO_2(NO_3)_2 \cdot 6H_2O$] with the ligand $\{C_6H_5\}_2POC_5H_5N$ yielded compound **8** (Scheme 4.2).

CHN analyses revealed that the ratio of uranyl nitrate to ligand is 1:2 in the compound. The IR spectrum of **8** shows that the water molecules from the starting compound $[UO_2(NO_3)_2{\cdot}6H_2O]$ are completely replaced by the ligand and that the ligand is bonded through the phosphoryl oxygen atom to the uranyl group. The observed frequency difference for the PO group ($\Delta\nu_{PO} = 30$ cm^{-1}, where $\Delta\nu_{PO} = \nu_{PO\ (free\ ligand\ )} - \nu_{PO(\ coordinated)}$) group shows that the phosphoryl group is bonded to the uranyl group directly [102, 154]. This difference is comparable in magnitude with those observed in $[UO_2(NO_3)_2\ (DPPMO_2)]$[102] , $[UO_2(NO_3)_2\ (DPPFO_2)]$[154b] and $[UO_2Cl_2(DPPFO_2))]$ [154c] $[UO_2(DPPMO_2)_2(OPPh_3)][(BF_4)_2]$ [171] and $[UO_2(OPPh_3)_4\ ][(OTf)_2\ ]$[172].

The $^{31}P\{^1H\}$ NMR spectrum of **8** shows single resonance at δ 36.7 ppm, which is 15.4 ppm downfield compared to the uncomplexed ligand. This observation further supports the coordination of the phosphoryl oxygen atom to uranyl group. The ^1H NMR spectrum of **8** shows the expected peaks and integrations. All protons are deshielded with respect to the free ligand indicating that the bonding between the ligand and uranyl group persists in solution. The ESI-MS spectrum of **8** in positive mode in acetonitrile shows the presence of a peak at *m/z* 581.5 $[\{(UO_2(\mathbf{L^8})_3(H_2O)_3+2H)\}^{2+}$, 100%] and 302 $[\{(UO_2(\mathbf{L^8})(H_2O)_3+H)\}^{2+}$, 100%], indicating that the metal ligand bonding is retained in solution. It is apparent from the IR and NMR spectral results that the ligand bonds through the phosphoric oxygen atoms to the uranyl group.

4.3.4 Synthesis of diphenyl-(2-pyridyl)-phosphine oxide uranyl bis(dibenzoyl methanate) complex: The reaction of $(C_6H_5)_2POC_5H_5N$ with $[UO_2(C_6H_5COCHCOC_6H_5)_2.2H_2O]$ yielded compound **9** (Scheme 4.2). CHN analyses revealed that the ratio of ligand to uranyl bis(dibenzoylmethanate) is 1:1 in the compound. The IR spectrum of **9** shows that the water molecules from the starting compound $[UO_2(C_6H_5COCHCOC_6H_5)_2.2H_2O]$ are completely replaced by the ligand and furthermore the observed frequency difference for thephosphoryl ($\Delta\nu_{PO}$ = 20 cm^{-1}, where $\Delta\nu_{PO} = \nu_{PO\ (free\ ligand\ )} - \nu_{PO(\ coordinated)}$) group is consistent with the supposition that the phosphoryl group is bonded to the uranyl group directly.

The ^{1}H NMR spectrum of **9** shows the expected peaks and integrations. The $^{31}P\{^{1}H\}$ NMR spectrum of **9** shows a single resonance at 31.8 ppm, which is deshielded about 10 ppm with respect to the uncomplexed ligand, indicating the metal ligand bonding persists in solution.

$$[UO_2(NO_3)_2\ .6H_2O] \quad + \quad \mathbf{2.\ L^8} \longrightarrow \quad [UO_2(NO_3)_2\ .2\ (\mathbf{L^8})]$$

(8)

$$[UO_2(DBM)_2\ .H_2O] \quad + \quad \mathbf{L^8} \longrightarrow \quad [UO_2(DBM)_2\ .(\mathbf{L^8})]$$

(9)

Scheme-4.2: Synthesis of the uranyl complexes

4.3.5 Molecular Structure of [$UO_2(NO_3)_2(\{C_6H_5\}_2POC_5H_5N)_2$] (8). The structure of **8** is shown in Figure 4.1, and selected bond distances and angles are given in Table 4.2. The pyridyl ring shows a disorder over two positions and was taken in to account during the refinement. The structure consists of a centrosymmetric [$UO_2(NO_3)_2(\{C_6H_5\}_2POC_5H_5N)_2$] moiety, in which the uranium atom is surrounded by eight oxygen atoms in a hexagonal bi-pyramidal geometry. Four oxygen atoms of the two bidentate nitrate groups, together with two oxygen atoms of diphenyl-(2-pyridyl)-phosphine oxide ligand form the equatorial hexagonal plane. The UO_6 atoms in the equatorial plane show an r.m.s deviation of 0.029Å. The two uranyl oxygen atoms occupy the axial positions.

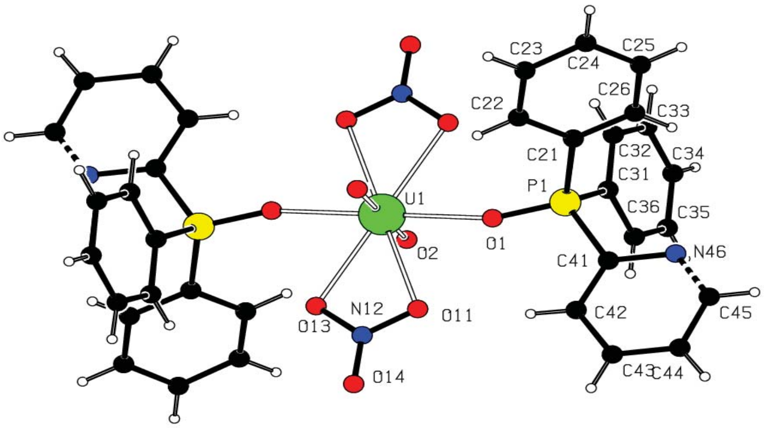

Figure 4.1 The Structure of complex $[UO_2(NO_3)_2(\{C_6H_5\}_2POC_5H_5N)_2]$ (8)

This type of co-ordination is similar to that observed in the compounds of phosphine oxide, amides and pyrolidone with uranyl nitrate such as, $[UO_2(NO_3)_2(OPBu_3)_2]$ [61], $[UO_2(NO_3)_2(amide)_2]$ [56], $[UO_2(NO_3)_2$(*N*-cyclohexyl,2-pyrrolidone)$_2]$ [118] and $[UO_2(NO_3)_2$(1,3-dimethyl,2-imidazolidone)$_2]$ [54] . The average U-O$_{(phosphine\ oxide)}$ distance (2. 350(4) Å) in **8** is comparable in magnitude with those of earlier reported uranyl nitrate-phosphine compounds such as, $[UO_2(NO_3)(TBPO))_2]$ [61] , $[UO_2(NO_3)_2(DPEPA)_2]$ (2.347(5) , 2.379(4) Å) [154a], $[UO_2(NO_3)_2(TPPA)_2]$ (2.340(3) Å) [154a], $[UO_2(NO_3)_2(DPPMO_2)]$ (2.386(9) Å) [102] , $[UO_2(NO_3)_2(CMPO)]$ (2.380 (2) Å) [59] , and $[UO_2(NO_3)_2(DPPFO_2)]$ (2.352(2) Å) [154b] . The observed average U-O(NO_3) (2.534(5) Å) and U-O(uranyl) (1.758(4) Å) distances are normal. The angles subtended at the metal atom show that the uranium atom has a slightly distorted hexagonal bi-pyramidal geometry.

It is interesting to note here that the ligand forms a 2:1 complex with the uranyl nitrate and bonds through the phosphine oxide oxygen atoms to metal centre leaving the pyridyl nitrogen un-coordinated. The chelating mode of bonding via the phophine oxide oxygen and pyridyl nitrogen atoms for this ligand with transition metal ions forming five membered metallocyclic rings is reported. We have also reported recently that the pyrazoyl urea ligand [120] forms five member metallocylcic rings with the uranyl(VI) ion via the pyrazolyl nitrogen and carbamoyl oxygen atoms. In order to find out the reason for not forming five member metallocyclic ring or not acting as a chelating ligand with the uranyl(VI) ion , theoretical studies were carried out. This study reveals clearly that the steric effect plays an important role in deciding the mode of bonding for this ligand. [173]

Table 4.2 : Important bond lengths (Å) and angles (°) for 8 and 9

	8		
U1 – O1	2.350(5)	U1 – O11	2.530(5)
U1 – O2	1.758(4)	U1 – O13	2.538(5)
P1 – O1	1.521(4)		
O2 – U1 – O2	180.0(2)	O2 – U1 – O1	89.73(19)
O2 – U1 – O11	89.83(19)	O2 – U1 – O13	90.34(18)
O1 – U1 – O11	64.45(15)	O1 – U1 – O13	114.55 (16)
O11 – U1 – O13	50.11(14)	P12– O1 – U1	159.6(3)
	9		
U1 – O1	1.770(5)	U1 – O31	2.357(6)
U1 – O2	1.775(5)	U1 – O35	2.352(6)
U1 – O15	2.381(6)	U1 – O11	2.329(5)
U1 – O3	2.389(5)	P3 – O3	1.487(5)
O1 – U1 – O2	178.7(2)	O31 – U1 – O35	70.10(19)
O31 – U1 – O3	73.88(19)	O3 – U1 – O15	74.25(18)
O11 – U1 – O15	69.64(19)	O11 – U1 – O35	72.9(2)
P3 – O3 – U1	167.4(3)	O3 – U1 – O35	143.85(19)
O3 – U1 – O11	142.9(2)		

4.3.6 Molecular Structure of [$UO_2(C_6H_5COCHCOC_6H_5)_2(C_6H_5)_2POC_5H_5N$] (9): The structure of **9** is shown in Figure 4.2 and selected bond distances and angles are given in Table 4.2. The structure shows that the uranyl group is bonded to two $C_6H_5COCHCOC_6H_5$ groups and a diphenyl-(2-pyridyl)-phosphine oxide ligand to give a coordination number of seven. The diphenyl-(2-pyridyl)-phosphine oxide ligand acts as a monodentate ligand and is bonded through the phosphine oxygen atom to the uranyl group. Four oxygen atoms from two bidentate $C_6H_5COCHCOC_6H_5$ groups and one oxygen from the phosphine oxide form the equatorial plane and together with two oxygen atoms of the uranyl group form a pentagonal bi-pyramidal geometry around the uranium(VI) ion.

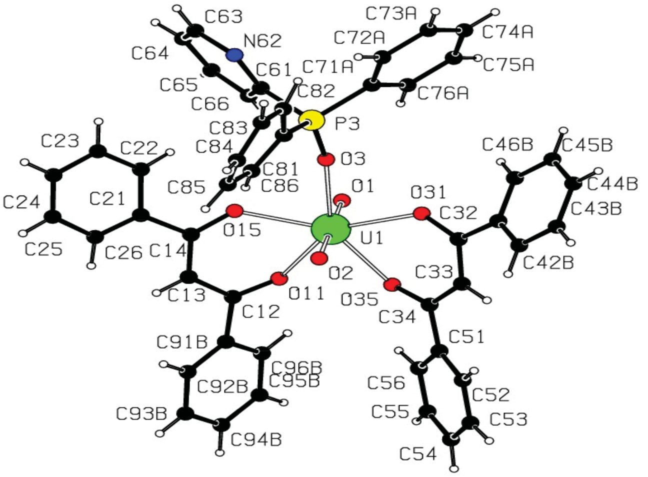

Figure 4.2: Structure of complex [$UO_2(C_6H_5COCHCOC_6H_5)_2(C_6H_5)_2POC_5H_5N$] (9)

The five oxygen atoms in the equatorial plane show an r.m.s deviation of 0.102 Å. Similar structures are also observed in the compounds of phosphine oxides, sulfoxides, ketones, *N*-oxides and amides with the uranyl(VI) bis (β-diketonates) viz: [$UO_2(DBM)_2(OPPh_3)$] [72b], [$UO_2(TTA)_2TIBP$] [174], [$UO_2(DBM)_2(C_6H_5SOCH_3)$] [175], [$UO_2(TTA)_2(C_5H_5NO)$] [72a], [$UO_2(DBM)_2(camphor]$[21], [$UO_2(DBM)_2(C_4H_9CON\{C_4H_9)_2)$] [176] and [$UO_2(DBM)_2({}^{i}C_3H_7CON\{{}^{i}C_3H_7)_2)$] [56]. The observed U-O phophine oxide bond distance

(2.389(5)Å) is comparable with the earlier reported uranyl(VI) bis (β-diketonate)-phosphine oxide compounds [177].

4.3.7 Theoretical studies on dipheny (2-pyridyl) phosphine oxide uranyl nitrate compound

To examine the feasibility of binding the uranyl(VI) ion with this compound as either a chelating ligand binding through both the phosphine oxide and pyridyl nitrogen atoms or as a monodentate ligand binding through phosphine oxide oxygen atom, quantum chemical calculations have been carried out. Full geometry optimization of possible complexes has been performed under isolated gas phase conditions as well as in solution following a macroscopic solvation model in dichloromethane. The minimum energy structures predicted in solution are presented in Figure 4.3 (a-b).

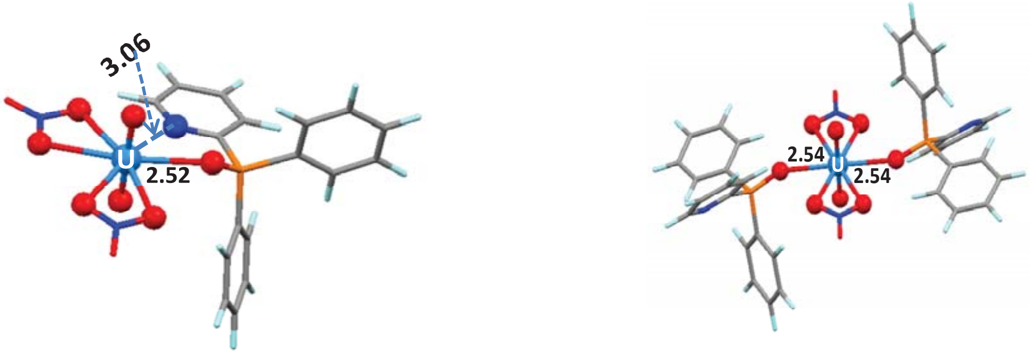

(a) (b)

Figure 4.3 (a) DFT optimized structures for $[UO_2(NO_3)_2PON]$ and (b) $[UO_2(NO_3)_2.2PON]$

In the chelated complex, the calculated bond distance between U and O atom of the ligand is 2.52 Å whereas the same between U and N atom of the ligand is 3.06 Å. The large bond distance appears to be due to steric hindrance. The calculated bond distance between U and O atom of the ligand is little longer as shown in Fig. 4.3. Note that these bond distance parameters are about 0.1 Å shorter compared to those calculated in gas phase. To calculate the binding energy of the chelating ligand and $UO_2(NO_3)_2$, the energy of the whole complex was calculated increasing the distance between the ligand and $UO_2(NO_3)_2$ unit to generate a dissociation curve and thus the binding energy is calculated as 37.7 kcal/mol. In case of monodentate complex, the dissociation curve is generated by calculating the energy at increasing distance of the U and O atoms of both ligands. The total binding energy is thus calculated as 52.2 kcal/mol. This suggests that binding energy per ligand is predicted as 25.6 kcal/mol. Thus, binding of the pyridyl nitrogen atom with U provides approximately 12.1 kcal/mol stability to the complex and this is quite low compared to the stability provided by the O atom of phosphine oxide of the ligand.

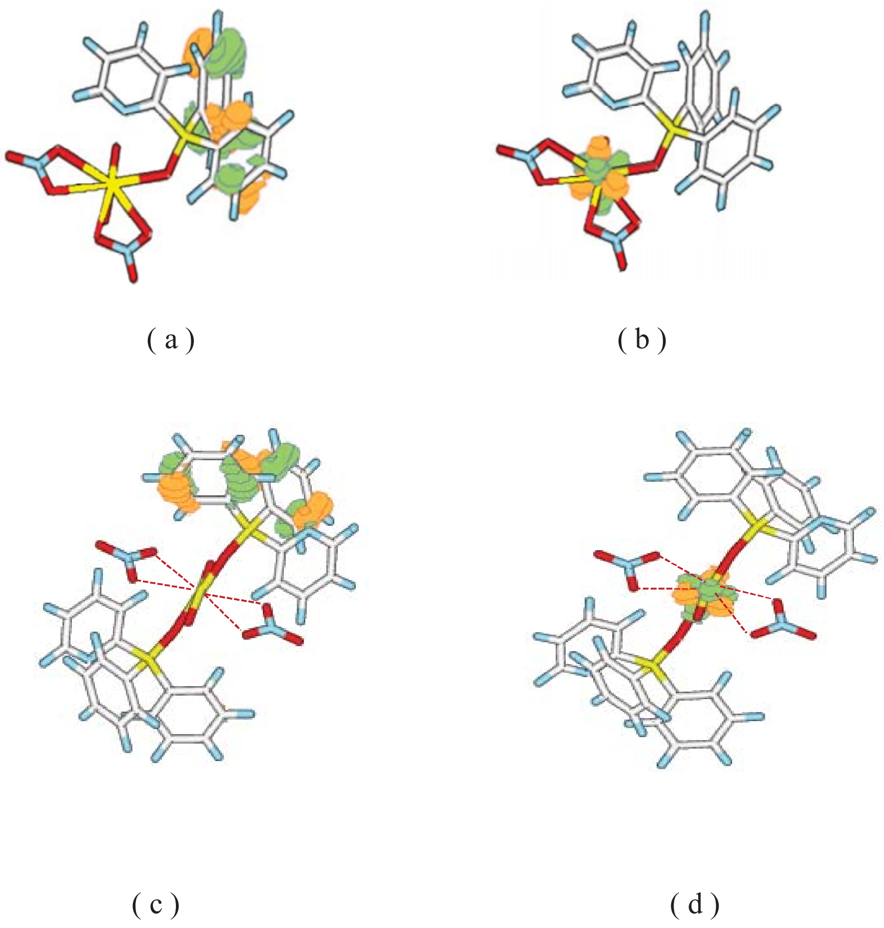

(a) (b)

(c) (d)

Figure 4.4 (a) HOMO of [$UO_2(NO_3)_2$PON], (b) LUMO of [$UO_2(NO_3)_2$PONO] , (c) HOMO of [$UO_2(NO_3)_2$.2PON] and (d) LUMO of [$UO_2(NO_3)_2$.2PON]

Figures 4.4 (a-d) display the HOMO and LUMO of [$UO_2(NO_3)_2$PON] and the [$UO_2(NO_3)_2$.2PON] complexes. It is observed that basic nature of these orbitals is quite similar in both the complexes. Phenyl π orbitals of the ligand participate in the HOMOs whereas the LUMOs are comprised of mainly the U[5f $_{z(x2-y2)}$] orbital.

4.3.8 Synthesis of complexes of europium and samarium β-diketonates with ligand L^8 and L^9: Complexes **10-17** were synthesized by reacting the corresponding Ln-β-diketonate aqua complexes with ligands $\mathbf{L^8}$ and $\mathbf{L^9}$ in dichloromethane as shown in Scheme-4.3. The IR spectra of the complexes **10-17** show the disappearance of the peaks in region of 3400-3600 cm^{-1}, indicating clearly that the removal of water molecules from the coordination sphere of starting complexes [$Ln(OO)_3.2H_2O$] (OO = diketonate). The $\nu_{P=O}$ in all complexes are shifted to a lower wavenumber region as compared to that of the uncomplexed ligands. For **10**, **12**, **14** and **16** the observed frequency difference for the P=O group ($\Delta\nu_{PO}$) is in the range of 31-36 cm^{-1}, (where $\Delta\nu_{PO} = \nu_{PO\ (free\ ligand\ )} - \nu_{PO(\ coordinated)}$), indicating clearly the direct bonding of $\mathbf{L^8}$ with the lanthanide ions through the P=O group. For **11**, **13**, **15** and **17** the observed frequency difference for the P=O group ($\Delta\nu_{PO}$) is in the range of 16-25 cm^{-1} and for the N-O group ($\Delta\nu_{NO}$) in the range of 43-54 cm^{-1} (where $\Delta\nu_{NO} = \nu_{NO\ (free\ ligand\ )} - \nu_{NO(coordinated)}$). The observed frequency differences for $\mathbf{L^9}$ show that the ligand bonds through both the P=O and N-O groups to metal centre. This in agreement with the earlier, reported values for the $\mathbf{L^9}$ complex of lanthanum nitrate [157b], in which $\mathbf{L^9}$ acts as a bidentate chelating ligand and bonds through both P=O and N-O groups to the metal centre. CHN analyses of the componds show that the $\mathbf{L^8}$ to metal ratio in **10**, **12**, **14** and **16** is 2:1, while the $\mathbf{L^9}$ to metal ratio in **11**, **13**, **15** and **17** is 1:1.

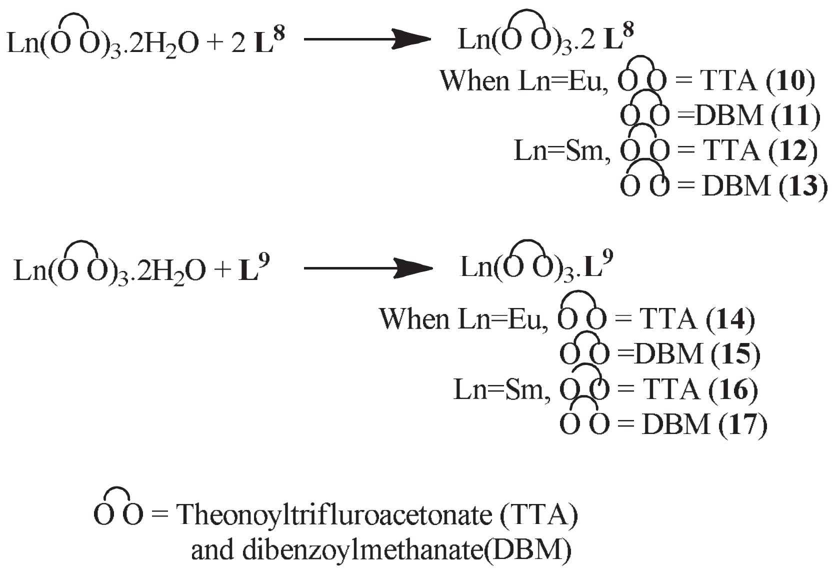

Scheme-4.3. Synthesis of Complexes of Europium(III) and Samarium(III) β-diketonates with ligands L^8 and L^9

4.3.9 Crystal Structure of [Sm(TTA)$_3$.(C$_6$H$_5$)$_2$POC$_5$H$_5$N)$_2$] (12): The crystal structure of complex **12** is shown in Fig. 4.5 and selected bond distances and angles are given in Table 4.3. The Sm^{3+} ion is coordinated to eight oxygen atoms, six of which are from three β-diketonate ligands and two oxygens are from two $\mathbf{L^8}$ ligands. There is no bonding of pyridyl nitrogen to the metal centre. This type of coordination is similar to observed in the complexes of [Ln(TTA)$_3$.2TPPO][178] . The geometry around the metal centre is bicapped trigonal prism as shown in Fig. 4.3. The Sm-O bond distances are in the range of 2.362 – 2.468 Å, which are comparable in magnitude to other reported samarium tris (beta-diketonate) complexes[179].

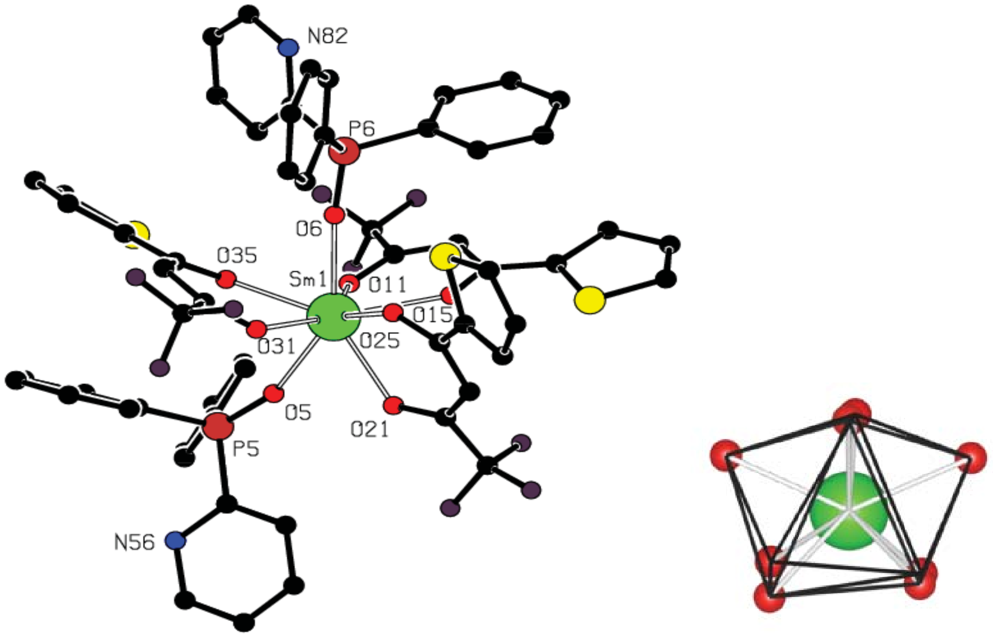

Figure 4.5: Crystal structure of complex [Sm(TTA)$_3$.(C$_6$H$_5$)$_2$POC$_5$H$_5$N)$_2$] (12)

Table 4.3: Important bond lengths and angles for 12 and 17

12			
Sm1 – O21	2.362 (2)	Sm1 – O5	2.398 (2)
Sm1 – O6	2.369 (2)	Sm1 – O35	2.430 (2)
Sm1 – O11	2.374 (2)	Sm1 – O15	2.446 (2)
Sm1 – O31	2.375 (4)	Sm1 – O25	2.468 (2)
P5 – O5	1.490 (2)	P6 – O6	1.490 (2)
O21 – Sm1 – O6	143.83 (8)	O5 – Sm1 – O35	70.96 (7)
O21 – Sm1 – O11	107.99 (8)	O21 – Sm1 – O15	72.26 (8)
O6 – Sm1 – O11	83.26 (8)	O6 – Sm1 – O15	80.29 (8)
O21 – Sm1 – O31	98.70 (8)	O11 – Sm1 – O15	69.92 (7)
O6 – Sm1 – O31	87.94 (8)	O31 – Sm1 – O15	141.02 (7)
O11 – Sm1 – O31	145.53 (7)	O5 – Sm1 – O15	123.88 (8)
O21 – Sm1 – O5	71.90 (8)	O35 – Sm1 – O15	138.34 (7)
O6 – Sm1 – O5	144.25(7)	O21 – Sm1 – O25	71.86 (8)
O11 – Sm1 – O5	82.02 (9)	O6 – Sm1 – O25	77.07 (7)

O31 – Sm1 – O5	86.09 (8)	O11 – Sm1 – O25	137.97 (8)
O21 – Sm1 – O35	141.86 (8)	O31 – Sm1 – O25	70.81 (7)
O6 – Sm1 – O35	73.82 (7)	O5 – Sm1 – O25	132.88 (7)
O11 – Sm1 – O35	75.03 (7)	O35 – Sm1 – O25	131.75 (7)
O31 – Sm1 – O35	70.51 (7)	O15 – Sm1 – O25	70.36 (7)
P5 – O5 – Sm1	160.37 (14)	P6 – O6 – Sm1	172.65 (14)

17

Sm1 – O1	2.546 (5)	Sm1 – O5	2.358 (4)
Sm1 – O2	2.497 (5)	Sm1 – O6	2.368 (4)
Sm1 – O3	2.344 (4)	Sm1 – O7	2.388 (5)
Sm1 – O4	2.334 (4)	Sm1 – O8	2.373 (5)
N1 – O1	1.332 (8)	P1 – O2	1.496 (4)
O1 – Sm1 – O2	67.86 (15)	O5 – Sm1 – O1	145.84(16)
O3 – Sm1 – O1	91.10 (16)	O5 – Sm1 – O2	145.00(16)
O3 – Sm1 – O2	74.61 (15)	O5 – Sm1 – O6	71.08(16)
O3 – Sm1 – O5	105.28(18)	O5 – Sm1 – O7	77.75(19)
O3 – Sm1 – O6	75.55(16)	O5 – Sm1 – O8	91.7(2)
O3 – Sm1 – O7	146.05(17)	O6 – Sm1 – O1	84.82(15)
O3 – Sm1 – O8	142.29(15)	O6 – Sm1 – O2	138.63(15)
O4 – Sm1 – O1	140.25(15)	O6 – Sm1 – O7	73.65(17)
O4 – Sm1 – O2	73.09(15)	O6 – Sm1 – O8	142.16(15)
O4 – Sm1 – O3	71.33(16)	O7 – Sm1 – O1	72.33(18)
O4 – Sm1 – O5	73.90(16)	O7 – Sm1 – O2	122.28(16)
O4 – Sm1 – O6	122.28(17)	O8 – Sm1 – O1	93.06(19)
O4 – Sm1 – O7	138.93(18)	O8 – Sm1 – O2	72.43(16)
O4 – Sm1 – O8	81.92(18)	O8 – Sm1 – O7	69.79(16)
N1 – O1 – Sm1	115.5 (3)	P1 – O2 – Sm1	128.5 (3)

4.3.10 Crystal Structure of [Sm(DBM)$_3$.(C$_6$H$_5$)$_2$POC$_5$H$_5$NO)] (17): The crystal structure of **17** is shown in Fig. 4.6 and selected bond distances and angles are given in Table 4.3. The

Sm^{3+} cation is coordinated to eight oxygen atoms, six of them are from three β-diketonate ligands as in complex **12** and the remaining two oxygen atoms are from the $\mathbf{L^9}$ ligand (one from the P=O group and other from the N-O group). This type of bidentate chelating mode of bonding for $\mathbf{L^9}$ is reported in literature for the complex $[La(NO_3)_3.2\mathbf{L^9}]$[157b]. The Sm-O (β-diketonate) distances are in good agreement with the literature values [179]. The Sm-O (P=O) distance and Sm-O (N-O) distances are 2.497(5) Å and 2.546(5) Å respectively. The bite angle for $\mathbf{L^9}$ is 75.55(16) (O1-Sm-O2) and is close to observed in $[UO_2(NO_3)_2.\mathbf{L^9}]$ (70.0 (3)°) and $[UO_2(NO_3)_2((EtO)_2P(O)pyO)]$ (68.3(4)°) [157a]. The geometry around the metal centre is similar to that seen in **12** i.e. a bicapped trigonal prism as shown in Fig. 4.6.

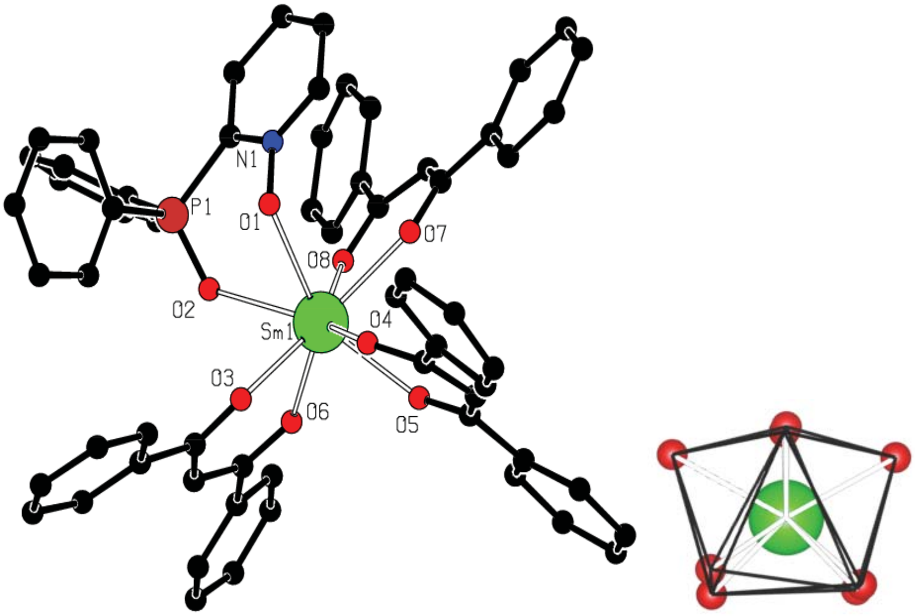

Figure 4.6:Crystal structure of complex $[Sm(DBM)_3(C_6H_5)_2POC_5H_5NO)]$ (17)

4.3.11 Emission properties of europium(III) complexes: The emission and excitation spectra of all the europium(III) complexes were recorded in chloroform. Emission spectra of all the europium complexes comprise of five transitions namely $^5D_0 \rightarrow {}^7F_0$ (zero-zero band), $^5D_0 \rightarrow {}^7F_1$ (magnetic dipole transtion), $^5D_0 \rightarrow {}^7F_2$ (induced electrical dipole transition) and $^5D_0 \rightarrow {}^7F_3$

(magnetic dipole transition) and $^5D_0 \rightarrow {}^7F_4$ (induced electrical dipole transition). The intensity of magnetic dipole transition $^5D_0 \rightarrow {}^7F_1$ is not affected by the asymmetry around the metal centre whereas the intensity of $^5D_0 \rightarrow {}^7F_2$ is highly dependent upon the ligand field around the metal centre and is called a hypersensitive transition. Hence, the asymmetric ratio R_{Eu} ($R_{Eu} = I(^5D_0 \rightarrow {}^7F_2)/ I(^5D_0 \rightarrow {}^7F_1)$) for the complexes is an important parameter to give the extent of asymmetry around the metal centre [180]. For the representative example, the emission spectra of **10** and **14** in chloroform are given in Fig. 4.7 upon excitation with 360 nm light.

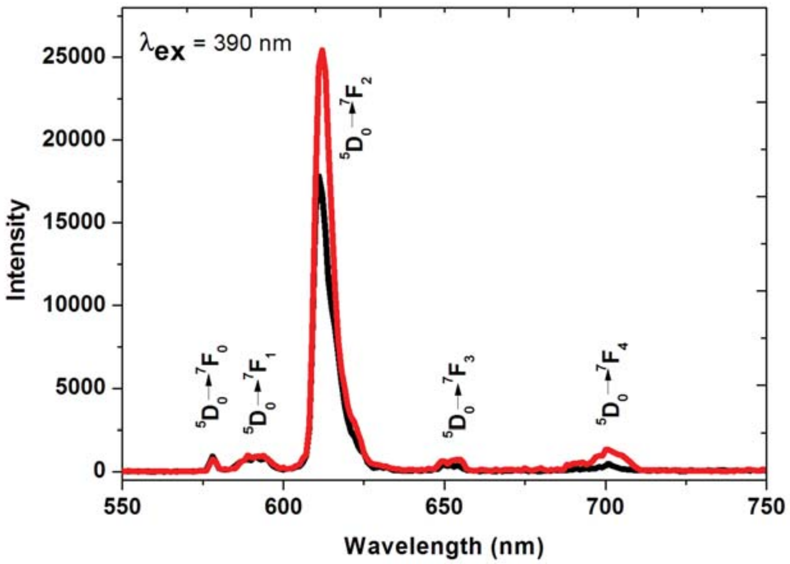

Figure 4.7: Emission spectrum of complex 10 (black) and complex 14 (red)

In case of **10** and **14**, the R_{Eu} values in chloroform are 19.14 and 28.55, respectively. The larger value of asymmetric ratio for **14** as compare to **10** certainly indicate that in **14**, the Eu^{3+} ion has a more asymmetric ligand field as compared to **10** as evident from the crystal structures obtained for the very similar samarium(III) complexes **12** and **17** (where two different donor groups i.e. N-O and P=O are bonded in **14** whereas two similar P=O groups are bonded in **10)**.

The quantum yield (Φ) of photoluminescence is defined as the product of intrinsic quantum yield (η) and energy transfer efficiency (η_{sens}) i.e.

$\Phi = \eta_{sens} * \eta$.........(4.1)

As shown in the excitation spectrum of **10** in chloroform (Fig. 4.8) there is broad absorption in range of 300 - 390 nm which corresponds to n→π* and π→π* transitions ($S_0 \rightarrow S_1$) of the β-diketone ligand (TTA) [181]. In both **10** and **14**, the β-diketone ligand (TTA) is the same and hence, the energy transfer efficiency (η_{sens}) is also expected to be same. The intrinsic quantum yield (η) which is dependent upon the asymmetry around the metal centre will be a direct a measure of quantum yield (Φ).

Intrinsic quantum yield (η) can be calculated by the following relation:

$$\eta = \frac{A_{rad}}{A_{rad} + A_{nr}}$$ ....(4.2)

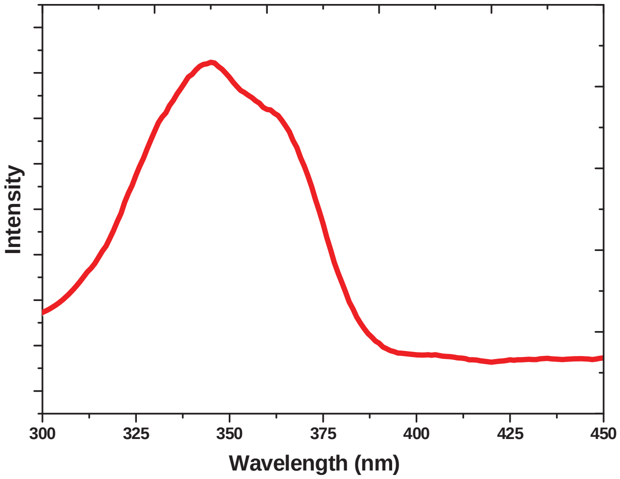

Figure 4.8: Excitation spectra of the complex 10 at λ_{em} = 612nm

Where, A_{rad} and A_{nr} are the radiative and non-radiative decay rate, respectively.

A_{rad} can be calculated from the following formula:

$$A_{rad} = A_{MD,0} \times n^3 \times \frac{I_{total}}{I_{mag}} = 1/\tau_{rad}$$ ....(4.3)

Where, $A_{MD,0}$ is spontaneous emission probability for $^5D_0 \rightarrow {}^7F_1$ transition in vacuum (14.65 s^{-1} for Eu^{3+}), *n* is the refractive index of the solvent (1.45 for chloroform), I_{total}/I_{mag} is the ratio of the integrated intensity of corrected emission spectrum to the integrated intensity ofthe $^5D_0 \rightarrow {}^7F_1$ transition and τ_{rad} is the radiative lifetime for the $^5D_0$ level of Eu^{3+}[182]. The non-radiative decay constant and non-radiative lifetime can be calculated from the following expressions:

$$A_{obs} = 1/\tau_{obs} = A_{rad} + A_{nr}$$ ....(4.4)

Where, τ_{obs} is observed lifetime of the $^5D_0 \rightarrow {}^7F_2$ transition.

In case of **10**, where the auxiliary ligand is $\mathbf{L^8}$, A_{rad} is 927.2 s^{-1} while in **14** the auxiliary ligand is $\mathbf{L^9}$, A_{rad} is 1363.5 s^{-1}. The significantly higher radiative decay rate and higher value of intrinsic quantum yield is obtained when ligand having two P=O groups (as in **10**) are replaced with ligand having one N-O and one P=O groups (as in **14**). Similarly, in **11** and **15** also the intrinsic quantum yields are 4.7 % and 12.8 %, respectively. Here also there is an enhancement (172%) in intrinsic quantum yields as we go from the $\mathbf{L^8}$ auxiliary ligand to the $\mathbf{L^9}$ ligand. Moreover, there is a decrease in the non radiative decay rate in **14** (1551.9 s^{-1}) as compared to that of **10** (1775.5 s^{-1}). These results clearly confirm that by changing one of the donor groups in auxiliary ligand i.e. introducing aymmetry of the ligand field around metal centre certainly increases the radiative rate in this metal ligand system. The intrinsic quantum yields (η) are 34.3 % and 46.8 % for **10** and **14**, respectively. There is a 36% increase in the intrinsic quantum yield in the more asymmetric ligand field design. The photoluminescence data for all the europium(III) complexes in chloroform are summarized in Table-4.4. Similarly, in the solid state, the R_{Eu} for complexes with $\mathbf{L^9}$ are higher than those of $\mathbf{L^8}$ (Table-4.5). However, in the solid state intermetallic non-radiative quenching (self-quenching) may give lower τ_{obs} values and thus inaccurate values for the quantum yields.

4.3.12 Emission properties of samarium(III) complexes: The emission spectra of samarium complexes **12** and **16** in chloroform are shown in Fig. 4.9 as a representative examples.

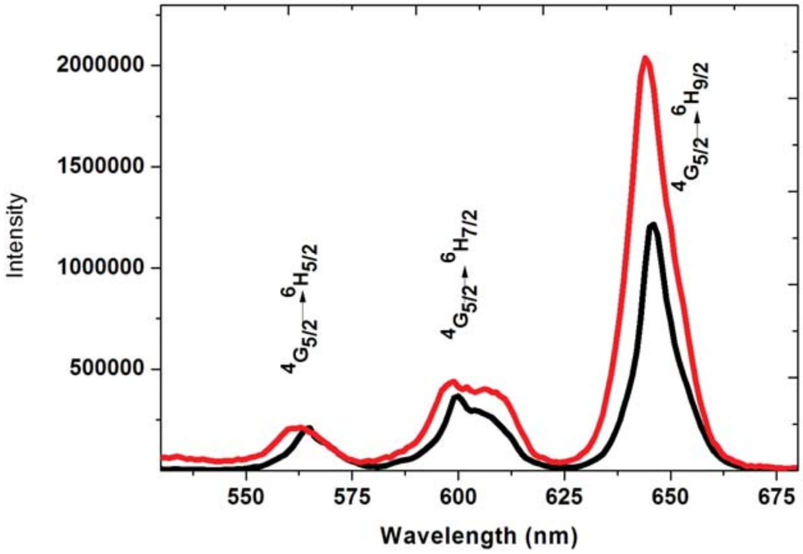

Figure 4.9: Emission spectrum of 12 (black) and 16 (red) in chloroform.

Table-4.4: Photoluminescence data for europium(III) complexes in chloroform solution at room temperature

S.No.	Compound	R_{Eu}	τ_{obs} (ms)	I_{tot}/I_{mag}	A_{rad}	A_{nr}	A_{obs}	τ_{rad} (ms)	τ_{nr} (ms)	η (%)
1	[Eu(TTA)$_3$.({C_6H_5}$_2$POC$_5$H$_5$N)$_2$] (**10**)	19.14	370	20.76	927.19	1775.51	2702.70	1078.53	563.22	34.0
2	[Eu(TTA)$_3$. ({C_6H_5}$_2$POC$_5$H$_5$NO)] (**14**)	28.55	343	30.53	1363.50	1551.91	2915.45	733.38	644.37	46.7
3	[Eu(DBM)$_3$.({C_6H_5}$_2$POC$_5$H$_5$N)$_2$] (**11**)	7.25	126	8.47	378.29	7558.22	7936.51	2643.43	132.31	4.7
4	[Eu(DBM)$_3$.({C_6H_5}$_2$POC$_5$H$_5$NO)] (**15**)	13.14	193	14.85	663.24	4518.11	5181.35	1507.76	221.33	12.8

Table 4.5: Photoluminescence characterstics for europium(III) complexes in the solid state at room temperature

S.No.	Compound	R_{Eu}	τ_{obs} (ms)
1	$[Eu(TTA)_3.(\{C_6H_5\}9_2POC_5H_5N)_2]$ (**10**)	22.22	608
2	$[Eu(TTA)_3.(\{C_6H_5\}_2POC_5H_5NO)]$ (**14**)	25.92	470
3	$[Eu(DBM)_3.(\{C_6H_5\}_2POC_5H_5N)_2]$ (**11**)	30.96	598
4	$[Eu(DBM)_3.(\{C_6H_5\}_2POC_5H_5NO)]$ (**15**)	32.66	230

Three observed emission bands are assigned as: $^4G_{5/2} \rightarrow {}^6H_{5/2}$ (magnetic dipole transition), $^4G_{5/2} \rightarrow {}^6H_{7/2}$ (magnetic dipole transition + electric dipole transition) and $^4G_{5/2} \rightarrow {}^6H_{9/2}$ (electric dipole transition) transitions. The electric dipole transition ($^4G_{5/2} \rightarrow {}^6H_{9/2}$) in all samarium(III) complexes is of maximum intensity which shows the asymmetric environment around the metal centre. The intensity ratio of electrical dipole transition to magnetic dipole transition (R_{sm}= $I(^4G_{5/2} \rightarrow {}^6H_{9/2})/ I(^4G_{5/2} \rightarrow {}^6H_{9/2})$) gives the idea about the extent of the asymmetry around the metal centre as discussed in the case of europium(III) complexes[183]. R_{sm} for all the samarium(III) complexes in solid as well as in solution state are given in the Table 4.6. It can be seen from the R_{sm} values that the complexes with ligand $\mathbf{L^9}$ (PONO) where the donor group are from N-O and P=O moieties have higher values as compared to the complexes with ligand $\mathbf{L^8}$ (PON), where the donor group is P=O only. So by introducing the different donor groups around the metal centre, one can tune the asymmetric ratio, and thereby enhance the quantum yield of emission in lanthanide complexes. This observation is in agreement with the recently proposed ECA principle for europium(III) complexes.

Table 4.6: Photoluminescence characterstics for samarium(III) complexes in the solid state and in chloroform at room temperature

S.No.	Compound	R_{Sm}	τ_{obs} (ms)
	For solid		
1	$[Sm(TTA)_3.(\{C_6H_5\}_2POC_5H_5N)_2]$ **(12)**	14.61	78
2	$[Sm(TTA)_3.(\{C_6H_5\}_2POC_5H_5NO)]$ **(16)**	17.84	121
3	$[Sm(DBM)_3.(\{C_6H_5\}_2POC_5H_5N)_2]$ **(13)**	16.51	73
4	$[Sm(DBM)_3.(\{C_6H_5\}_2POC_5H_5NO)]$ **(17)**	18.06	88
	For Solution		
1	$[Sm(TTA)_3.(\{C_6H_5\}_2POC_5H_5N)_2]$ **(12)**	6.60	38
2	$[Sm(TTA)_3.(\{C_6H_5\}_2POC_5H_5NO)]$ **(16)**	13.34	45
3	$[Sm(DBM)_3.(\{C_6H_5\}_2POC_5H_5N)_2]$ **(13)**	7.27	8.6
4	$[Sm(DBM)_3.(\{C_6H_5\}_2POC_5H_5NO)]$ **(17)**	7.69	11

4.4 Conclusions:

The structural studies on the complexes of diphenyl-(2-pyridyl)phosphine oxide with uranyl(VI) nitrate (complex **8)** and uranyl(VI) bis(dibenzoylmethanate) (complex **9**) show a monodentate mode of bonding for the ligand. Theoretical studies reveal that the steric effects play an important role in deciding the mode of bonding for the ligand. The 2:1 complex $[UO_2(NO_3)_2\cdot 2\mathbf{L}^8]$, in which the ligand acts as a monodentate ligand, is energetically more stable by 13.5 kcal/mol than the 1:1 complex $[UO_2(NO_3)_2\cdot \mathbf{L}^8]$, in which the ligand acts as a bidentate chelating ligand. Eight new complexes of europium(III) and samarium(III) β-diketonates with two auxiliary ligands namely diphenyl-(2-pyridyl)-phosphine oxide (**L**^{8}) and diphenyl-(2-pyridyl-*N*-oxide)-phosphine oxide (**L**^{9}) were synthesized. The crystal structure of complex **17** and complex **22**, clearly shows monodentate behavior for **L^8** in **17** and bidentate behavior for **L^9** in **22**. Photophysical measurementsfor all the complexes show good photophysical properties in solid as well as in solution states. In the complexes as from the ligand field asymmetry changes from lower to higher, the asymmetry ratio increases which in turn increases the intrinsic quantum yield as observed in the synthesized complexes.z

Chapter – 5

Synthesis, coordination, structural and extraction studies of (*N*,*N*-dialkyl carbamoyl methyl) (2-pyridyl-*N*-oxide) sulfide ligands with the uranyl(VI) ion.

5.1: Introduction:

Many ligands systems have been proposed for the extraction of actinides from spent fuel as the requirement for the sustainable nuclear fuel cycle as well as for reducing the long term storage of spent fuel [135a]. Tri *n*-butyl phosphate (TBP) is used as an extractant for tetravalent and hexavalent actinides in the PUREX process at industrial scale. However, it has its own disadvantages [184]. Many new ligand systems with mono as well as bifunctional donor groups based on amide, phosphine oxide and very few with *N*-oxide and sulphoxide have been reported. Isobutyramide [49c], malonamide[185], diglycolamide[135b] and carbamoyl methyl phosphine oxide (CMPO) [186] ligand systems have been studied very well in the context of actinide partitioning. A new bifunctional ligand system, carbamoyl methyl sulphoxide (CMSO) has been explored for actinide extractions [24] which shows extraction for U(VI) and Pu(VI) from acidic solutions. Paine et al. have been involved in the coordination chemistry of some of the newly synthesized ligand systems containing *N*-oxide and phosphine oxide groups (NOPO, NOPOPO) with lanthanides and actinides [153a, 187]. A new trifunctional ligand system containing both an *N*-oxide and a carbamoyl group (NOCOCO) [188] has been explored for the coordination chemistry of lanthanides. However, to the best of our knowledge, no coordination chemistry of bifunctional ligands containing an *N*-oxide and a carbamoyl group (NOCO) with actinides or lanthanides has been reported. In this report, we synthesized a new ligand system namely (*N,N*-dialkyl carbamoyl methyl) (2-pyridyl-*N*-oxide) sulfide (NOCO type) and studied the extraction and coordination behaviour with uranium and plutonium.

5.2 Experimental:

5.2.1 General consideration: All starting materials and other chemicals were reagent grade and were commercially available. *N,N*-dialkylcarbamoyl methyl chloride were prepared by the literature procedure[189]. The FTIR spectra were obtained on a ATR-IR platinum Bruker spectrometer. The ^{1}H NMR in $CDCl_3$ or DMSO-d_6 for ligands and compounds were recorded on Bruker 300 or 500 MHz spectrometers.

5.2.2 Synthesis of Ligand [$C_5H_4NOSCH_2CON(^iC_3H_7)_2$] ($L^{10}$): Sodium hydroxide (40 mg, 1 mmol) is taken in 5 mL ethanol and stirred until all NaOH is dissolved. 2-mercapto pyridyl-*N*-oxide (127 mg, 1mmol) is added into it. After stirring for 15 minutes, *N,N'*-diisopropyl carbamoyl methyl chloride (177.6 mg, 1mmol) is added to reaction mixture. The solution is stirred for another hour. After 1 hour, the solution is filtered and evaporated to dryness to obtain the pure compound. Yield 71% ^{1}H-NMR ($CDCl_3$ δ ppm): 1.26 (d, 6H, -CH_3, ^{i}Pr, J = 6.6 Hz), 1.35 (d, 6H, -CH_3, ^{i}Pr, 6.9 Hz), 3.43 (m. 1H, -CH, ^{i}Pr), 3.74 (s, 2H, -CH_2), 4.04 (m, 1H, -CH, ^{i}Pr), 7.07 (m, 1H, Py), 7.26 (m, 1H, Py), 7.84 (dd, 1H, Py, J = 8.5 Hz, 1.8 Hz), 8.23 (dd, 1H, Py, J = 6.3 Hz, 1.8 Hz) IR (KBr, ν cm^{-1}): 1631 (s, C=O), 1252 (s, N-O), Elemental analysis (%): Calc.for, $C_{13}H_{20}N_2O_2S$: C 58.2, H 7.5, N 10.4. Found: C 58.0, H 7.3, N 10.1.

5.2.3 Synthesis of Ligand [$C_5H_4NOSCH_2CON(^iC_4H_9)_2$] ($L^{11}$) : Sodium hydroxide (40 mg, 1 mmol) is taken in 5 mL ethanol and stirred until all NaOH is dissolved. 2-mercapto pyridyl-*N*-oxide (127.2 mg, 1mmol) is added into it. After stirring for 15 minutes, *N,N'*-diisobutyl carbamoyl methyl chloride (205.6 mg, 1mmol) is added into reaction mixture. The solution is stirred for another hour. After 1 hour, the solution is filtered and evaporated to dryness to obtain the pure compound. Yield 72%. ^{1}H-NMR ($CDCl_3$ δ ppm): 0.72 (d, 6H, -CH_3 ^{i}Bu, J = 6.6 Hz), 0.87 (d, 6H, -CH_3 ^{i}Bu, J = 6.6 Hz), 1.88 (m, 2H, -CH ^{i}Bu), 3.11 (d, 2H, -CH_2 ^{i}Bu, J = 5.4 Hz), 3.14 (d, 2H, -CH_2 ^{i}Bu, J = 5.7 Hz), 3.75 (s, 2H, -CH_2), 7.02 (m, 1H, Py), 7.20 (m, 1H, Py), 7.68 (dd, 1H, py, J = 8.4 Hz, 1.5 Hz), 8.16 (d, 1H, Py, J = 5.7 Hz) IR (KBr, ν cm^{-1}): 1636 (s, C=O), 1242 (s, N-O stretch), Elemental analysis (%): Calc. for $C_{15}H_{24}N_2O_2S$: C 60.8, H 8.2, N 9.5. Found: C 60.5, H 8.0, N 9.6.

5.2.4 Synthesis of Ligand [$C_5H_4NOSCH_2CON(C_4H_9)_2$] ($L^{12}$): Sodium hydroxide (40 mg, 1 mmol) is taken in 5 mL ethanol and stirred until all NaOH is dissolved. 2-mercapto pyridyl-*N*-oxide (127.2 mg, 1mmol) is added into it. After stirring for 15 minutes, *N,N*'-dibutyl carbamoyl methyl chloride (205.6 mg, 1mmol) is added into reaction mixture. The solution is stirred for another hour. After 1 hour, the solution is filtered and evaporated to dryness to obtain the pure compound. Yield 72%. ^{1}H-NMR (CDCl$_3$ δ ppm): 0.82 (t, 3H, -CH$_3$, ^{n}Bu, J = 7.5 Hz), 0.91 (t, 3H, -CH$_3$, ^{n}Bu, J = 7.5 Hz), 1.20 (m, 2H, -C$\mathbf{H_2}$CH$_3$, ^{n}Bu), 1.30 (m, 2H, -C$\mathbf{H_2}$CH$_3$, ^{n}Bu), 1.41 (m, 2H, -C$\mathbf{H_2}$CH$_2$CH$_3$, ^{n}Bu), 1.54 (m, 2H, -C$\mathbf{H_2}$CH$_2$CH$_3$, ^{n}Bu), 3.26 (t, 2H, -NCH$_2$, ^{n}Bu, J = 7.5 Hz), 3.29 (t, 2H, -NCH$_2$, ^{n}Bu, J = 7.5 Hz), 3.72 (s, 2H, -CH$_2$), 7.06 (m, 1H, Py), 7.23 (m, 1H, Py), 7.74 (dd, 1H, py, J = 8.4 Hz, 1.5 Hz), 8.19 (d, 1H,Py, J = 6.3 Hz). IR (KBr, ν cm^{-1}): 1642 (s, C=O), 1248 (s, N-O), Elmental analysis(%): Calc. for $C_{15}H_{24}N_2O_2S$: C 60.8, H 8.2, N 9.5. Found: C 60.6, H 8.1, N 9.5.

5.2.5 Synthesis of Ligand [$C_5H_4NOSCH_2CON(C_8H_{17})_2$] ($L^{13}$): Sodium hydroxide (40 mg, 1 mmol) is taken in 5 mL ethanol and stirred until all NaOH is dissolved. 2-mercapto pyridyl-*N*-oxide (127.2 mg, 1mmol) is added into it. After stirring for 15 minutes, *N,N*'-dioctyl carbamoyl methyl chloride (317.6 mg, 1mmol) is added into reaction mixture. The solution is stirred for another hour. After 1 hour, the solution is filtered and evaporated to dryness to obtain the pure compound.Yield 75%. ^{1}H-NMR (CDCl$_3$, δ ppm): 0.95 (m, 6H, -CH$_3$, *n*-octyl,), 1.21 (m, 20H, -NCH$_2$CH$_2$(C$\mathbf{H_2}$)$_5$CH$_3$, 1.46 (m, 4H, -NCH2C**H2(**CH$_2$)$_5$CH$_3$), 3.30 (m, 4H, -NC$\mathbf{H_2}$, *n*-octyl), 3.74 (s, 2H, -SC$\mathbf{H_2}$CO-), 7.06 (m, 1H, py,), 7.26 (m, 1H, py), 7.79 (m, 1H, py), 8.21 (m, 1H, py). IR (KBr, ν cm^{-1}): 1636 (s, C=O,), 1251 (s, N-O), Elemental analysis (%): Calc. for $C_{23}H_{40}N_2O_2S$: C 67.6, H 9.9, N 6.9. Found: C 67.4, H 9.8, N 6.7.

5.2.6 Synthesis of Complex [$UO_2(NO_3)_2(C_5H_4NOSCH_2CON(^iC_3H_7)_2)$] (18): Uranyl nitrate hexahydrate (185 mg, 0.37 mmol) is added to a solution of Ligand $\mathbf{L^{10}}$ (100 mg, 0.37 mmol) in methylene chloride, and left to stirfor 1 hour. After filtraation and evaporation, a yellow compound is obtained. Yield 71% ^{1}H-NMR (DMSO-d_6, δ ppm): 1.17 (d, 6H, -CH_3, ^{i}Pr, J = 6.6 Hz), 1.28 (d, 6H, -CH_3, ^{i}Pr, J = 6.6 Hz), 3.43 (merged with DMSO-d6, 1H, -CH, ^{i}Pr), 4.02 (s, 2H, -CH_2), 4.14 (m, 1H, -CH, ^{i}Pr), 7.19 (m, 1H, Py), 7.34 (m, 1H, Py), 7.50 (dd, 1H. Py, j = 8.5 Hz, 1.5 Hz), 8.26 (d, 1H, Py, J = 6.5 Hz). IR (KBr, ν cm^{-1}): 1589 (s, C=O), 1209 (s, N-O), 930 (s, O=U=O). Elememtal analysis (%): Calc. for $C_{13}H_{20}N_4O_{10}SU$: C 23.6, H 3.0, N 8.5. Found: C 23.4, H 3.2, N 8.3.

5.2.7 Synthesis of Complex [$UO_2(NO_3)_2(C_5H_4NOSCH_2CON(i\text{-}C_4H_9)_2)$] (19): Uranyl nitrate hexahydrate (185 mg, 0.37 mmol) is added to a solution of Ligand **L^{11}** (100 mg, 0.34 mmol) in methylene chloride, and stirred for 1 hour. After filtration and evaporation, a yellow compound is obtained. Yield 71% , ^{1}H-NMR (DMSO-d_6, δ ppm): 0.78 (d, 6H, -CH_3 ^{i}Bu, J = 6.6 Hz), 0.89 (d,-CH_3, ^{i}Bu, J = 6.6 Hz), 1.94 (m, 2H, -CH, ^{i}Bu), 3.12 (d, 2H, -CH_2, ^{i}Bu, J = 7.5 Hz), 3.23 (d, 2H, -CH_2, ^{i}Bu, J = 7.5 Hz), 4.04 (s, 2H, -CH_2), 7.20 (m, 1H, Py), 7.35 (m, 1H, Py), 7.48 (dd, 1H, py, j = 8.2 Hz, 1.5 Hz), 8.26 (d, 1H,Py, J = 6.5 Hz) IR (KBr, ν cm^{-1}): 1591 (s, C=O,), 1210 (s, N-O), 927 (s, O=U=O). Elemental analysis (%): Calc.for $C_{15}H_{24}N_4O_{10}SU$: C 26.1, H 3.5, N 8.1. Found: C 26.3, H 3.3, N 8.2.

5.2.8 Synthesis of Complex [$UO_2(NO_3)_2(C_5H_4NOSCH_2CON(C_4H_9)_2)$] (20): Uranyl nitrate hexahydrate (185 mg, 0.37 mmol) is added to a solution of Ligand **L^{12}** (100 mg, 0.34 mmol) in methylene chloride, and left to stir for 1 hour. After filtraation and evaporation, a yellow compound is obtained. Yield 72%. ^{1}H-NMR (DMSO-d_6, δ ppm): 0.85 (t, 3H, -CH_3, ^{n}Bu, J = 7.2 Hz), 0.91 (t, 3H,-CH_3, ^{n}Bu, J = 7.2 Hz), 1.23 (m, 2H, -C**H$_2$**CH_3, ^{n}Bu), 1.32 (m, 2H, -C**H$_2$**CH_3, ^{n}Bu), 1.45 (m, 2H, -C**H$_2$**CH_2CH_3, ^{n}Bu), 1.55 (m, 2H, -C**H$_2$**CH_2CH_3, ^{n}Bu), 3.25 (t, 2H, -NCH_2, *n*-Bu, J = 7.8 Hz), 3.35 (t, 2H, -NCH_2, ^{n}Bu, J = 7.2 Hz), 4.02 (s, 2H, -CH_2), 7.21 (m, 1H, Py), 7.35(m, 1H, Py), 7.44 (dd, 1H, py, J = 8.2 Hz, 1.5 Hz), 8.28 (dd, 1H, Py, J = 6.4

Hz, 0.9 Hz). IR (KBr, ν cm^{-1}): 1598 (s, C=O), 1208 (s, N-O), 925 (s, O=U=O). Elemental analysis (%): Calc. for $C_{15}H_{24}N_4O_{10}SU$: C 26.1, H 3.5, N 8.1. Found: C 25.9, H 3.3, N 8.3.

5.2.9 Crystallogarphy: For complex **19**, the data were collected on a Agilent SuperNova system equipped with Titan CCD detector at 293(2) K using CuK_{α} radiation (λ = 1.5418 Å). The crystals were positioned at 101 mm from the CCD. 973 frames were measured for **19** with an integration time of 2s. Data analyses were carried out with the CrysAlis program[111] for all compounds. The structures were solved using direct methods with the Shelxs97 program[112]. All non hydrogen atoms were refined with anisotropic thermal parameters. The hydrogen atoms bonded to carbon atoms were included in the geometric positions and given thermal parameters equivalent to 1.2 times those of the atoms to which they attached. Empirical absorption corrections were carried out using the ABSPACK program [113] for all compounds. The structures were refined to convergence on F^2 using Shelxl97[112] . Selected crystallographic data for **19** is summarized in Table 5.1.

5.2.10 Thermogravimetric studies: Simultaneous thermogravimetric (TG) and differential thermal analysis (DTA) data for all complexes were recorded on a Mettler thermoanalyzer (model: TGA/SDTA 851e/MT5/LF1600). All the samples were heated up to 800°C a at the rate of 10°C min^{-1} in an alumina crucible in air (flow rate 50 ml min^{-1}). All the weight changes were corrected for buoyancy corrections.

Table 5.1: Crystal data refinement of complex 19

	19
Empirical Formula	$C_{15}H_{24}N_4O_{10}SU$
Crystal system	triclinic
Space group	P- $\bar{1}$
a (Å)	8.2961 (3)
b (Å)	8.4702 (4)
c (Å)	17.6140 (9)
α (°)	79.383 (4)
β (°)	77.265(8)
γ (°)	79.107 (4)
V (cm^3)	1173.73 (10)
Z	2
ρ_{calcd} [g cm^{-3}]	1.954
μ [mm^{-1}]	20.80
Reflections collected/ unique	4532/3621
Data/restrains/parameters	4532/18/295
Goodness of fit on F^2	1.006
Final R_1 indices [$I > 2\sigma(I)$]	0.0832
wR_2 indices (all data)	0.2209

Where $w = 1/[\sigma^2(Fo^2)+(0.1704P)^2$ where $P = (Fo^2 + 2Fc^2)/3$

5.2.11 Solvent extraction studies: Distribution studies were performed by using 0.5ml solution of $\mathbf{L^{13}}$ in *n*-dodecane (0.2 M) with 0.5 ml of required aqueous phase spiked with ^{233}U, ^{239} Pu or ^{241}Am tracers at 25 ± 0.1 C. Assays of organic and aqueous phases were done in duplicate by alpha counting using a dioxane based liquid scintillator for ^{233}U and ^{239}Pu and direct γ counting for ^{241}Am. Plutonium was adjusted to the tetravalent state by the addition of 0.01M $NaNO_2$ with 0.005M NH_4VO_3 as the holding oxidant. The distribution ratio (D) is calculated as the ratio of the concentration of uranium in the organic phase to that of the aqueous phase. For acid uptake studies, the organic phase (0.2 M ligand $\mathbf{L^{13}}$ in dodecane) was contacted with an equal volume of HNO_3 at varying initial acid concentrations (0.5 to 5.0 M). The acidity of the aqueous as well as the organic phase was determined by using standard acid-base titrations.

5.3. Results and discussion:

5.3.1 Characterization of ligands and complexes: The ligands $\mathbf{L^{10}}$ – $\mathbf{L^{13}}$ were obtained by reacting the sodium salt of 2-mercapto pyridine-N-oxide with the respective *N,N'*-dialkyl methyl carbamoyl chloride in a 1:1 ratio in good yields as shown in Scheme 5.1. The complexes were prepared by adding the ligands to uranyl nitrate hexahydrate in a 1:1 ratio. All the ligands and complexes were characterized by CHN analyses, FTIR and NMR spectroscopy. The IR spectra of the ligands show the characteristic peak of the amide group (-C=O) as well as the peak corresponding to the N-O groups. The IR spectra of the complexes show that the water molecule from the starting compound $UO_2(NO_3)_2.6H_2O$ has been completely replaced by the ligands and the ligands are coordinated to uranyl through C=O and N-O groups. The above suppositions are supported by the absence of the broad peak of the water molecule at around 3400 cm^{-1} and observed frequency differences between the amidic –C=O and N-O strectch for the ligands and the corresponding complexes (C=O ($\Delta\nu_{C=O}$ = 42 – 44 cm^{-1}) and N-O ($\Delta\nu_{N-O}$ = 32 – 43 cm^{-1})) in the IR spectra. Earlier, also similar decrease in frequency of amidic C=O is reported in uranyl amide complexes [120, 190]. In uranyl and lanthanide *N*-oxide complexes also there is around 35-50 cm^{-1} shift in *N*-oxide IR frequency after complexation reported in literature [153g, 191].The OUO asymmetric frequency in uranyl(VI) complexes ranges from 925 to 930 cm-1 which are close to the earlier reported uranyl complexes in this thesis.These IR frequencies are downfielded shifted than that of uranyl nitrate hexahydrate (949 cm^{-1}) which shows that these ligands are stronger as compared to the inner sphere water molecule attached to the uranyl (VI) in uranyl nitrate hexa hydrate The ^{1}H NMR spectra of the complexes show that the CH_2 protons of the ligands are deshielded as compared to that of the uncomplexed ligands which further confirms the coordination of these ligands to the metal centre also exists in solution. The ^{1}H-NMR spectra of the ligands and complexes shows the expected integration and multiplicity. CHN analyses of the complexes agree well with the calculated values.

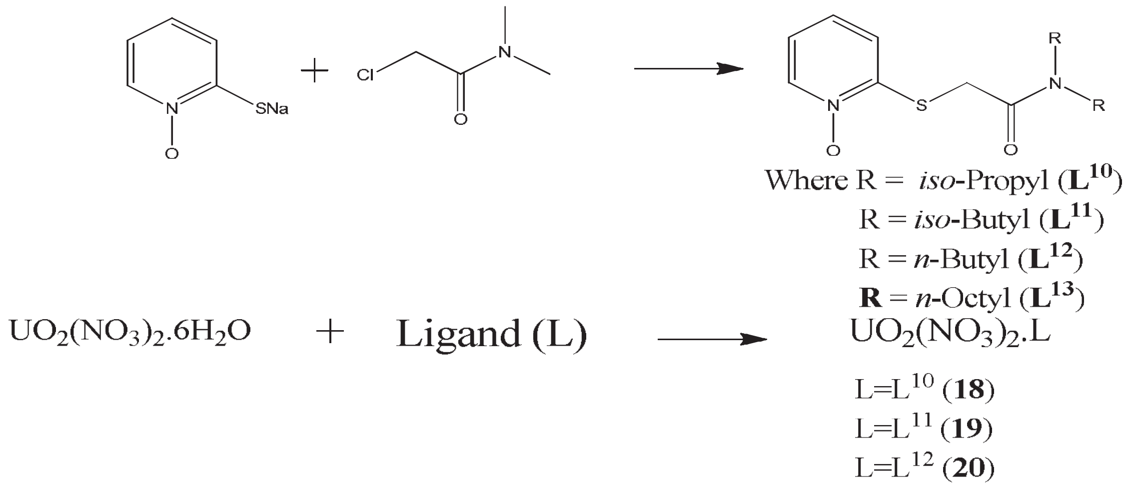

Where R = *iso*-Propyl (**L^{10}**)
R = *iso*-Butyl (**L^{11}**)
R = *n*-Butyl (**L^{12}**)
R = *n*-Octyl (**L^{13}**)

$UO_2(NO_3)_2.6H_2O$ + Ligand (L) ⟶ $UO_2(NO_3)_2.L$

$L=L^{10}$ (**18**)
$L=L^{11}$ (**19**)
$L=L^{12}$ (**20**)

Scheme 5.1: Synthesis of ligands (*N,N*-dialkyl carbamoyl methyl) (2-pyridyl-*N*-oxide) sulfide and their uranyl(VI) complexes

5.3.2 Molecular Structure of the complex 19: The molecular structure of complex **19** is shown in Fig. 5.1. The structure shows that uranium atom is surrounded by eight oxygen atoms in a hexagonal-bi-pyramidal geometry. The four oxygen atoms of the two nitrate groups and the two oxygen atoms of the ligand, from C=O and N-O groups forms the equatorial hexagonal plane. A similar cordination geometry has been obtained earlier for CMPO [59], CMSO [24] and malonamide [58a] ligands with uranyl(VI) nitrate. The observed U-O (amide) and U-O (N-O) bond lengths in complex **2** are 2.393 (12) Å 2.389 (12) Å, which are comparable to, or slightly shorter than those of the other reported bi-functional ligands such as $[UO_2(NO_3)_2(CH_3)_2NCOCH_2CON(CH_3)_2]$ (2.41(2) Å)[58a], $[UO_2(NO_3)_2Ph$[178]

$POCH_2CONEt_2$](2.426(8)Å)[59],[$UO_2(NO_3)_2Ph_2POCH_2CONEt_2$] (2.404(5))[59] and [$UO_2(NO_3)_2C_6H_5SOCH_2CON(C_4H_9)_2$] (2.442(9)Å)[24]. The average U=O (1.790 (12)-1.795 (11) and U-O (NO_3) (2.504 (15)-2.548 (15)) bond distances agree well with the reported uranyl(VI) nitrate neutral ligand complexes.[24, 106, 190]. All Important bond distances and angles are given in Table 5.2.

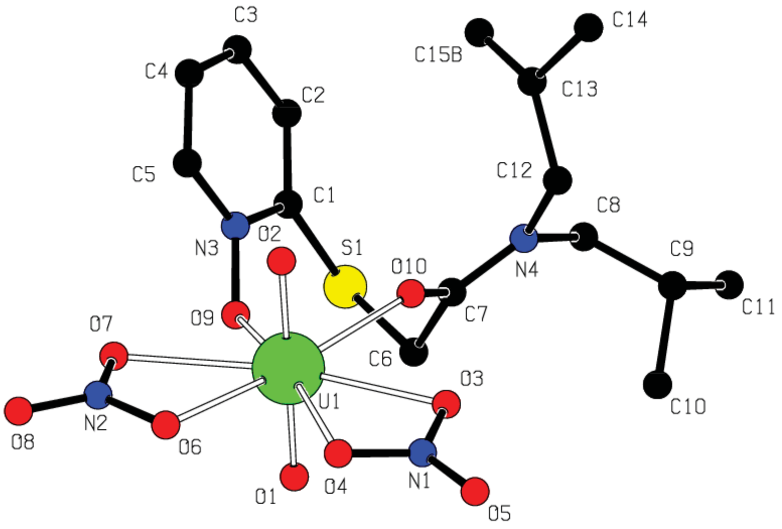

Figure 5.1: Crystal structure of compound 19

Table 5.2. Important bond lengths (Å) and angles (°) for 19.

		19	
U1 – O1	1.789 (12)	U1 – O6	2.518(14)
U1 – O2	1.795 (11)	U1 – O7	2.549(15)
U1 – O3	2.506 (16)	U1 – O9	2.389(12)
U1 – O4	2.504 (15)	U1 – O10	2.393 (12)
C7 – O10	1.26 (2)	N3 – O9	1.344 (19)
O1 – U1 – O2	178.7(5)	O9 – U1 – O10	70.0 (4)
O7 – U1 – O6	49.8 (5)	O4 – U1 – O3	49.7 (3)

5.3.3 Thermal studies of the complexes 18, 19 and 20

Thermogravimetric (TG) and Differential Thermal Analyses (DTA) of complexes **18, 19** and **20** were carried out to find out the metal to ligand ratio and product of the decomposition reaction. These compounds decompose in four to five steps to give U_3O_8 as a final product. The TGA and DTA curves for complexes **18**, **19** and **20** are been shown in Fig. 5.2. The first two exothermic peaks in DTA correspond to nitrate decomposition as is earlier reported [192]. Powder XRD pattern of the residue obtained after the TGA experiment shows U_3O_8 phase formation without any other phase impurities as shown in Fig. 5.3 The total weight loss expected from the ligand and nitrate decomposition for the complexes **18**, **19** and **20** to give U_3O_8 is 57.63%, 59.4% and 59.4%, respectively which is very close to the observed values of 59.5%, 59.4% and 60.2% for the complexes **18**, **19** and **20**, respectively. This observation again supports the ligand to metal ratio is 1:1 in the complex. However, the decomposition product of the phosphine oxide compounds of uranyl(VI) nitrate yielded the corresponding uranyl phosphate as a final product [154a]. This observation clearly shows that the present ligand system can be completely destroyed on incineration, as indeed can the amide ligands [193].

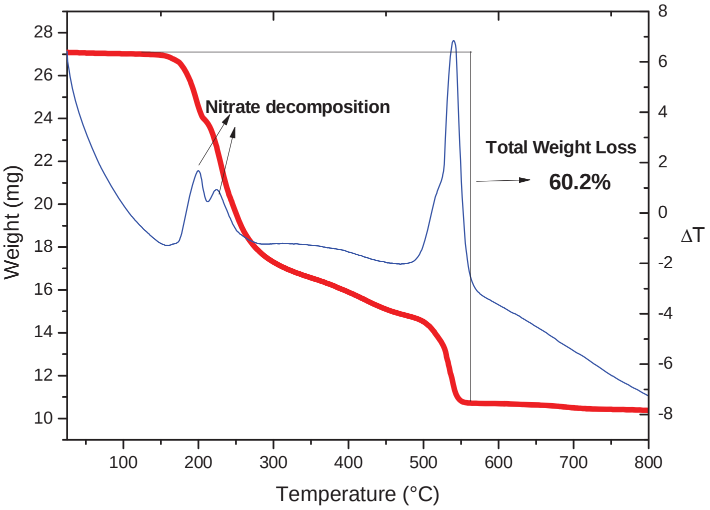

Figure 5.2: TGA (red) and DTA (blue) curve for complex 20 in an air atmosphere.

5.3.4 Extraction studies of UO_2(VI) and Pu(IV) with L^{13} from nitric acid medium: The extraction studies were carried out by using ligand $\mathbf{L^{13}}$ in *n*-dodecane with UO_2(VI) and Pu(IV) at tracer levels (using the ^{233}U and ^{239}Pu isotopes) from nitric acid medium to assess the feasibility of using these ligands for extraction purposes.

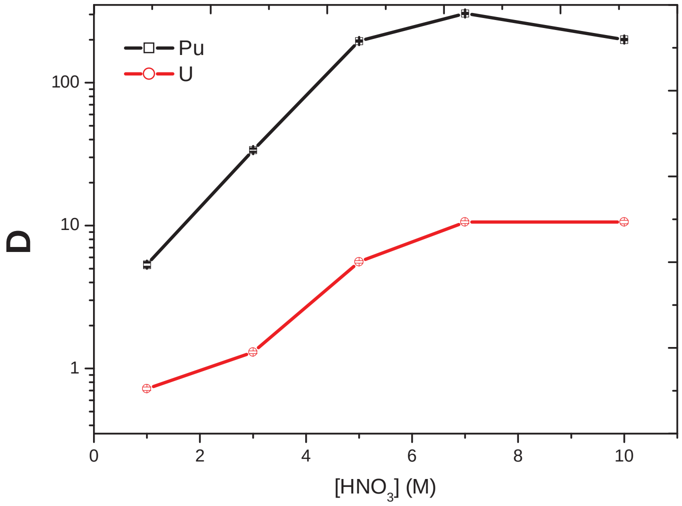

Figure 5.3: Graph showing the variation of D values of UO_2(VI) and Pu(IV) with L^{13} with HNO_3 concentration.

Distribution ratios (D) for UO_2(VI) and Pu(IV) as a function of nitric acid concentration (Fig. 5.3) shows clearly that UO_2(VI) and Pu(IV) are extracted significantly from a nitric acid concentrations of 1–7 M into *n*-dodecane. The observed distribution ratios follow the order : $D_{Pu(IV)} >> D_{UO2(IV)}$ and are comparable to those observed for the malonamides, CMP, CMPO, CMSO or malonamide ligands with these metal ions[125a, 185].All the D values and separation factors (S.F. = D_{Pu}/D_U) at different acidities have been summarized in Table 5.3. The highest separation factor of ~35 is realized for 5 M HNO_3. Hence from the data, it can be stated that the newly synthesized ligand is a promising bi-functional extractant for the separation of tetravalent and hexavalent actinides from the nitric acid medium.

Table 5.3: D values and S.F. at different acidity

Acidity	D_{Pu}	D_U	S.F. (D_{Pu}/D_U)
1	5.33±0.19	0.72±0.02	7.40
3	33.72±0.91	1.30±0.03	25.93
5	195.65±1.91	5.57±0.12	35.13
7	304.58±2.50	10.57±0.25	28.82
10	200.58±1.85	10.60±0.31	18.92

5.3.5 Acid uptake study by the ligand: The uptake of nitric acid by the ligand $\mathbf{L^{13}}$ involves the protonation of ligand according to the following equation:

$E\ (org.) + n.H^+(aq) + n.NO_3^-(aq) = E.nHNO_3\ (org.)$ .... (5.1)

Where, 'E' is the neutral extractant and 'n' is the number of nitric acid molecules involved in the formation of acid adduct. The acid uptake constant K_H is given by:

$K_H = [E.nHNO_3]_{org}/[E]_{org}.[H^+]^n_{aq}[NO_3^-]^n_{aq}$ ....(5.2)

Where, $[E]_{org}$ is concentration of uncomplexed organic ligand

As the data for the activities of HNO_3 and uncomplexed ligand in the organic phase were not available in the literature, the concentration terms have therefore been used and the equilibrium constant is referred as conditional acid uptake constant.

Taking logarithm of equation (2) and rearranging

$\log [H^+]_{org} - \log [E]_{org} = \log K_H + 2n \log [H^+]_{aq}$ ....(5.3)

Where $[H^+]_{aq} = [NO_3^-]_{aq}$ and $[E.nHNO3]_{org} = [H^+]_{org}$

Here, $[H^+]_{aq.}$ can be calculated from the titre value (T) and dissociation constant (K_a) of HNO_3 (K_a=23.5).

$K_a = [\ H^+]^2_{aq.} / [HNO_3]_{aq.}$, Where, $[HNO_3]_{aq.} = T - [H^+]_{\ aq}$............(5.4)

Thus, from equation (3) the plot of $\log [H^+]_{org} - \log [E]_{org}$ vs. $\log [H^+]_{aq}$ gives a straight line slope of 2n as shown in Fig. 5.4. The slope value obtained from Fig. 4 is 0.64 ± 0.02 which suggests the stoichiometry for the extracted acid adduct is 1:0.32 for ligand $\mathbf{L^{13}}$: HNO_3.

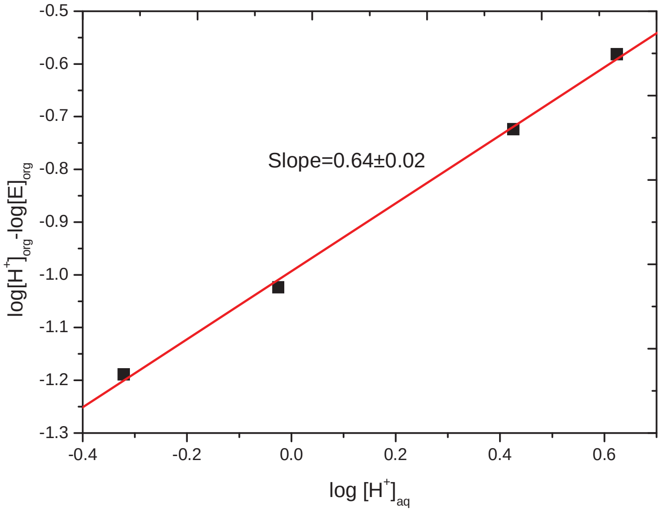

Figure 5.4: HNO_3 uptake by ligand L^{13}

5.3.6 The effect of extractant concentration on metal extraction and stoichiometry of the extractant in complex: The effect of ligand concentration variation on extraction of metal ions needs to be evaluated to assess the stoichiometry of the ligand in metal complexes. Distribution ratio (D_{Pu} and D_U) values for plutonium and uranium were determined at varying concentrations (0.0125 M – 0.2M) of ligand $\mathbf{L^{13}}$ at a fixed nitrate concentration i.e. 0.5M HNO_3 + 2.5M $NaNO_3$ feed solution as shown in Fig. 5.5. The logD vs. log [Extractant] plot showed a straight line with slope values ~1.07 and 1.02 for plutonium(IV) and uranyl(VI), respectively. This means that only one ligand is involved per metal ion in the extraction process.

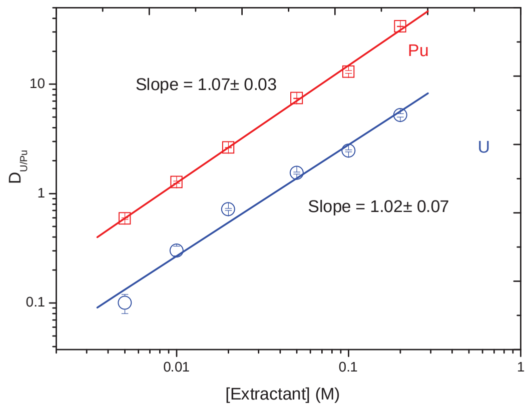

Figure 5.5: plot of [Extractant] vs. D at a constant nitric acid concentration of 0.5M HNO_3 + 2.5 M $NaNO_3$

5.4 Conclusions:

The novel bi-functional ligands having N-O and C=O oxygen donor groups have been synthesized and characterized by IR and ^1H NMR spectroscopy. The complexes of uranyl(VI) nitrate with these ligands show that the ligands are connected to the uranyl(VI) centre by two oxygen atoms from the amidic C=O and N-O in a chelating mode. The ligand $\mathbf{L^{13}}$ shows that uranyl(VI) and plutonium(IV) can be extracted from nitric acid medium significantly and can be extracted from each other. The maximum S.F. values are obtained in 5M HNO_3.

Chapter 6

Summary and future outlook

Coordination chemistry of neutral oxygen donor ligands with lanthanides and actinides is a well established branch of coordination chemistry of f-block elements. The solvation mechanism is at play to carry the metal ion from the aqueous phase to the organic phase with the neutral oxygen donor ligands. Mono functional oxygen donor ligands are good at the extraction of hexavalent and tetravalent actinides from nitric acid medium whilst bifunctional and trifunctional ligands are commonly used for the extraction of trivalent actinides and lanthanides. The coordination chemistry of monofuctional ligand sysytems such as phosphine oxides, *N*-oxides and amides with actinides is well established while bifunctional ligands containg two oxygen donors are still in progress. Many combinations including diamide (malonamide) (C=O and C=O), carbamoyl phosphine oxide (C=O and P=O) etc. are available in the literature to induce selectivilty in the extraction process towards one oxidation state over another. In this thesis, we have evaluated new bifunctional oxygen donor ligand systems towards the coordination chemistry of uranyl(VI) and lanthanide(III) and the summary of the key findings are listed below:

1. Chapter one gives the general introduction about the coordination chemistry of actinides and lanthanides relevant to separation studies.

2. In the second chapter, the synthesis, coordination and extraction properties of new dithiodiglycolamide based ligand system with uranyl(VI) ion are discussed. The two amide groups in this ligand sysytem are separated by a six atom bridge, but the ligand still behaves as a chelator to form 11-membered metallacycle rings upon coordination with uranium. Theoretical studies reveal that the chelating mode of binding for these ligands is more energetically favorable than monodentate or bridging bidentate modes of binding due to the two sulfur atoms in between the

metallacyclic ring. The dioctyl based ligand shows an appreciable extraction for uranyl(VI) and plutonium(IV) ions from nitric acid medium ($D_{UO2(VI)}$ ~1 and $D_{Pu(IV)}$~10 at 3M HNO_3).

3. The third chapter, deals with the synthesis of the *N*,*N*-dialkyl-α-hydroxyacetamide based ligand system containing one amide group and one hydoxyl group. The coordination chemistry of this ligand system with uranyl(VI) nitrate shows that two of the ligands are bound to the metal centre in a chelating mode and out of the two nitrate groups, only one is bound to the metal centre and the other remains uncoordinated and outside the metal coordination sphere. The molecular structure of the europium(III) complex shows that three ligands are bound to the metal centre in a chelating mode and only one nitrate is in the primary coordination whilst the other two are outside the primary coordination sphere. Solvent extraction studies with this ligand system show promising behaviour for trivalent lanthanides and actinides separation ($D > 100$ at 4M HNO_3). This ligand behaviour is similar to the other reported diglycolamide ($D>100$) and the CMPO ($D>20$) based ligand system. High extraction behavior for trivalent lanthanide and actinide ions above 3 M HNO_3 and quantitative back extraction by 0.5M HNO_3 showed the potential capability of this novel monoamide extractant. Poor extraction for Sr(II) ions (D~10^{-4}) from 3-4M HNO_3 and Ru(III) from real HLLW solution makes it advantageous over other extractants by reducing extra steps needed during the back extraction process. This ligand is also capable of extracting the actinides from highly complexing media such as HF and phosphoric acid..
4. In the fouth chapter, the coordination chemistry of diphenyl-(2-pyridyl) phosphine oxide (PON) and diphenyl-(2-pyridyl-N-oxide) phosphine oxide (PONO) with lanthanide(III) and uranyl(VI) nitrate is discussed. In the case of the PON ligand, the

phophine oxide is an oxygen donor while the pyridyl group is a nitrogen donor while in the case of the PONO ligand, the phosphine oxide and pyridine *N*-oxide are the donor groups. The coordination chemistry of PON with uranyl(VI) nitrate clearly shows that this ligand behaves as monodentate ligand with phosphine oxide as a donor while the pyridyl nitrogen remains uncoordinated. Theoretical studies clearly conclude that the 1:2 complex, with two ligands bonded through the phosphine oxide is more favorable than the 1:1 complex with a bidentate chelating mode, where both phosphine oxide and pyridyl nitrogen atoms are bonded to the uranium centre. Furthermore, the coordination behaviour of the lanthanide(III) β-diketonates (TTA, Ln(III) = Eu and Sm) with PON and PONO ligands are studied. The PON ligand behaves as a monodentate ligand bonded through the phosphine oxide, while the PONO ligand behaves as bidentate ligand bonded through both the phosphine oxide and pyridine *N*-oxide groups. The europium(III) and samarium(III) complexes show very good luminescence behaviour and their luminescence quantum yield is controlled by the ligand field asymmetry around the metal entre.

5. The fifth chapter, deals with the synthesis of a new ligand system (*N*,*N*'-dialkyl carbamoyl methyl-2-pyridyl-N-oxide) sulfide (NOSCO) containing the *N*-oxide and amide groups and where the alkyl groups are *iso*-propyl, *iso*-butyl, *n*-butyl and *n*-octyl. The coordination chemistry of this ligand system with uranyl(VI) nitrate shows the bidentate behaviour of the ligand with the metal centre. The ligands are bound through the pyridine *N*-oxide and carbamoyl groups in a chelating manner. The ligand shows that uranyl(VI) and plutonium(IV) can be extracted significantly from nitric acid medium. The maximum separation factor for uranyl(VI) and plutonium(IV) is ~35 at 5 M HNO_3.

Actinide chemistry research has mainly begun for the use of nuclear energy in a sustainable way. The bifunctional ligands synthesized here show promising behaviour with respect to actinides separation and pave the way for further fine tuning to improve and add to the available the separation strategies for spent fuel. The dithiodiglycolamide ligand design shows how to tune the bridging ligand to chelating mode by introducing a sulfur atom in between the two amide groups in the ligand which further demonstrates a way to stabilise macrocyclic chelate rings with more than 6-atoms. In future, there is scope to further improve the ligand design to impart selectivity by tuning the spacer length i.e. number of atoms in the macrocyclic ring. The α-hyroxyacetamide based ligands show selectivity towards trivalent actinides and lanthanides over hexavalent actinides. This ligand is superior to the well established ligands such as the diglycolamide and CMPO based ligand systems. Many macrocyclic ligands containg diglycolamide and CMPO have been reported to improve the selectivity. Hence, there is now ample scope for the α-hyroxyacetamide ligand to be incorporated in such macrocyclic platforms and to improve the extraction behaviour with respect to selectivity for the metal ions. Studies on ionic liquids based on this functionality will also be very interesting for future separation methodologies. Diphenyl (2-pyridyl)-phosphine oxide (PON) and diphenyl (2-pyridyl-*N*-oxide) phosphine oxide (PONO) complexes with europium(III) and samarium(III) β-diketonates show that the luminescence behaviour can be controlled by the ligand field aroun the metal centre and these findings can be very useful in developing high efficiency luminescence devices and even for determining the exact nature of the species extracted in separations chemistry. The (*N*,*N*-dialkyl carbamoyl methyl-2-pyridyl-*N*-oxide) sulfide ligand systems which have N-O and C=O functionalities reported for the first time for actinide extractions and this ligand type shows some selectivity towards tetravalent plutonium as compared to hexavalent uranium. Further tuning of the ligand through design is highly probable to achieve practical usefulness of this new ligand system for actinide partitioning.

References:

1. Klaproth, M. H., Chemische Untersuchung des Uranits, einer neuentdeckten metallische Substanz. *Chem. Ann. Freunde Naturl.* **1789,** *2*, 387-403.

2. Stanton, A., Wilhelm Conrad Röntgen on a new kind of rays: translation of a paper read before the Würzburg Physical and Medical Society, 1895. *Nature* **1896,** *53* (1369), 274-276.

3. Joliot, F.; Curie, I., Artificial production of a new kind of radio-element. *Nature* **1934,** *133* (3354), 201-202.

4. Meitner, L.; Frisch, O. R., When Man Became God. *Nature* **1939,** *143*, 239-240.

5. Nash, K. L.; Braley, J. C., Challenges for actinide separations in advanced nuclear fuel cycles. In *Nuclear Energy and the Environment*, ACS Publications: 2010; pp 19-38.

6. Beatty, R., *The Lanthanides*. Marshall Cavendish: 2007.

7. (a) Wells, A. F., *Structural inorganic chemistry*. Oxford University Press: 2012; (b) Pyykko, P., Relativistic effects in structural chemistry. *Chemical Reviews* **1988,** *88* (3), 563-594.

8. Fortier, S.; Walensky, J. R.; Wu, G.; Hayton, T. W., High-Valent Uranium Alkyls: Evidence for the Formation of UVI(CH2SiMe3)6. *Journal of the American Chemical Society* **2011,** *133* (30), 11732-11743.

9. (a) Katz, J. J., *The Chemistry of the Actinide and Transactinide Elements (Volumes 1-5)*. Springer Science & Business Media: 2007; Vol. 1; (b) Burns, C. J.; Neu, M. P.; Boukhalfa, H.; Gutowshi, K. E.; Bridges, N. J.; Rogers, R. D.; McCleverty, J. A.; Meyer, T. J.; Parkin, G. F. R., *Comprehensive Coordination Chemistry II*. 2004; Vol. 3, p 189.

10. Burns, C. J.; Bursten, B. E., Covalency in f-element organometallic complexes: Theory and experiment. *Comments on Inorganic Chemistry* **1989,** *9* (2), 61-93.

11. Cotton Simon, A., *Scandium, Yttrium & the Lanthanides: Inorganic & Coordination Chemistry*.

12. Marçalo, J.; De Matos, A. P., A new definition of coordination number and its use in lanthanide and actinide coordination and organometallic chemistry. *Polyhedron* **1989,** *8* (20), 2431-2437.

13. Dunbar, A. C.; Gozum, J. E.; Girolami, G. S., Synthesis and characterization of phosphine adducts of thorium borohydride, Th (BH 4) 4: Crystal structures of Th (BH4) 4 (PEt3) 2 and Th (BH4) 4 (Me2PCH2CH2PMe2) 2. *Journal of Organometallic Chemistry* **2010,** *695* (25), 2804-2808.

14. Rietz, R. R.; Edelstein, N. M.; Ruben, H. W.; Templeton, D. H.; Zalkin, A., Preparation and crystal structure of uranium (IV) borohydride-bis (tetrahydrofuran), U (BH4) 4.20 C4H8. *Inorganic Chemistry* **1978,** *17* (3), 658-660.

15. Daly, S. R.; Piccoli, P.; Schultz, A. J.; Todorova, T. K.; Gagliardi, L.; Girolami, G. S., Synthesis and Properties of a Fifteen-Coordinate Complex: The Thorium Aminodiboranate [Th (H3BNMe2BH3) 4]. *Angewandte Chemie International Edition* **2010,** *49* (19), 3379-3381.

16. Gaunt, A. J.; Enriquez, A. E.; Reilly, S. D.; Scott, B. L.; Neu, M. P., Structural characterization of Pu [N (SiMe3) 2] 3, a synthetically useful nonaqueous plutonium (iii) precursor. *Inorganic Chemistry* **2008,** *47* (1), 26-28.

17. Andersen, R. A., Tris ((hexamethyldisilyl) amido) uranium (III): preparation and coordination chemistry. *Inorganic Chemistry* **1979,** *18* (6), 1507-1509.

18. Berg, J. M.; Clark, D. L.; Huffman, J. C.; Morris, D. E.; Sattelberger, A. P.; Streib, W. E.; Van der Sluys, W. G.; Watkin, J. G., Early actinide alkoxide chemistry. Synthesis, characterization, and molecular structures of thorium (IV) and uranium (IV) aryloxide complexes. *Journal of the American Chemical Society* **1992,** *114* (27), 10811-10821.

19. (a) Reynolds, J. G.; Zalkin, A.; Templeton, D. H.; Edelstein, N. M.; Templeton, L. K., Crystal structure and optical and magnetic properties of tetrakis (diethylamido) uranium (IV), a five-coordinate dimeric complex in the solid state. *Inorganic Chemistry* **1976,** *15* (10), 2498-2502; (b) Burns, C. J.; Clark, D. L.; Donohoe, R. J.; Duval, P. B.; Scott, B. L.; Tait, C. D., A trigonal bipyramidal

uranyl amido complex: synthesis and structural characterization of [Na (THF) 2][UO2 (N (SiMe3) 2) 3]. *Inorganic Chemistry* **2000,** *39* (24), 5464-5468.

20. Kannan, S.; Barnes, C. L.; Duval, P. B., Versatile new uranyl(vi) dihalide complexes supported by tunable organic amide ligands. *Chemical Communications* **2005,** (48), 5997-5998.

21. Kannan, S.; Pillai, M. R. A.; Venugopal, V.; Droege, P. A.; Barnes, C. L., The camphor adducts of uranyl bis (β-diketonates). The low temperature 19 F NMR behaviour of [UO 2 (TTA) 2· camphor] and the crystal structure of [UO 2 (DBM) 2· camphor]. *Inorganica Chimica Acta* **1997,** *254* (1), 113-117.

22. Willis, B. T. M., Structures of UO2, UO2+ x andU4O9 by neutron diffraction. *Journal de Physique* **1964,** *25* (5), 431-439.

23. Zalkin, A.; Forrester, J. D.; Templeton, D. H., The Crystal Structure of Thorium Tetraiodide. *Inorganic Chemistry* **1964,** *3* (5), 639-644.

24. Kannan, S.; Chetty, K. V.; Venugopal, V.; Drew, M. G. B., Extraction and coordination studies of the unexplored bifunctional ligand carbamoyl methyl sulfoxide (CMSO) with uranium(vi) and cerium(iii) nitrates. Synthesis and structures of [UO2(NO3)2(PhSOCH2CONiBu2)] and [Ce(NO3)3(PhSOCH2CONBu2)2]. *Dalton Transactions* **2004,** (21), 3604-3610.

25. Levy, J. H.; Taylor, J. C.; Wilson, P. W., The structure of uranium (III) triiodide by neutron diffraction. *Acta Crystallographica Section B: Structural Crystallography and Crystal Chemistry* **1975,** *31* (3), 880-882.

26. Matonic, J. H.; Scott, B. L.; Neu, M. P., High-yield synthesis and single-crystal X-ray structure of a plutonium (III) aquo complex:[Pu (H2O) 9][CF3SO3] 3. *Inorganic Chemistry* **2001,** *40* (12), 2638-2639.

27. Leipoldt, J. G.; Wessels, G. F. S.; Bok, L. D. C., The crystal and molecular structure of tetrakis (1, 1, 1-trifluoro-3-2′-thenoylacetonato) tri-n-octylphosphine oxide thorium (IV). *Journal of Inorganic and Nuclear Chemistry* **1975,** *37* (12), 2487-2490.

28. Day, V. W.; Hoard, J. L., Stereochemistry of tropolonato complexes utilizing the higher coordination numbers. I. Nine-coordinate tetrakis (tropolonato)-N, N'-dimethylformamidethorium (IV). *Journal of the American Chemical Society* **1970,** *92* (12), 3626-3635.

29. Akhtar, M. N.; Smith, A. J., The crystal structure of tetrapotassium tetraoxalatothorium (IV) tetrahydrate, K4Th (C2O4) 4.4 H2O. *Acta Crystallographica Section B: Structural Crystallography and Crystal Chemistry* **1975,** *31* (5), 1361-1366.

30. Caughlan, C. N.; Hart, F. A.; VanNice, R., Crystal and molecular structure of tetranitratobis (triphenylphosphine oxide) cerium (IV). *Inorganic Chemistry* **1971,** *10* (1), 115-122.

31. Ueki, T.; Zalkin, A.; Templeton, D. H., Crystal structure of thorium nitrate pentahydrate by X-ray diffraction. *Acta Crystallographica* **1966,** *20* (6), 836-841.

32. Rammo, N. N.; Hamid, K. R.; Khaleel, B. A., Synthesis and crystal structure analysis of 4, 4'-dipyridinium 4, 4'-dipyridinium (II) nitrate hexanitratothorate (IV)[(C10H8N2H)(C10H8N2H2) NO3][Th (NO3) 6]. *Journal of the Less Common Metals* **1990,** *162* (1), 1-9.

33. (a) Brady, E. D.; Clark, D. L.; Gordon, J. C.; Hay, P. J.; Keogh, D. W.; Poli, R.; Scott, B. L.; Watkin, J. G., Tris (bis (trimethylsilyl) amido) samarium: X-ray Structure and DFT Study. *Inorganic Chemistry* **2003,** *42* (21), 6682-6690; (b) Andersen, R. A.; Templeton, D. H.; Zalkin, A., Structure of tris (bis (trimethylsilyl) amido) neodymium (III), Nd [N (Si (CH3) 3) 2] 3. *Inorganic Chemistry* **1978,** *17* (8), 2317-2319.

34. Zhou, S.-L.; Wang, S.-W.; Yang, G.-S.; Liu, X.-Y.; Sheng, E.-H.; Zhang, K.-H.; Cheng, L.; Huang, Z.-X., Synthesis, structure, and catalytic activity of tetracoordinate lanthanide amides [(Me 3 Si) 2 N] 3 Ln (μ-Cl) Li (THF) 3 (Ln= Nd, Sm, Eu). *Polyhedron* **2003,** *22* (7), 1019-1024.

35. Dröse, P.; Hrib, C. G.; Hilpert, L.; Edelmann, F. T., Synthesis and Structure of a Rare Unsolvated Bis (amidinato) Lanthanide Chloride,(Piso) 2CeCl (Piso=[tBuC (NAr) 2]–, Ar= C6H3iPr2–2, 6). *Zeitschrift für anorganische und allgemeine Chemie* **2011,** *637* (1), 31-33.

36. Bassett, A. P.; Van Deun, R.; Nockemann, P.; Glover, P. B.; Kariuki, B. M.; Van Hecke, K.; Van Meervelt, L.; Pikramenou, Z., Long-lived near-infrared luminescent lanthanide complexes of imidodiphosphinate “shell” ligands. *Inorganic Chemistry* **2005,** *44* (18), 6140-6142.

37. Wang, J.; Takahashi, M.; Takeda, M., Crystal Structures and 166Er Mössbauer Spectra for Some β-Diketonatoerbium (III) Complexes. *Bulletin of the Chemical Society of Japan* **2002,** *75* (4), 735-740.

38. Biju, S.; Raj, D. B. A.; Reddy, M. L. P.; Kariuki, B. M., Synthesis, crystal structure, and luminescent properties of novel Eu3+ heterocyclic β-diketonate complexes with bidentate nitrogen donors. *Inorganic Chemistry* **2006,** *45* (26), 10651-10660.

39. Tanase, S.; Gallego, P. M.; de Gelder, R.; Fu, W. T., Synthesis, crystal structure and photophysical properties of europium (III) and terbium (III) complexes with pyridine-2, 6-dicarboxamide. *Inorganica Chimica Acta* **2007,** *360* (1), 102-108.

40. Parker, D.; Puschmann, H.; Batsanov, A. S.; Senanayake, K., Structural Analysis of Nine-Coordinate Lanthanide Complexes: Steric Control of the Metal− Water Distance Across the Series. *Inorganic Chemistry* **2003,** *42* (26), 8646-8651.

41. Gourbatsis, S.; Plakatouras, J. C.; Nastopoulos, V.; Cardin, C. J.; Hadjiliadis, N., [Pr (NO 3) 3 L]: a mononuclear ten-coordinate lanthanide (III) complex with a tetradentate di-Schiff base. *Inorganic Chemistry Communications* **1999,** *2* (10), 468-471.

42. Sharma, C. V. K.; Rogers, R. D., ‘Molecular Chinese blinds’: self-organization of tetranitrato lanthanide complexes into open, chiral hydrogen bonded networks. *Chemical Communications* **1999,** (1), 83-84.

43. Jones, P. L.; Amoroso, A. J.; Jeffery, J. C.; McCleverty, J. A.; Psillakis, E.; Rees, L. H.; Ward, M. D., Lanthanide complexes of the hexadentate N-donor podand tris [3-(2-pyridyl) pyrazolyl] hydroborate: Solid-state and solution properties. *Inorganic Chemistry* **1997,** *36* (1), 10-18.

44. (a) Marks, T. J., Actinide organometallic chemistry. *Accounts of Chemical Research* **1976,** *9* (6), 223-230; (b) Behrle Andrew, C.; Walensky Justin, R., *Actinides: Organometallic Chemistry*.

45. Fox, A. R.; Bart, S. C.; Meyer, K.; Cummins, C. C., Towards uranium catalysts. *Nature* **2008,** *455* (7211), 341-349.

46. Fleming, J. E.; Lynton, H., Crystal structure of uranyl nitrate hexahydrate. SOC CHEMICAL INDUSTRY 14 BELGRAVE SQUARE, LONDON SW1X 8PS, ENGLAND: 1960; pp 1416-1417.

47. McKay, H. A. C., The PUREX process. In *Science and technology of tribuytl phosphate*, 1990.

48. (a) Puzikov, E. A.; Zilberman, B. Y.; Fedorov, Y. S.; Blazheva, I. V.; Kudinov, A. S.; Goletskiy, N. D.; Ryabkov, D. V., A New Approach to Simulation of Extraction Equilibria in the PUREX Process. *Solvent Extraction and Ion Exchange* **2015,** *33* (4), 362-384; (b) Paiva, A. P.; Malik, P., Recent advances on the chemistry of solvent extraction applied to the reprocessing of spent nuclear fuels and radioactive wastes. *Journal of radioanalytical and nuclear chemistry* **2004,** *261* (2), 485-496.

49. (a) Ruikar, P. B.; Nagar, M. S.; Subramanian, M. S.; Gupta, K. K.; Varadarajan, N.; Singh, R. K., Extraction behavior of uranium (VI), plutonium (IV), zirconium (IV), ruthenium (III) and europium (III) with γ-pre-irradiated solutions of N, N’-methylbutyl substituted amides in n-dodecane. *Journal of radioanalytical and nuclear chemistry* **1995,** *201* (2), 125-134; (b) Musikas, C.; Hubert, H., EXTRACTION BY N, N'-TETRAALKYLMALONAMIDES II. *Solvent Extraction and Ion Exchange* **1987,** *5* (5), 877-893; (c) Siddall, T. H., EFFECTS OF STRUCTURE OF N,N-DISUBSTITUTED AMIDES ON THEIR EXTRACTION OF ACTINIDE AND ZIRCONIUM NITRATES AND OF NITRIC ACID1. *The Journal of Physical Chemistry* **1960,** *64* (12), 1863-1866.

50. Laskorin, B. N.; Skorovarov, D. I.; Philipp, E. A.; Volodin, II, Extraction of uranium and plutonium by tertiary aliphatic phosphine oxides. *Journal of Radioanalytical Chemistry* **1974,** *21* (1), 65-79.

51. (a) Shukla, J. P.; Pai, S. A.; Subramanian, M. S., Solvent extraction of plutonium (IV), uranium (VI), and some fission products with di-n-octylsulfoxide. *Separation Science and Technology* **1979,** *14* (10), 883-894; (b) Chaohong, S.; Borong, B.; Yizhi, B.; Gaodong, W.; Ju, Q.; Zhengbei, C., Extraction of

U (VI), Th (IV) and some fission products from nitric acid medium by sulfoxides and effect of γ-irradiation on the extraction. *Journal of radioanalytical and nuclear chemistry* **1994,** *178* (1), 91-98.

52. Ramakrishna, V. V.; Patil, S. K., Synergic extraction of actinides. In *New Developments*, Springer: 1984; pp 35-90.

53. Burns, J. H.; Brown, G. M.; Ryan, R. R., Structure of dinitratodioxobis (triisobutyl phosphate) uranium (VI) at 139 K. *Acta Crystallographica Section C: Crystal Structure Communications* **1985,** *41* (10), 1446-1448.

54. Koshino, N.; Harada, M.; Nogami, M.; Morita, Y.; Kikuchi, T.; Ikeda, Y., A structural study on uranyl (VI) nitrate complexes with cyclic amides: N-n-butyl-2-pyrrolidone, N-cyclohexylmethyl-2-pyrrolidone, and 1,3-dimethyl-2-imidazolidone. *Inorganica Chimica Acta* **2005,** *358* (6), 1857-1864.

55. (a) Pathak, P. N.; Veeraraghavan, R.; Prabhu, D. R.; Mahajan, G. R.; Manchanda, V. K., Separation studies of uranium and thorium using di-2-ethylhexyl isobutyramide (D2EHIBA). *Separation Science and Technology* **1999,** *34* (13), 2601-2614; (b) Prabhu, D. R.; Mahajan, G. R.; Nair, G. M., Di (2-ethyl hexyl) butyramide and di (2-ethyl hexyl) isobutyramide as extractants for uranium (VI) and plutonium (IV). *Journal of radioanalytical and nuclear chemistry* **1997,** *224* (1-2), 113-117.

56. Kannan, S.; Deb, S. B.; Gamare, J. S.; Drew, M. G. B., Coordination and separation studies of the uranyl ion with iso-butyramide based ligands: Synthesis and structures of [UO 2 (NO 3) 2 (i C 3 H 7 CON {i C 4 H 9} 2) 2] and [UO 2 (C 6 H 5 COCHCOC 6 H 5) 2 (i C 3 H 7 CON {i C 3 H 7} 2)]. *Polyhedron* **2008,** *27* (12), 2557-2562.

57. (a) Malik, K. M. A.; Jeffery, J. W., The crystal structure of tetranitratobis (triphenylphosphine oxide) thorium (IV). *Acta Crystallographica Section B: Structural Crystallography and Crystal Chemistry* **1973,** *29* (12), 2687-2692; (b) Dillen, J. L. M.; van Rooyen, P. H.; Strydom, C. A.; van Vuuren, C. P. J., Structures of tetranitratobis (tripyrrolidinophosphine oxide) uranium (IV) and tetranitratobis (triphenylphosphine oxide) uranium (IV). *Acta Crystallographica Section C: Crystal Structure Communications* **1988,** *44* (11), 1921-1923.

58. (a) Lumetta, G. J.; McNamara, B. K.; Rapko, B. M.; Sell, R. L.; Rogers, R. D.; Broker, G.; Hutchison, J. E., Synthesis and characterization of mono- and bis-(tetraalkylmalonamide)uranium(VI) complexes. *Inorganica Chimica Acta* **2000,** *309* (1–2), 103-108; (b) Singh, S. K.; Dhami, P. S.; Dakshinamoorthy, A.; Sundersanan, M., Studies on the recovery of uranium from phosphoric acid medium using synergistic mixture of 2-ethyl hexyl hydrogen 2-ethyl hexyl phosphonate and octyl (phenyl)-N, N-diisobutyl carbamoyl methyl phosphine oxide. *Separation Science and Technology* **2009,** *44* (2), 491-505; (c) Zhu, Z.-X.; Sasaki, Y.; Suzuki, H.; Suzuki, S.; Kimura, T., Cumulative study on solvent extraction of elements by N, N, N′, N′-tetraoctyl-3-oxapentanediamide (TODGA) from nitric acid into n-dodecane. *Analytica chimica acta* **2004,** *527* (2), 163-168; (d) Kannan, S.; Moody, M. A.; Barnes, C. L.; Duval, P. B., Lanthanum(III) and Uranyl(VI) Diglycolamide Complexes: Synthetic Precursors and Structural Studies Involving Nitrate Complexation. *Inorganic Chemistry* **2008,** *47* (11), 4691-4695.

59. Caudle, L. J.; Duesler, E. N.; Paine, R. T., Formation and crystal and molecular structures of dioxouranium(VI) complexes containing bidentate carbamoylmethylphosphinate and phosphine oxide ligands. *Inorganica Chimica Acta* **1985,** *110* (2), 91-100.

60. Henderson, W.; Leach, M. T.; Nicholson, B. K.; Wilkins, A. L.; Hoye, P. A. T., Uranyl nitrate complexes of camphene-derived organophosphorus ligands, and the X-ray crystal structure of [UO 2 (NO 3) 2 (RPO3Me 2) 2](R= endo-8-camphanyl). *Polyhedron* **1998,** *17* (21), 3747-3752.

61. Burns, J. H., Solvent-extraction complexes of the uranyl ion. 1. Crystal and molecular structure of bis(nitrato)bis(tri-n-butylphosphine oxide)dioxouranium(VI). *Inorganic Chemistry* **1981,** *20* (11), 3868-3871.

62. Bowen, S. M.; Duesler, E. N.; Paine, R. T., Synthesis and crystal and molecular structure of a [diethyl (N,N-diethylcarbamyl)methylenephosphonate]thorium nitrate complex. *Inorganic Chemistry* **1982,** *21* (1), 261-265.

63. Sasaki, Y.; Sugo, Y.; Suzuki, S.; Tachimori, S., The novel extractants, diglycolamides, for the extraction of lanthanides and actinides in HNO3–n-dodecane system. *Solvent Extraction and Ion Exchange* **2001,** *19* (1), 91-103.

64. Tian, G.; Xu, J.; Rao, L., Optical absorption and structure of a highly symmetrical neptunium (V) diamide complex. *Angewandte Chemie International Edition* **2005,** *44* (38), 6200-6203.

65. Lewis, F. W.; Harwood, L. M.; Hudson, M. J.; Drew, M. G. B.; Desreux, J. F.; Vidick, G.; Bouslimani, N.; Modolo, G.; Wilden, A.; Sypula, M., Highly efficient separation of actinides from lanthanides by a phenanthroline-derived bis-triazine ligand. *Journal of the American Chemical Society* **2011,** *133* (33), 13093-13102.

66. Clark, D. L.; Keogh, D. W.; Palmer, P. D.; Scott, B. L.; Tait, C. D., Synthesis and Structure of the First Transuranium Crown Ether Inclusion Complex:[NpO2 ([18] Crown-6)] ClO4. *Angewandte Chemie International Edition* **1998,** *37* (1-2), 164-166.

67. Bombieri, G.; De Paoli, G.; Immirzi, A., Crown ether complexes of actinide elements an X-ray study of the conformational change of the crown ether within the UO2 (NO3) 2 (H2O) 2 (18-crown-6) molecule. *Journal of Inorganic and Nuclear Chemistry* **1978,** *40* (5), 799-802.

68. (a) Fedoseev, E. V.; Aizenberg, M. I.; Davydov, A. V.; Myasoedov, B. F., Separation of actinide and fission product elements by means of thermochromatography and fractional sublimation of their β-diketonates. *Journal of radioanalytical and nuclear chemistry* **1989,** *136* (6), 395-403; (b) Shcherbakova, L. L.; Mishin, V. Y.; Rubtsov, E. M., NMR investigation of actinide (4) beta-diketonates. *Radiokhimiya* **1984,** *26* (5), 698-700.

69. Baskin, Y.; Ferraro, J. R., Studies on TTA complexes with metal ions-IV: Investigations of some crystalline forms of uranyl-TTA complex. *Journal of Inorganic and Nuclear Chemistry* **1968,** *30* (1), 241-251.

70. Baskin, Y.; Prasad, N. S. K., Studies on TTA complexes with metal ions—II: Investigations of some tetravalent complexes in the solid state. *Journal of Inorganic and Nuclear Chemistry* **1963,** *25* (8), 1011-1019.

71. (a) Irving, H.; Edgington, D. N., Synergic effects in the solvent extraction of the actinides—I uranium (VI). *Journal of Inorganic and Nuclear Chemistry* **1960,** *15* (1-2), 158-170; (b) Patil, S. K.; Ramakrishna, V. V.; Haraprakas, B., Synergistic extraction of metal ions involving mixed adduct formation by β-diketone-neutral donor mixtures. *Journal of Inorganic and Nuclear Chemistry* **1981,** *43* (6), 1377-1382; (c) Felinto, M.; Almeida, V. F., Solvent extraction separation of uranium (VI) with acetatecalix [n] arene and β-diketone (HTTA). *Journal of alloys and compounds* **2000,** *303*, 524-528.

72. (a) Kannan, S.; Usman, A.; Fun, H. K., Synthesis and characterization of [bis (β-diketonato) uranium (VI)] nitrone compounds. The crystal and molecular structure of [UO 2 (TTA) 2· p-NO 2瑕 C 5 H 4 NO]. *Polyhedron* **2002,** *21* (23), 2403-2407; (b) Alagar, M.; Rajagopal, K.; Krishnakumar, R. V.; Subha Nandhini, M.; Kannan, S.; Natarajan, S., Bis (1, 3-diphenylpropane-1, 3-dionato-κ2O, O′) dioxo (triphenylphosphine oxide-κO) uranium (VI). *Acta Crystallographica Section E: Structure Reports Online* **2003,** *59* (7), m524-m526.

73. (a) Nigond, L.; Musikas, C.; Cuillerdier, C., EXTRACTION BY N, N, N', N-TETRAALKYL-2 ALKYL PROPANE-1, 3 DIAMIDES. I. H2O, HNO3 and HClO4. *Solvent Extraction and Ion Exchange* **1994,** *12* (2), 261-296; (b) Subramanian, M. S., Carbamoylmethyl sulfoxides as novel extractants for actinides. *Journal of radioanalytical and nuclear chemistry* **1994,** *187* (2), 91-97; (c) Biswas, S. S.; Murty, P. S.; Sethumadhavan, A.; Kaimal, R.; Sankaran, A. V., Separation of some trace rare earths from uranium by two-step liquid-liquid extraction and estimation by ICP-AES. *Analytical letters* **1991,** *24* (5), 887-901.

74. (a) Bosson, M.; Levason, W.; Patel, T.; Popham, M. C.; Webster, M., Lanthanide nitrate complexes of diphenylmethylphosphine oxide: synthesis and spectroscopic studies. Crystal structures of [La (Ph 2 MePO) 3 (NO 3) 3],[La (Ph 2 MePO) 4 (NO 3) 3]· xMe 2 CO and [Yb (Ph 2 MePO) 4 (NO 3) 2] PF 6. *Polyhedron* **2001,** *20* (15), 2055-2062; (b) Levason, W.; Newman, E. H.; Webster, M., Tetrakis (triphenylphosphine oxide) complexes of the lanthanide nitrates; synthesis,

characterisation and crystal structures of [La (Ph 3 PO) 4 (NO 3) 3]· Me 2 CO and [Lu (Ph 3 PO) 4 (NO 3) 2] NO 3. *Polyhedron* **2000,** *19* (28), 2697-2705.

75. (a) Hudson, M. J.; Lewis, F. W.; Harwood, L. M., The circuitous journey from malonamides to BTPhens: ligands for separating actinides from lanthanides. *Strategies and Tactics in Organic Synthesis. Academic Press, London* **2013**, 177-202; (b) Nagar, M. S.; Ruikar, P. B.; Mathur, J. N.; Lyer, R. H., Synthesis and Characterization of Plutonium (IV), Uranium (VI), Morium (IV) and Neodymium (III) Nitrate Complexes with Bidentate Organophosphorus Ligands. *Synthesis and reactivity in inorganic and metal-organic chemistry* **1998,** *28* (4), 621-636; (c) Kulyako, Y.; Malikov, D.; Trofimov, T.; Chmutova, M.; Myasoedov, B., Extraction of Actinides and Lanthanides with Diphenyl [dibutylcarbamoylmethyl] phosphine Oxide in the Absence of a Solvent. *Journal of Nuclear Science and Technology* **2002,** *39* (sup3), 302-305.

76. Antonio, M. R.; McAlister, D. R.; Horwitz, E. P., An europium (III) diglycolamide complex: insights into the coordination chemistry of lanthanides in solvent extraction. *Dalton Transactions* **2015,** *44* (2), 515-521.

77. (a) Panak, P. J.; Geist, A., Complexation and extraction of trivalent actinides and lanthanides by triazinylpyridine N-donor ligands. *Chemical Reviews* **2013,** *113* (2), 1199-1236; (b) Iveson, P. B.; Rivière, C.; Guillaneux, D.; Nierlich, M.; Thuéry, P.; Ephritikhine, M.; Madic, C., Selective complexation of uranium (III) over cerium (III) by 2, 6-bis (5, 6-dialkyl-1, 2, 4-triazin-3-yl) pyridines: 1H NMR and X-ray crystallography studies. *Chemical Communications* **2001,** (16), 1512-1513; (c) Berthet, J.-C.; Miquel, Y.; Iveson, P. B.; Nierlich, M.; Thuéry, P.; Madic, C.; Ephritikhine, M., The affinity and selectivity of terdentate nitrogen ligands towards trivalent lanthanide and uranium ions viewed from the crystal structures of the 1∶ 3 complexes. *Journal of the Chemical Society, Dalton Transactions* **2002,** (16), 3265-3272.

78. Backer-Dirks, J. D. J.; Cooke, J. E.; Galas, A. M. R.; Ghotra, J. S.; Gray, C. J.; Hart, F. A.; Hursthouse, M. B., Complexes of lanthanide ions with the crown ether 1, 4, 7, 10, 13, 16-hexaoxacyclo-octadecane. *Journal of the Chemical Society, Dalton Transactions* **1980,** (11), 2191-2198.

79. Bünzli, J. C.; Wessner, D.; Klein, B., Complexes of the Heavier Lanthanoid Nitrates with Crown Ethers. In *The Rare Earths in Modern Science and Technology*, Springer: 1980; pp 99-104.

80. Bünzli, J.-C. G.; Wessner, D., Complexes of lanthanoid nitrates with 12-crown-4 Ether: Synthesis and characterization. *Inorganica Chimica Acta* **1980,** *44*, L55-L58.

81. Rogers, R. D.; Rollins, A. N.; Benning, M. M., f-Element/crown ether complexes. 22. Preparation and structural characterization of lanthanide chloride complexes of 12-crown-4. *Inorganic Chemistry* **1988,** *27* (21), 3826-3835.

82. Rogers, R. D., f-Element/crown ether complexes. 26. Crystallization of two hydrated forms of hydrogen bonded complexes of NdCl3·nH2O and 15-crown-5. Crystal structures of [Nd(OH2)9]Cl3·15-crown-5·H2O and [NdCl2(OH2)6]Cl·15-crown-5. *Inorganica Chimica Acta* **1988,** *149* (2), 307-314.

83. Rogers, R. D.; Rollins, A. N.; Henry, R. F.; Murdoch, J. S.; Etzenhouser, R. D.; Huggins, S. E.; Nunez, L., Direct comparison of the preparation and structural features of crown ether and polyethylene glycol complexes of neodymium trichloride hexahydrate. *Inorganic Chemistry* **1991,** *30* (26), 4946-4954.

84. (a) Furphy, B. M.; Harrowfield, J. M.; Kepert, D. L.; Skelton, B. W.; White, A. H.; Wilner, F. R., Bimetallic lanthanide complexes of the calixarenes: europium (III) and tert-butylcalix [8] arene. *Inorganic Chemistry* **1987,** *26* (25), 4231-4236; (b) Furphy, B. M.; Harrowfield, J. M.; Ogden, M. I.; Skelton, B. W.; White, A. H.; Wilner, F. R., Lanthanide ion complexes of the calixarenes. Part 4. Double inclusion by p-t-butylcalix [4] arene (H 4 L). Crystal structures of [Eu 2 (HL) 2 (dmf) 4]. 7dmf (dmf= dimethylformamide) and H 4 L. dmso (dmso= dimethyl sulphoxide). *Journal of the Chemical Society, Dalton Transactions* **1989,** (11), 2217-2221.

85. Zalkin, A.; Templeton, D. H.; Karraker, D. G., Crystal and molecular structure of the heptacoordinate complex tris (diphenylpropanedionato) aquoholmium, Ho (PhCOCHCOPh) 3. H2o. *Inorganic Chemistry* **1969,** *8* (12), 2680-2684.

86. (a) Sood, D. D.; Patil, S. K., Chemistry of nuclear fuel reprocessing: current status. *Journal of radioanalytical and nuclear chemistry* **1996,** *203* (2), 547-573; (b) Nash, K. L.; Choppin, G. R., Separations chemistry for actinide elements: recent developments and historical perspective. *Separation Science and Technology* **1997,** *32* (1-4), 255-274; (c) Warin, D. In *Future nuclear fuel cycles: prospect and challenges for actinide recycling*, 2010; IOP Publishing: p 012063.

87. (a) Madic, C.; Hudson, M. J.; Liljenzin, J.-O.; Glatz, J.-P.; Nannicini, R.; Facchini, A.; Kolarik, Z.; Odoj, R., Recent achievements in the development of partitioning processes of minor actinides from nuclear wastes obtained in the frame of the NEWPART European programme (1996–1999). *Progress in Nuclear Energy* **2002,** *40* (3-4), 523-526; (b) Grouiller, J.-P.; Pillon, S.; de Saint Jean, C.; Varaine, F.; Leyval, L.; Vambenepe, G.; Carlier, B., Minor actinides transmutation scenario studies with PWRs, FRs and moderated targets. *Journal of Nuclear Materials* **2003,** *320* (1), 163-169.

88. Geist, A.; Hill, C.; Modolo, G.; Foreman, M. R. S. J.; Weigl, M.; Gompper, K.; Hudson, M. J., 6, 6′-Bis (5, 5, 8, 8-tetramethyl-5, 6, 7, 8-tetrahydro-benzo [1, 2, 4] triazin-3-yl)[2, 2′] bipyridine, an Effective Extracting Agent for the Separation of Americium (III) and Curium (III) from the Lanthanides. *Solvent Extraction and Ion Exchange* **2006,** *24* (4), 463-483.

89. (a) Foreman, M. R. S.; Hudson, M. J.; Drew, M. G. B.; Hill, C.; Madic, C., Complexes formed between the quadridentate, heterocyclic molecules 6, 6′-bis-(5, 6-dialkyl-1, 2, 4-triazin-3-yl)-2, 2′-bipyridine (BTBP) and lanthanides (III): implications for the partitioning of actinides (III) and lanthanides (III). *Dalton Transactions* **2006,** (13), 1645-1653; (b) Drew, M. G. B.; Foreman, M. R. S. J.; Hill, C.; Hudson, M. J.; Madic, C., 6, 6′-bis-(5, 6-diethyl-[1, 2, 4] triazin-3-yl)-2, 2′-bipyridyl the first example of a new class of quadridentate heterocyclic extraction reagents for the separation of americium (III) and europium (III). *Inorganic Chemistry Communications* **2005,** *8* (3), 239-241.

90. Nilsson, M.; Nash, K. L., A review of the development and operational characteristics of the TALSPEAK process. *Solvent Extraction and Ion Exchange* **2007,** *25* (6), 665-701.

91. (a) Gelis, A. V.; Vandegrift, G. F.; Bakel, A.; Bowers, D. L.; Hebden, A. S.; Pereira, C.; Regalbuto, M., Extraction behaviour of actinides and lanthanides in TALSPEAK, TRUEX and NPEX processes of UREX+. *Radiochimica Acta* **2009,** *97* (4-5), 231-232; (b) Mincher, B. J.; Schmitt, N. C.; Case, M. E., A TRUEX-based separation of americium from the lanthanides. *Solvent Extraction and Ion Exchange* **2011,** *29* (2), 247-259.

92. Magnusson, D.; Christiansen, B.; Foreman, M. R. S.; Geist, A.; Glatz, J. P.; Malmbeck, R.; Modolo, G.; Serrano-Purroy, D.; Sorel, C., Demonstration of a SANEX Process in Centrifugal Contactors using the CyMe4-BTBP Molecule on a Genuine Fuel Solution. *Solvent Extraction and Ion Exchange* **2009,** *27* (2), 97-106.

93. Modolo, G.; Vijgen, H.; Serrano-Purroy, D.; Christiansen, B.; Malmbeck, R.; Sorel, C.; Baron, P., DIAMEX Counter-Current Extraction Process for Recovery of Trivalent Actinides from Simulated High Active Concentrate. *Separation Science and Technology* **2007,** *42* (3), 439-452.

94. (a) Hill, C.; Guillaneux, D.; Berthon, L.; Madic, C., SANEX-BTP process development studies. *Journal of Nuclear Science and Technology* **2002,** *39* (sup3), 309-312; (b) Kolarik, Z.; Müllich, U.; Gassner, F., Selective extraction of Am (III) over Eu (III) by 2, 6-ditriazolyl-and 2, 6-ditriazinylpyridines 1. *Solvent Extraction and Ion Exchange* **1999,** *17* (1), 23-32.

95. Magnusson, D.; Christiansen, B.; Malmbeck, R.; Glatz, J.-P., Investigation of the radiolytic stability of a CyMe4-BTBP based SANEX solvent. *Radiochimica Acta International journal for chemical aspects of nuclear science and technology* **2009,** *97* (9), 497-502.

96. Brown, J.; McLachlan, F.; Sarsfield, M.; Taylor, R.; Modolo, G.; Wilden, A., Plutonium loading of prospective grouped actinide extraction (GANEX) solvent systems based on diglycolamide extractants. *Solvent Extraction and Ion Exchange* **2012,** *30* (2), 127-141.

97. Aneheim, E.; Ekberg, C.; Fermvik, A.; Foreman, M. R. S. J.; Retegan, T.; Skarnemark, G., A TBP/BTBP-based GANEX separation process. Part 1: feasibility. *Solvent Extraction and Ion Exchange* **2010,** *28* (4), 437-458.
98. Schulz, W. W.; Bender, K. P.; Burger, L. L.; Navratil, J. D., *Science and technology of tributyl phosphate*. Baca Raton, FL (United States); CRC Press, Inc.: United States, 1990.
99. Ban, Y.; Hotuku, S.; Morita, Y., Distribution of U(VI) and Pu(IV) by N,N-di(2-ethylhexyl)Butanamide in Continuous Counter-Current Extraction with Mixer-Settler Extractor. *Solvent Extraction and Ion Exchange* **2012,** *30* (2), 142-155.
100. de Almeida, K. C. S.; Martins, T. S.; Isolani, P. C.; Vicentini, G.; Zukerman-Schpector, J., Uranyl nitrate complexes with diphenylsulfoxide and dibenzylsulfoxide: characterization, luminescence and structures. *Journal of Solid State Chemistry 171* (1–2), 230-234.
101. Ahuja, I. S.; Singh, R., Uranyl nitrate and thiocyanate complexes with some pyridine N-oxides. *Journal of Inorganic and Nuclear Chemistry* **1973,** *35* (2), 561-566.
102. Kannan, S.; Rajalakshmi, N.; Chetty, K. V.; Venugopal, V.; Drew, M. G. B., Complexes of the uranyl ion with bis(diphenylphosphino)methane dioxide. *Polyhedron* **2004,** *23* (9), 1527-1533.
103. Varga, T. R.; Bényei, A. C.; Fazekas, Z.; Tomiyasu, H.; Ikeda, Y., Molecular and crystal structure of bis(N-cyclohexyl-2-pyrrolidone)dioxouranium(VI) nitrate. *Inorganica Chimica Acta* **2003,** *342*, 291-294.
104. Cherfa, S.; Pecaut, J.; Nierlich, M., Crystal structure of octyl(phenyl)-N,N-diisobutylcarbamoylmethylphosphine dioxouranium nitrate, C48H84N6O20P2U2. In *Zeitschrift für Kristallographie - New Crystal Structures*, 1999; Vol. 214, p 523.
105. Wahu, S.; Berthet, J.-C.; Thuéry, P.; Guillaumont, D.; Ephritikhine, M.; Guillot, R.; Cote, G.; Bresson, C., Structural Versatility of Uranyl(VI) Nitrate Complexes That Involve the Diamide Ligand Et2N(C=O)(CH2)n(C=O)NEt2 (0 ≤ n ≤ 6). *European Journal of Inorganic Chemistry* **2012,** *2012* (23), 3747-3763.
106. Deb, S. B.; Gamare, J. S.; Kannan, S.; Drew, M. G. B., Uranyl(VI) and lanthanum(III) thio-diglycolamides complexes: Synthesis and structural studies involving nitrate complexation. *Polyhedron* **2009,** *28* (13), 2673-2678.
107. Deb, S. B.; Kannan, S.; Drew, M. G. B., Synthesis and structural studies of a bis(carbamoyl methyl) sulfoxide complex of uranyl nitrate. *Journal of Coordination Chemistry* **2010,** *63* (20), 3620-3626.
108. Kannan, S.; Deb, S. B.; Drew, M. G. B., Synthesis, structural and emission studies of a bis (carbamoyl methyl) sulfone complex of uranyl nitrate. *Inorganic Chemistry Communications* **2011,** *14* (1), 225-227.
109. Charpin, P.; Lance, M.; Nierlich, M.; Vigner, D.; Charbonnel, M. C.; Musikas, C., Complexes of uranyl nitrate and dialkyldiamides: structures of dinitratodioxo[N,N,N',N'-tetrabutyl-1,2-phenylenebis(oxyacetamide)-O,O']uranium(VI) and catena-poly{[dinitratodioxouranium(VI)]-[mu]-(N,N,N',N',-tetrabutylglutaramide-O:O')}. *Acta Crystallographica Section C* **1987,** *43* (3), 442-445.
110. Vats, B.; Kannan, S.; Sundararajan, M.; Kumar, M.; Drew, M. G. B., Synthesis, structural and theoretical studies of dithiodiglycolamide compounds of palladium(ii). *Dalton Transactions* **2015,** *44* (26), 11867-11876.
111. *CrysAlis*, Oxford Diffraction Ltd.: Abingdon, U.K., 2006.
112. Sheldrick, G., A short history of SHELX. *Acta Crystallographica Section A* **2008,** *64* (1), 112-122.
113. *ABSPACK*, Oxford Diffraction Ltd.: Oxford, U.K., 2005.
114. Pantazis, D. A.; Neese, F., All-electron scalar relativistic basis sets for the actinides. *Journal of Chemical Theory and Computation* **2011,** *7* (3), 677-684.
115. Schuchardt, K. L.; Didier, B. T.; Elsethagen, T.; Sun, L.; Gurumoorthi, V.; Chase, J.; Li, J.; Windus, T. L., Basis set exchange: a community database for computational sciences. *Journal of chemical information and modeling* **2007,** *47* (3), 1045-1052.

116. Schmidt, M. W.; Baldridge, K. K.; Boatz, J. A.; Elbert, S. T.; Gordon, M. S.; Jensen, J. H.; Koseki, S.; Matsunaga, N.; Nguyen, K. A.; Su, S. J., Iowa State University J. *Comput. chem* **1993,** *14*, 1347.

117. Ruhela, R.; Sharma, J. N.; Tomar, B. S.; Murali, M. S.; Hubli, R. C.; Suri, A. K., Dithiodiglycolamide: novel ligand with highest selectivity and extractability for palladium. *Tetrahedron Letters* **2011,** *52* (30), 3929-3932.

118. Varga, T. R.; Bényei, A. C.; Fazekas, Z.; Tomiyasu, H.; Ikeda, Y., Molecular and crystal structure of bis (N-cyclohexyl-2-pyrrolidone) dioxouranium (VI) nitrate. *Inorganica Chimica Acta* **2003,** *342*, 291-294.

119. Kannan, S.; Gamare, J. S.; Chetty, K. V.; Drew, M. G. B., Coordination and extraction studies of an unexplored bi-functional ligand, carbamoyl methyl pyrazole (CMPz) with uranium (VI), lanthanum (III) and cerium (III) nitrates. *Polyhedron* **2007,** *26* (14), 3810-3816.

120. Das, D.; Kannan, S.; Maity, D. K.; Drew, M. G. B., Steric Effects on Uranyl Complexation: Synthetic, Structural, and Theoretical Studies of Carbamoyl Pyrazole Compounds of the Uranyl(VI) Ion. *Inorganic Chemistry* **2012,** *51* (8), 4869-4876.

121. Martin-Gil, J.; Martin-Gil, F. J.; Perales, A.; Fayos, J.; Martinez-Ripoll, M., Bis (N, N-dimethylformamide) dinitratodioxouranium (VI), C6H14N4O10U. *Acta Crystallographica Section C: Crystal Structure Communications* **1983,** *39* (1), 44-45.

122. Charpin, P.; Lance, M.; Nierlich, M.; Vigner, D.; Descouls, N.; Musikas, C., Structure du bis (N, N-dibutyldodécanamide) dinitratodioxouranium (VI). *Acta Crystallographica Section C: Crystal Structure Communications* **1986,** *42* (5), 560-563.

123. (a) Alcock, N. W.; Flanders, D. J.; Brown, D., Actinide structural studies. Part 7. The crystal and molecular structures of (2, 2′-bipyridyl) dinitratodioxo-uranium (VI) and-neptunium (VI), and diacetato-(2, 2′-bipyridyl) dioxo-uranium (VI) and-neptunium (VI). *Journal of the Chemical Society, Dalton Transactions* **1985,** (5), 1001-1007; (b) Alcock, N. W.; Flanders, D. J.; Pennington, M.; Brown, D., Actinide structural studies. 15. Two 1, 10-phenanthroline complexes of uranium (VI). *Acta Crystallographica Section C: Crystal Structure Communications* **1988,** *44* (2), 247-250.

124. Schöne, S.; Radoske, T.; März, J.; Stumpf, T.; Patzschke, M.; Ikeda-Ohno, A., [UO2Cl2(phen)2], a Simple Uranium(VI) Compound with a Significantly Bent Uranyl Unit (phen=1,10-phenanthroline). *Chemistry – A European Journal* **2017,** *23* (55), 13574-13578.

125. (a) Schulz, W. W.; Horwitz, E. P., The Truex Process and the Management of Liquid Tru Uwaste. *Separation Science and Technology* **1988,** *23* (12-13), 1191-1210; (b) Musikas, C., Solvent extraction for the chemical separations of the 5f elements. *Inorganica Chimica Acta* **1987,** *140*, 197-206; (c) Condamines, N.; Musikas, C., The extraction by NN-dialkylamides. II. Extraction of actinide cations. *Solvent Extraction and Ion Exchange* **1992,** *10* (1), 69-100.

126. (a) Nair, G.; Prabhu, D.; Mahajan, G., Methylbutylmalonamide as an extractant for U (VI), Pu (IV) and Am (III). *Journal of radioanalytical and nuclear chemistry* **1994,** *186* (1), 47-55; (b) Kannan, S.; Chetty, K. V.; Usman, A.; Fun, H. K., Extraction and coordination studies of carbamoyl methyl sulfoxide (CMSO) with uranyl bis (β-diketonates). Synthesis and molecular structure of [{UO 2 (DBM) 2} 2 C 6 H 5 CH 2 SOCH 2 CONHC 6 H 5]. *Polyhedron* **2007,** *26* (7), 1383-1387.

127. Baisden, P. A. C., G. R., Nuclear Waste Management and Nuclear Fuel Cycle. In *Encyclopedia of Life Support System (EOLLS)*, Nagyl, S., Ed. EOLLS: Oxford, U. K., 2007.

128. *Actinide and fission product partioning and transmutation: Status and assesment report*

OECD/NEA: Paris, 1999.

129. (a) Madic, C. H., M.J.; Liljenzin, J.O.; Glatz, J.P.; Nannicini, R.; Facchini, A.; Kolarik; Z. Odoj, R. *New Partiotioning Techniques for Minor Actinides*; Luxembourg, 2000; (b) Dam, H. H.; Reinhoudt, D. N.; Verboom, W., Multicoordinate ligands for actinide/lanthanide separations. *Chemical Society Reviews* **2007,** *36* (2), 367-377.

130. Horwitz, E. P.; Schulz, W. W., The Truex process: A vital tool for disposal of US defense nuclear waste. In *New separation chemistry techniques for radioactive waste and other specific applications*, Springer: 1991; pp 21-29.

131. Zhu, Y.; Jiao, R., Chinese experience in the removal of actinides from highly active waste by trialkylphosphine-oxide extraction. *Nuclear Technology* **1994,** *108* (3), 361-369.

132. Morita, Y.; Glatz, J. P.; Kubota, M.; Koch, L.; Pagliosa, G.; Roemer, K.; Nicholl, A., Actinide partitioning from HLW in a continuous DIDPA extraction process by means of centrifugal extractors. *Solvent Extraction and Ion Exchange* **1996,** *14* (3), 385-400.

133. Serrano-Purroy, D.; Baron, P.; Christiansen, B.; Glatz, J.-P.; Madic, C.; Malmbeck, R.; Modolo, G., First demonstration of a centrifugal solvent extraction process for minor actinides from a concentrated spent fuel solution. *Separation and purification technology* **2005,** *45* (2), 157-162.

134. Sasaki, Y.; Tsubata, Y.; Kitatsuji, Y.; Sugo, Y.; Shirasu, N.; Morita, Y.; Kimura, T., Extraction behavior of metal ions by TODGA, DOODA, MIDOA, and NTAamide extractants from HNO3 to n-Dodecane. *Solvent Extraction and Ion Exchange* **2013,** *31* (4), 401-415.

135. (a) Mathur, J. N.; Murali, M. S.; Nash, K. L., Actinide partitioning—a review. *Solvent Extraction and Ion Exchange* **2001,** *19* (3), 357-390; (b) Ansari, S. A.; Pathak, P.; Mohapatra, P. K.; Manchanda, V. K., Chemistry of Diglycolamides: Promising Extractants for Actinide Partitioning. *Chemical Reviews* **2012,** *112* (3), 1751-1772; (c) Ansari, S. A.; Pathak, P.; Mohapatra, P. K.; Manchanda, V. K., Aqueous partitioning of minor actinides by different processes. *Separation & Purification Reviews* **2011,** *40* (1), 43-76.

136. Ansari, S. A.; Pathak, P. N.; Manchanda, V. K.; Husain, M.; Prasad, A. K.; Parmar, V. S., N,N,N′,N′-Tetraoctyl Diglycolamide (TODGA): A Promising Extractant for Actinide-Partitioning from High-Level Waste (HLW). *Solvent Extraction and Ion Exchange* **2005,** *23* (4), 463-479.

137. Suzuki, H.; Sasaki, Y.; Sugo, Y.; Apichaibukol, A.; Kimura, T., Extraction and separation of Am (III) and Sr (II) by N, N, N, N-tetraoctyl-3-oxapentanediamide (TODGA). *Radiochimica Acta* **2004,** *92* (8), 463-466.

138. (a) Matloka, K.; Sah, A. K.; Peters, M. W.; Srinivasan, P.; Gelis, A. V.; Regalbuto, M.; Scott, M. J., CMPO-Functionalized C 3-Symmetric Tripodal Ligands in Liquid/Liquid Extractions: Efficient, Selective Recognition of Pu (IV) with Low Affinity for 3+ Metal Ions. *Inorganic Chemistry* **2007,** *46* (25), 10549-10563; (b) Grüner, B.; Kvíčalová, M.; Plešek, J.; Šícha, V.; Císařová, I.; Lučaníková, M.; Selucký, P., Cobalt bis (dicarbollide) ions functionalized by CMPO-like groups attached to boron by short bonds; efficient extraction agents for separation of trivalent f-block elements from highly acidic nuclear waste. *Journal of Organometallic Chemistry* **2009,** *694* (11), 1678-1689; (c) Odinets, I. L.; Sharova, E. V.; Artyshin, O. I.; Lyssenko, K. A.; Nelyubina, Y. V.; Myasoedova, G. V.; Molochnikova, N. P.; Zakharchenro, E. A., Novel class of functionalized ionic liquids with grafted CMPO-moieties for actinides and rare-earth elements recovery. *Dalton Transactions* **2010,** *39* (17), 4170-4178; (d) Mohapatra, P. K.; Kandwal, P.; Iqbal, M.; Huskens, J.; Murali, M. S.; Verboom, W., A novel CMPO-functionalized task specific ionic liquid: synthesis, extraction and spectroscopic investigations of actinide and lanthanide complexes. *Dalton Transactions* **2013,** *42* (13), 4343-4347; (e) Mohapatra, P. K.; Sengupta, A.; Iqbal, M.; Huskens, J.; Verboom, W., Diglycolamide-functionalized calix [4] arenes showing unusual complexation of actinide ions in room temperature ionic liquids: role of ligand structure, radiolytic stability, emission spectroscopy, and thermodynamic studies. *Inorganic Chemistry* **2013,** *52* (5), 2533-2541; (f) Mohapatra, P. K.; Sengupta, A.; Iqbal, M.; Huskens, J.; Verboom, W., Highly efficient diglycolamide-based task-specific ionic liquids: synthesis, unusual extraction behaviour, irradiation, and fluorescence studies. *Chemistry-A European Journal* **2013,** *19* (9), 3230-3238.

139. Sugo, Y.; Sasaki, Y.; Tachimori, S., Studies on hydrolysis and radiolysis of N, N, N′, N′-tetraoctyl-3-oxapentane-1, 5-diamide. *Radiochimica Acta* **2002,** *90* (3), 161-165.

140. Dicholkar, D. D.; Kumar, P.; Heer, P. K.; Gaikar, V. G.; Kumar, S.; Natarajan, R., Synthesis of N, N, N′, N′-tetraoctyl-3-oxapentane-1, 5-diamide (TODGA) and its steam thermolysis-nitrolysis as a nuclear waste solvent minimization method. *Industrial & Engineering Chemistry Research* **2013,** *52* (7), 2457-2469.

141. Den Auwer, C.; Charbonnel, M. C.; Drew, M. G. B.; Grigoriev, M.; Hudson, M. J.; Iveson, P. B.; Madic, C.; Nierlich, M.; Presson, M. T.; Revel, R.; Russell, M. L.; Thuéry, P., Crystallographic, X-ray Absorption, and IR Studies of Solid- and Solution-State Structures of Tris(nitrato) N,N,N‘,N‘-Tetraethylmalonamide Complexes of Lanthanides. Comparison with the Americium Complex. *Inorganic Chemistry* **2000,** *39* (7), 1487-1495.

142. Pailloux, S.; Binyamin, I.; Deck, L. M.; Hay, B. P.; Duesler, E. N.; Zakharov, L. N.; Scott Kassel, W.; Rheingold, A. L.; Paine, R. T., Unexpected chelation interaction for 2-hydroxy-2-(1-oxy-pyridin-2-yl)-N,N-diphenyl acetamide with La(III). *Polyhedron* **2009,** *28* (18), 3979-3984.

143. Caudle, L. J.; Duesler, E. N.; Paine, R. T., Preparation and structure of a neodymium complex containing bidentate (carbamoylmethyl)phosphine oxide ligands. *Inorganic Chemistry* **1985,** *24* (25), 4441-4444.

144. B. Iveson, P.; G. B. Drew, M.; J. Hudson, M.; Madic, C., Structural studies of lanthanide complexes with new hydrophobic malonamide solvent extraction agents [dagger]. *Journal of the Chemical Society, Dalton Transactions* **1999,** (20), 3605-3610.

145. Davies, W.; Gray, u., A rapid and specific titrimetric method for the precise determination of uranium using iron (II) sulphate as reductant. *Talanta* **1964,** *11* (8), 1203-1211.

146. McPheeters, C. C.; Pierce, R. D.; Mulcahey, T. P., Application of the pyrochemical process to recycle of actinides from LWR spent fuel. *Progress in Nuclear Energy* **1997,** *31* (1-2), 175-186.

147. Rogers, R. D.; Seddon, K. R., *Ionic liquids: industrial applications for green chemistry*. ACS Publications: 2002.

148. Hallett, J. P.; Welton, T., Room-temperature ionic liquids: solvents for synthesis and catalysis. 2. *Chemical Reviews* **2011,** *111* (5), 3508-3576.

149. Visser, A. E.; Rogers, R. D., Room-temperature ionic liquids: new solvents for f-element separations and associated solution chemistry. *Journal of Solid State Chemistry* **2003,** *171* (1), 109-113.

150. Dai, S.; Ju, Y. H.; Barnes, C. E., Solvent extraction of strontium nitrate by a crown ether using room-temperature ionic liquids. *Journal of the Chemical Society, Dalton Transactions* **1999,** (8), 1201-1202.

151. (a) Szigethy, G.; Raymond, K. N., The Influence of Linker Geometry in Bis (3-hydroxy-N-methyl-pyridin-2-one) Ligands on Solution Phase Uranyl Affinity. *Chemistry–A European Journal* **2011,** *17* (6), 1818-1827; (b) Ni, C.; Shuh, D. K.; Raymond, K. N., Uranyl sequestration: synthesis and structural characterization of uranyl complexes with a tetradentate methylterephthalamide ligand. *Chemical Communications* **2011,** *47* (22), 6392-6394; (c) Szigethy, G.; Raymond, K. N., Influence of Linker Geometry on Uranyl Complexation by Rigidly Linked Bis(3-hydroxy-N-methyl-pyridin-2-one). *Inorganic Chemistry* **2010,** *49* (14), 6755-6765; (d) Szigethy, G.; Raymond, K. N., Hexadentate Terephthalamide (bis-hydroxypyridinone) Ligands for Uranyl Chelation: Structural and Thermodynamic Consequences of Ligand Variation (1). *Journal of the American Chemical Society* **2011,** *133* (20), 7942-7956; (e) Gorden, A. E. V.; Xu, J.; Raymond, K. N.; Durbin, P., Rational design of sequestering agents for plutonium and other actinides. *Chemical Reviews* **2003,** *103* (11), 4207-4282; (f) Drouza, C.; Gramlich, V.; Sigalas, M. P.; Pashalidis, I.; Keramidas, A. D., Synthesis, Structure, and Solution Dynamics of UO22+− Hydroxy Ketone Compounds [UO2 (ma) 2 (H2O)] and [UO2 (dpp)(Hdpp) 2 (H2O)] ClO4 [ma= 3-Hydroxy-2-methyl-4-pyrone, Hdpp= 3-Hydroxy-1, 2-dimethyl-4 (1 H)-pyridone]. *Inorganic Chemistry* **2004,** *43* (26), 8336-8345; (g) Sather, A. C.; Berryman, O. B.; Rebek Jr, J., Selective recognition and extraction of the uranyl ion. *Journal of the American Chemical Society* **2010,** *132* (39), 13572-13574; (h) Sinha, R. K.; Kakodkar, A., Design and development of the AHWR—the Indian thorium fuelled innovative nuclear reactor. *Nuclear Engineering and Design* **2006,** *236* (7), 683-700; (i) Seko, N.; Katakai, A.; Hasegawa, S.; Tamada, M.; Kasai, N.; Takeda, H.; Sugo, T.; Saito, K., Aquaculture of uranium in seawater by a fabric-adsorbent submerged system. *Nuclear Technology* **2003,** *144* (2), 274-278.

152. Nash, K. L.; Lavallette, C.; Borkowski, M.; Paine, R. T.; Gan, X., Features of the Thermodynamics of Two-Phase Distribution Reactions of Americium (III) and Europium (III) Nitrates into Solutions of 2, 6-Bis [(bis (2-ethylhexyl) phosphino) methyl] pyridine N, P, P ‘-Trioxide. *Inorganic Chemistry* **2002,** *41* (22), 5849-5858.

153. (a) Paine, R. T.; Bond, E. M.; Parveen, S.; Donhart, N.; Duesler, E. N.; Smith, K. A.; Nöth, H., Synthesis and Coordination Properties of 1-(Diphenylphosphine oxide)-1-(2‘-pyridyl N-oxide)-3-(diphenylphosphine oxide)propane. *Inorganic Chemistry* **2002,** *41* (2), 444-448; (b) Tan, Y.-C.; Gan, X.-M.; Stanchfield, J. L.; Duesler, E. N.; Paine, R. T., Synthesis and Coordination Chemistry of 1, 3-Bis (diphenylphosphinomethyl) benzene P, P ‘-Dioxide. *Inorganic Chemistry* **2001,** *40* (12), 2910-2913; (c) Bond, E. M.; Duesler, E. N.; Paine, R. T.; Neu, M. P.; Matonic, J. H.; Scott, B. L., Synthesis and Molecular Structure of a Plutonium (IV) Coordination Complex:[Pu (NO3) 2 {2, 6-[(C6H5) 2P (O) CH2] 2C5H3NO} 2](NO3) 2• 1.5 H2O• 0.5 MeOH. *Inorganic Chemistry* **2000,** *39* (18), 4152-4155; (d) Peters, M. W.; Werner, E. J.; Scott, M. J., Enhanced selectivity for actinides over lanthanides with CMPO ligands secured to a C 3-symmetric triphenoxymethane platform. *Inorganic Chemistry* **2002,** *41* (7), 1707-1716; (e) Lees, A. M. J.; Platt, A. W. G., Complexes of lanthanide nitrates with bis (diphenylphosphino) methane dioxide. *Inorganic Chemistry* **2003,** *42* (15), 4673-4679; (f) Bowden, A.; Coles, S. J.; Pitak, M. B.; Platt, A. W. G., Complexes of lanthanide nitrates with tri tert butylphosphine oxide. *Inorganic Chemistry* **2012,** *51* (7), 4379-4389; (g) Rosario-Amorin, D.; Ouizem, S.; Dickie, D. A.; Wen, Y.; Paine, R. T.; Gao, J.; Grey, J. K.; de Bettencourt-Dias, A.; Hay, B. P.; Delmau, L. H., Synthesis, Lanthanide Coordination Chemistry, and Liquid–Liquid Extraction Performance of CMPO-Decorated Pyridine and Pyridine N-Oxide Platforms. *Inorganic Chemistry* **2013,** *52* (6), 3063-3083.

154. (a) de Aquino, A. R.; Bombieri, G.; Isolani, P. C.; Vicentini, G.; Zukerman-Schpector, J., Characterization, luminescence and crystal structure of uranyl nitrate complexes with diphenyl-N-ethylphosphine amide and tripiperidinephosphine oxide. *Inorganica Chimica Acta* **2000,** *306* (1), 101-105; (b) Kannan, S.; Deb, S. B.; Drew, M. G. B., Synthesis, characterization and molecular structure of 1, 1’ bis (diphenylphosphino ferrocene) dioxide complex of uranyl nitrate. *Inorganica Chimica Acta* **2010,** *363* (10), 2338-2340; (c) Kannan, S.; Deb, S. B.; Drew, M. G. B., Synthesis, characterization and molecular structure of 1, 1’ bis (diphenyl phosphino ferrocene) dioxide complex of the cis-uranyl dichloride. *Journal of Organometallic Chemistry* **2012,** *701*, 93-95.

155. (a) Hancock, R. D.; Martell, A. E., Ligand design for selective complexation of metal ions in aqueous solution. *Chemical Reviews* **1989,** *89* (8), 1875-1914; (b) Martell, A. E., Hancock, R. D. , *Metal complexes in aqueous solution*. Plenum Press: New York, 1996.

156. (a) Freiberg, E.; Davis, W. M.; Nicholson, T.; Davison, A.; Jones, A. G., Reduction of the pertechnetate anion with bidentate phosphine ligands. *Inorganic Chemistry* **2002,** *41* (22), 5667-5674; (b) Machura, B.; Jankowska, A.; Kruszynski, R.; Kłak, J.; Mroziński, J., Structural and spectroscopic studies on rhenium (III) diphenyl (2-pyridyl) phosphine oxide complexes. *Polyhedron* **2006,** *25* (14), 2663-2672; (c) Diaz, O.; Medina, S.; Valderrama, M.; Lahoz, F. J.; Martin, M. L., Synthesis and structure of dicarbonyldichloro {2-(diphenylphosphineoxide) pyridine} ruthenium (II). *Journal of the Chilean Chemical Society* **2008,** *53* (2), 1480-1482.

157. (a) McCabe, D. J.; Russell, A. A.; Karthikeyan, S.; Paine, R. T.; Ryan, R. R.; Smith, B., Synthesis and coordination chemistry of 2-(diethoxyphosphino)- and 2-(diphenylphosphino)pyridine N,P-dioxides. Crystal and molecular structures of bis(nitrato)[2-(diethoxyphosphino)pyridine N,P-dioxide]dioxouranium(VI) and bis(nitrato)[2-(diphenylphosphino)pyridine N,P-dioxide]dioxouranium(VI). *Inorganic Chemistry* **1987,** *26* (8), 1230-1235; (b) Conary, G. S.; Russell, A. A.; Paine, R. T.; Hall, J. H.; Ryan, R. R., Synthesis and coordination chemistry of 2-(diisopropoxyphosphino) pyridine N, P-dioxide. crystal and molecular structure of bis [2-(diisopropoxyphosphino) pyridine N, P-dioxide] lanthanum nitrate. *Inorganic Chemistry* **1988,** *27* (18), 3242-3245.

158. (a) Shinoda, S.; Tsukube, H., Luminescent lanthanide complexes as analytical tools in anion sensing, pH indication and protein recognition. *Analyst* **2011,** *136* (3), 431-435; (b) Binnemans, K., Lanthanide-based luminescent hybrid materials. *Chemical Reviews* **2009,** *109* (9), 4283-4374; (c) Eliseeva, S. V.; Bünzli, J.-C. G., Lanthanide luminescence for functional materials and bio-sciences. *Chemical Society Reviews* **2010,** *39* (1), 189-227; (d) Kido, J.; Okamoto, Y., Organo lanthanide metal complexes for electroluminescent materials. *Chemical Reviews* **2002,** *102* (6), 2357-2368; (e) Cui, Y.; Xu, H.; Yue, Y.; Guo, Z.; Yu, J.; Chen, Z.; Gao, J.; Yang, Y.; Qian, G.; Chen, B., A luminescent mixed-lanthanide metal–organic framework thermometer. *Journal of the American Chemical Society* **2012,** *134* (9), 3979-3982; (f) Miyata, K.; Konno, Y.; Nakanishi, T.; Kobayashi, A.; Kato, M.; Fushimi, K.; Hasegawa, Y., Chameleon Luminophore for Sensing Temperatures: Control of Metal-to-Metal and Energy Back Transfer in Lanthanide Coordination Polymers. *Angewandte Chemie International Edition* **2013,** *52* (25), 6413-6416.

159. (a) Weissman, S. I., Intramolecular energy transfer the fluorescence of complexes of europium. *The Journal of Chemical Physics* **1942,** *10* (4), 214-217; (b) Balzani, V., Scandola, F., *Supramolecular Photochemistry*. Ellis Horwood: Chichester, 1991.

160. Moudam, O.; Rowan, B. C.; Alamiry, M.; Richardson, P.; Richards, B. S.; Jones, A. C.; Robertson, N., Europium complexes with high total photoluminescence quantum yields in solution and in PMMA. *Chemical Communications* **2009,** (43), 6649-6651.

161. Lima, N. B. D.; Gonçalves, S. M. C.; Júnior, S. A.; Simas, A. M., A comprehensive strategy to boost the quantum yield of luminescence of europium complexes. *Scientific reports* **2013,** *3*, 2395.

162. Gago, S.; Fernandes, J. A.; Rainho, J. P.; Sá Ferreira, R. A.; Pillinger, M.; Valente, A. A.; Santos, T. M.; Carlos, L. D.; Ribeiro-Claro, P. J. A.; Gonçalves, I. S., Highly luminescent tris (β-diketonate) europium (III) complexes immobilized in a functionalized mesoporous silica. *Chemistry of materials* **2005,** *17* (20), 5077-5084.

163. (a) Archer, R. D.; Chen, H.; Thompson, L. C., Synthesis, Characterization, and Luminescence of Europium (III) Schiff Base Complexes1a. *Inorganic Chemistry* **1998,** *37* (8), 2089-2095; (b) Li, C.-J.; Peng, M.-X.; Leng, J.-D.; Yang, M.-M.; Lin, Z.; Tong, M.-L., Synthesis, structure, photoluminescence and magnetic properties of new 3-D lanthanide-pyridine-2, 4, 6-tricarboxylate frameworks. *CrystEngComm* **2008,** *10* (11), 1645-1652.

164. Binnemans, K.; Lenaerts, P.; Driesen, K.; Görller-Walrand, C., A luminescent tris (2-thenoyltrifluoroacetonato) europium (III) complex covalently linked to a 1, 10-phenanthroline-functionalised sol–gel glass. *Journal of Materials Chemistry* **2004,** *14* (2), 191-195.

165. He, Y.; Liu, L.; Zhang, Z.; Fu, G.; Lü, X.; Wong, W.-K.; Jones, R. A., A tris-diketonate-Eu(III) complex with the brominated 2,2′-bpy ancillary ligand doped in PMMA for high color-purity red luminescence. *Inorganic Chemistry Communications* **2016,** *64*, 13-15.

166. Brites, C. D. S.; Lima, P. P.; Carlos, L. D., Tuning the sensitivity of Ln 3+-based luminescent molecular thermometers through ligand design. *Journal of Luminescence* **2016,** *169*, 497-502.

167. Kang, J.-S.; Jeong, Y.-K.; Shim, Y. S.; Rout, S.; Leung, K. T.; Sohn, Y.; Kang, J.-G., Structures, and luminescence and magnetic properties of Ln (III) complexes bearing dibenzoylmethane ligand (Ln= Eu and Gd). *Journal of Luminescence* **2016,** *178*, 368-374.

168. Zhang, H.; Song, H.; Yu, H.; Li, S.; Bai, X.; Pan, G.; Dai, Q.; Wang, T.; Li, W.; Lu, S., Modified photoluminescence properties of rare-earth complex/polymer composite fibers prepared by electrospinning. *Applied Physics Letters* **2007,** *90* (10), 103103.

169. Malta, O. L.; Brito, H. F.; Menezes, J. F. S.; e Silva, F. R. G.; de Mello Donegá, C.; Alves, S., Experimental and theoretical emission quantum yield in the compound Eu (thenoyltrifluoroacetonate) 3. 2 (dibenzyl sulfoxide). *Chemical Physics Letters* **1998,** *282* (3), 233-238.

170. Yu, J.; Zhou, L.; Zhang, H.; Zheng, Y.; Li, H.; Deng, R.; Peng, Z.; Li, Z., Efficient electroluminescence from new lanthanide (Eu3+, Sm3+) complexes. *Inorganic Chemistry* **2005,** *44* (5), 1611-1618.

171. Kannan, S.; Moody, M. A.; Barnes, C. L.; Duval, P. B., Fluoride abstraction and reversible photochemical reduction of cationic uranyl (VI) phosphine oxide complexes. *Inorganic Chemistry* **2006,** *45* (23), 9206-9212.
172. Kannan, S.; Vaughn, A. E.; Weis, E. M.; Barnes, C. L.; Duval, P. B., Anhydrous Photochemical Uranyl(VI) Reduction: Unprecedented Retention of Equatorial Coordination Accompanying Reversible Axial Oxo/Alkoxide Exchange. *Journal of the American Chemical Society* **2006,** *128* (43), 14024-14025.
173. Vats, B. G.; Kannan, S.; Parvathi, K.; Maity, D. K.; Drew, M. G. B., Steric effects in complexes of diphenyl(2-pyridyl)phosphine oxide with the uranyl ion. Synthetic, structural and theoretical studies. *Polyhedron* **2015,** *89*, 116-121.
174. Kannan, S.; Raj, S.; Fun, H.-K., Synergistic complexes of tributyl phosphate and dibutyl (butyl) phosphonate with uranyl bis (β-diketonates). Synthesis, characterisation and molecular structure of [UO2 (TTA) 2. TIBP]. *Journal of Chemical Research* **2001,** *2001* (2), 50-51.
175. Kannan, S.; Venugopal, V.; Pillai, M. R. A.; Droege, P. A.; Barnes, C. L., Synthesis and characterization of sulphoxide adducts of uranyl bis (β-diketonates): The crystal and molecular structure of [UO2 (DBM) 2· C6H5CH2SOCH3]. *Polyhedron* **1996,** *15* (1), 97-101.
176. Rajagopal, K.; Kannan, S.; Venugopal, V.; Krishnakumar, R. V.; Nandhini, M. S.; Natarajan, S., Syntheses and characterisation of amide adducts of uranyl bis (β-diketonates) the molecular structure of [UO2 (DBM) 2. C4H9CON (3-C5H11)(sec-C4H9)]. *Journal of Chemical Research* **2003,** *2003* (8), 468-469.
177. (a) Taylor, J. C.; McLaren, A. B., Crystal and molecular structure of bis (3-chloropentane-2, 4-dionato)-dioxo (triphenylphosphine oxide) uranium (VI) and dioxobis (pentane-2, 4-dionato)(triphenylphosphine oxide) uranium (VI)–benzene (1/1). *Journal of the Chemical Society, Dalton Transactions* **1979,** (3), 460-464; (b) Taylor, J. C.; Waugh, A. B., Polymorphism in uranyl chelates. Part 3. The crystal and molecular structure of the β form of bis (1, 1, 1, 5, 5, 5-hexafluoropentane-2, 4-dionato) dioxo (trimethyl phosphate) uranium (VI). *Journal of the Chemical Society, Dalton Transactions* **1977,** (17), 1636-1640.
178. Leipoldt, J. G.; Bok, L. D. C.; Laubscher, A. E.; Basson, S. S., The crystal structure of tris (thenoyltrifluoroacetonato) bis (triphenylphosphine oxide) neodymium (III). *Journal of Inorganic and Nuclear Chemistry* **1975,** *37* (12), 2477-2480.
179. (a) Li, J.; Li, H.; Yan, P.; Chen, P.; Hou, G.; Li, G., Synthesis, crystal structure, and luminescent properties of 2-(2, 2, 2-trifluoroethyl)-1-indone lanthanide complexes. *Inorganic Chemistry* **2012,** *51* (9), 5050-5057; (b) Burns, J. H.; Baldwin, W. H., Crystal structures of aquotris (salicylato) samarium (III), and aquotris (salicylato) americium (III). *Inorganic Chemistry* **1977,** *16* (2), 289-294.
180. Kirby, A. F.; Foster, D.; Richardson, F. S., Comparison of 7FJ← 5DO emission spectra for Eu (III) in crystalline environments of octahedral, near-octahedral, and trigonal symmetry. *Chemical Physics Letters* **1983,** *95* (6), 507-512.
181. Shahi, P. K.; Singh, A. K.; Singh, S. K.; Rai, S. B.; Ullrich, B., Revelation of the Technological Versatility of the Eu (TTA) 3Phen Complex by Demonstrating Energy Harvesting, Ultraviolet Light Detection, Temperature Sensing, and Laser Applications. *ACS applied materials & interfaces* **2015,** *7* (33), 18231-18239.
182. Werts, M. H. V.; Jukes, R. T. F.; Verhoeven, J. W., The emission spectrum and the radiative lifetime of Eu 3+ in luminescent lanthanide complexes. *Physical Chemistry Chemical Physics* **2002,** *4* (9), 1542-1548.
183. Liang, H.; Xie, F., Optical investigation of Sm (III)-β-diketonate complexes with different neutral ligands. *Spectrochimica Acta Part A: Molecular and Biomolecular Spectroscopy* **2009,** *73* (2), 309-312.
184. Kumari, N.; Prabhu, D. R.; Kanekar, A. S.; Pathak, P. N., Validation of Solvent Extraction Scheme for the Reprocessing of Advanced Heavy Water Reactor Spent Fuel Using N,N-Dihexyl Octanamide as Extractant. *Industrial & Engineering Chemistry Research* **2012,** *51* (44), 14535-14542.

185. Cuillerdier, C.; Musikas, C.; Hoel, P.; Nigond, L.; Vitart, X., Malonamides as New Extractants for Nuclear Waste Solutions. *Separation Science and Technology* **1991,** *26* (9), 1229-1244.
186. Philip Horwitz, E.; Kalina, D. C.; Diamond, H.; Vandegrift, G. F.; Schulz, W. W., THE TRUEX PROCESS - A PROCESS FOR THE EXTRACTION OF THE TKANSURANIC ELEMENTS EROM NITRIC AC In WASTES UTILIZING MODIFIED PUREX SOLVENT*. *Solvent Extraction and Ion Exchange* **1985,** *3* (1-2), 75-109.
187. (a) Matonic, J. H.; Neu, M. P.; Enriquez, A. E.; Paine, R. T.; Scott, B. L., Synthesis and crystal structure of a ten-coordinate plutonium(iv) ion complexed by 2-[(diphenylphosphino)methyl]pyridine N,P-dioxide: [Pu(NO3)3{2-[(C6H5)2P(O)CH2]C5H4NO}2][Pu(NO3)6]0.5. *Journal of the Chemical Society, Dalton Transactions* **2002,** (11), 2328-2332; (b) Pailloux, S.; Shirima, C. E.; Ray, A. D.; Duesler, E. N.; Smith, K. A.; Paine, R. T.; Klaehn, J. R.; McIlwain, M. E.; Hay, B. P., Synthesis and lanthanide coordination chemistry of trifluoromethyl derivatives of phosphinoylmethyl pyridine N-oxides. *Dalton Transactions* **2009,** (36), 7486-7493.
188. Binyamin, I.; Pailloux, S.; Duesler, E. N.; Rapko, B. M.; Paine, R. T., Synthesis and Lanthanide Coordination Properties of New 2,6-Bis(N-tert-butylacetamide)pyridine and 2,6-Bis(N-tert-butylacetamide)pyridine-N-oxide Ligands. *Inorganic Chemistry* **2006,** *45* (15), 5886-5892.
189. Speziale, A. J.; Hamm, P. C., Preparation of Some New 2-Chloroacetamides. *Journal of the American Chemical Society* **1956,** *78* (11), 2556-2559.
190. Vats, B. G.; Kannan, S.; Pius, I. C.; Noronha, D. M.; Maity, D. K.; Drew, M. G. B., Synthetic, structural, extraction and theoretical studies of uranyl nitrate dithio-diglycolamide compounds. *Polyhedron* **2014,** *75*, 81-87.
191. Hnatejko, Z.; Lis, S.; Starynowicz, P.; Stryła, Z., Synthesis, spectroscopic and structural properties of uranyl complexes based on bipyridine N-oxide ligands. *Polyhedron* **2011,** *30* (5), 880-885.
192. Dash, S.; Kamruddin, M.; Bera, S.; Ajikumar, P. K.; Tyagi, A. K.; Narasimhan, S. V.; Raj, B., Temperature programmed decomposition of uranyl nitrate hexahydrate. *Journal of Nuclear Materials* **1999,** *264* (3), 271-282.
193. C. Medic, M. J. H. *High-level liquid waste partitioning by means of completely incinerable extractants*; European commision, Nuclear Science and Technology: Luxemberg, 1998.